

In situ IR spectroscopy of intermediates in heterogeneous oxidative catalysis

V.A. Matyshak *, O.V. Krylov

N.N. Semenov Institute of Chemical Physics, Russian Academy of Science, ul. Kosygin, 4, Moscow, 117334, Russia

1. Introduction

The construction of a theory of heterogeneous catalysis is hampered by the absence of information on detailed reaction mechanisms. Such information could possibly be obtained on the basis of the quantum-mechanical description of catalytic systems, but this approach is not feasible at present since the number of calculations needed is too large to be performed. The use of semiempirical methods is simpler, but their results are often ambiguous.

Furthermore, the last ten years have seen the considerable advance in the level of experimental facilities available. New methods have been evolved and are now advancing successfully; the sensitivity of traditional methods (Fourier-transform IR spectroscopy, etc.) has considerably increased. It has become possible to employ physical methods to investigate reactions in situ and to determine the real structure of surface intermediates.

At present, in our view, the most promising approach to the determination of a heterogeneous catalytic reaction mechanism is the systematic investigation of the structure and properties of the intermediate compounds. In the conventional meaning of the term, the reaction mechanism is a set of elementary steps resulting in the formation of products. Intermediates are substances which are involved in the elementary steps but which are not released with the reaction products [1].

To determine the mechanism of a catalytic reaction we have to identify the nature of its intermediates X, Y, Z



and also the sequence of their conversion into the reaction products.

Currently fundamental information on complexes formed at the surface during a reaction is derived from molecular spectroscopy. Information has been accumulated about the properties of such complexes, and assumptions about their role have been expressed. However, in order to determine with certainty whether or not the surface complex is an intermediate in the reaction, it is necessary to compare the rate of its formation and consumption with the rate of formation of the products, i.e., we must study the conversion kinetics of the surface compounds at the same time as we measure the rate of the catalytic reaction [2].

* Corresponding author.

A procedure for such (spectrokinetic) measurements has been developed [3]. It includes the use of an IR spectrophotometer which enables spectra to be measured at high temperature, and reactor-sample cells of special construction [4,5], which make it possible to record spectra and to study reaction kinetics under gradientless conditions at the same time. Such measurements can be made under both steady-state and nonsteady-state conditions.

This review deals with the results of the spectrokinetic study of the following reactions: oxidation of propylene to acrolein over simple and complex oxides; interaction of CO and NO over supported metals and oxides; C₃H₆, interaction of CO and NO over zeolites; and oxidation of ammonia over oxides and bulk metals. Note that all these reactions are oxidation reactions, where different molecules play the role of an oxidant. The reactions listed above were also selected for investigation because the adsorption of the reagents (CO, NO, NH₃, C₃H₆ etc.) on a variety of systems has been studied in detail by spectral methods and the structure of the surface compounds is well known. Many of the molecules mentioned above are used as test molecules to characterize the surface of solids. All this allows us to pay basic attention, not to specific spectral problems, such as the assignment of spectral bands, but to the investigation of the formation of surface compounds and their decomposition.

This review is concerned mainly with the results obtained in the Institute of Chemical Physics in Moscow. Data from other authors and some questions concerning the conduct of spectrokinetic investigations are also presented.

2. Molecular spectroscopic study of the properties of intermediates in heterogeneous catalytic reaction

The information obtained via IR spectroscopy may possibly even increase if one studies complexes on solid surfaces (in comparison with molecules in the gas phase), the reason being that, in the gas phase a rather large number of vibrations are not active in the IR range of the spectrum (they are active in the Raman spectrum). However, when molecules interact with the surface, their symmetry decreases and practically all vibrations become active in the IR spectrum. N₂, H₂, O₂ and other molecules adsorbed on a variety of solid surfaces, can be distinctly observed by IR spectroscopy.

The capabilities of IR spectroscopy were greatly extended with the introduction of the Fourier technique (FTIR) [6]. It has become possible to undertake spectral measurements at high temperatures, in situ [7,8], and at the same time to measure kinetic and spectral parameters of a catalytic system [3,9].

Processes which occur on bulk metal surfaces cannot be studied by the traditional transmission methods, but the emission spectroscopy method can be used for these purposes. The smooth surface of bulk metals is usually studied by reflection absorption IR spectroscopy [10]. The diffuse reflectance method is also used to study surface complexes in order to overcome some difficulties connected with rather strong intrinsic absorption of the catalyst.

We consider below some basic features of the IR spectroscopic methods used in our experiments.

2.1. Transmission spectroscopy

The fundamentals of this method have been presented in a great number of monographs (see, for example, Refs. [11–13]). Briefly, they are as follows: the spectrometer records the transmission T

$$T = J/J_0 = \exp(-kl) \quad (2.1)$$

where k is the absorption coefficient, and l is the thickness of the absorbing layer.

According to the Lambert–Bouguer–Beer law

$$D = \ln(1/T) = \ln(J_0/J) = \epsilon cl \quad (2.2)$$

where ϵ is the extinction coefficient, and c and l are the concentration and thickness of an adsorbed layer, respectively. This expression is the basic one for the quantitative analysis of spectroscopic data.

The sensitivity of the method is defined both by the characteristics of the emission recorder and by the extinction coefficient of the medium. For some traditionally used spectrometers it is possible to estimate the number of absorbing molecules which are necessary to obtain absorption bands of sufficiently intensity. For CO, for example, this number is about 10^{12} CO molecules/cm², corresponding to a coverage of about 0.1%. Because other vibrations are characterized by a lower extinction coefficient (by a factor of 10^{-2} – 10^{-3}), sensitivity to them is proportionately lower.

The use of the Fourier technique has improved the situation in this field. Calculations reveal [13] that when an interferometer is used instead of a dispersion element the sensitivity increases a hundred times. In actual practice, however, it is increased only tenfold, because of the intrinsic noise in the receiver.

The intrinsic emission of the sample hinders the use of transmission spectroscopy for the investigation of catalytic reactions. In this case, instead of a real spectrum one can only obtain a sum of emission and transmission spectra. It is possible to eliminate the emission by modulating it with a special device placed in front of the sample, but this requires a modification of serial spectrometers. Some firms produce spectrometers for high temperature measurements.

It is important to note that Fourier spectrometers also allow the performance of measurements at high temperatures. The spectra are distorted only because the emission of the heated sample can change the temperature of the globar. Fourier spectroscopy also makes it possible to deal with small energies, which means that one can use it to study surface complexes even on catalysts with strong intrinsic absorption.

Because spectrokinetic measurements are carried out under stationary and nonstationary conditions a question arises about the characteristic times of the processes which could be studied by such a technique. These times are estimated to be about 10 s. The value of the time constant for Fourier spectroscopy is very close to this value (the time of one scan is 1 s). A great number of scans is required to obtain a well-defined spectrum of the sample having strong intrinsic absorption (the signal/noise ratio increases as the square root of the number of scans). In this case the time required to obtain one spectrum is about 1 h. It is clear that such systems can be investigated only under stationary conditions.

A recent report [14] concerned measurements with the Fourier spectrometer that required a very brief period of time for one scan (1/25 s). The application of such devices will allow the investigation of reactions with a characteristic time considerably shorter than 1 s.

The need to simultaneously study both catalytic and kinetic properties of a system defines the sample cell construction: it has to be a catalytic reactor, in which it is possible to carry out kinetic measurements (relatively small volume and facility for heating). It is also essential that the reaction cell is gradient-free. Such cells are shown in Figs. 1 and 2 [4,5]. They allow the study of catalysts with different activities.

2.2. Diffuse reflectance IR spectroscopy

In experiments with transmission IR spectroscopy rather thin pellets of the substance (10–20 mg/cm²) are usually used in order to suppress scattering. So the success of this technique is defined by the ability to prepare such pellets. Moreover, the sensitivity of transmission spectroscopy in the range over 2000 cm⁻¹ is low due to the rather high intrinsic adsorption of the catalyst. And finally, sometimes because of the long optical path-length in the transmission cell, the absorption bands of the molecules

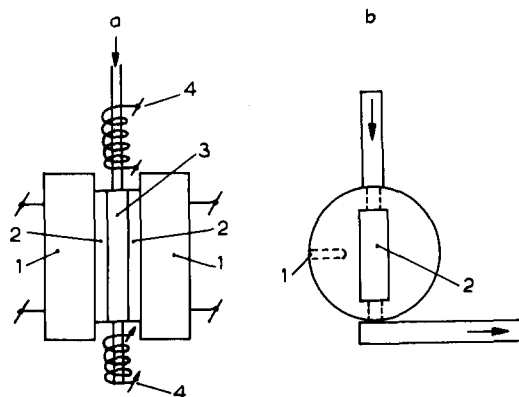


Fig. 1. The sample cell reactor. (a) Diagram of the sample cell reactor: 1, principal heater; 2, 'window'; 3, reactor; 4, the auxiliary heater. (b) Diagram of the reactor: 1, thermocouple pocket; 2, sample position.

and surface compounds may be superimposed. Furthermore, some diffusion complications may arise when the kinetics of the catalytic reaction is studied in pressed pellets.

All these limitations are absent when one uses diffuse reflectance spectroscopy [15,16]. A schematic diagram of this method is presented in Fig. 3. The special device allows the measurement of diffuse reflectance spectra at high temperatures.

The diffuse reflectance spectra are governed by the Kubelka–Munk formula [15], which links a portion of light reflected by the infinitely thick medium (R_∞) with absorption (K) and scattering (S) coefficients

$$K/S = (1 - R_\infty)^2 / 2R_\infty \quad (2.3)$$

When some molecules are adsorbed on this infinitely thick sample, formula (2.3) changes to:

$$(K + \epsilon c) / S = (1 - R)^2 / 2R \quad (2.4)$$

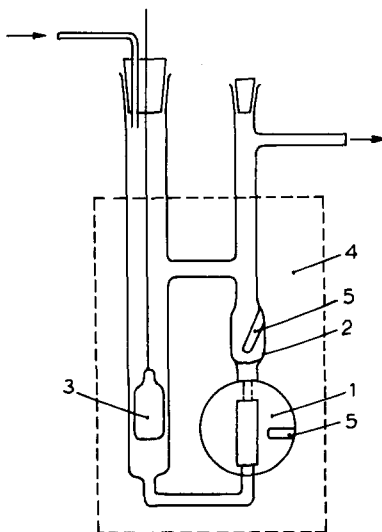


Fig. 2. Diagram of gradientless cell reactor for spectrokinetic measurements: 1, IR cell; 2, additional volume for catalyst; 3, plunger; 4, heater; 5, thermocouple pocket.

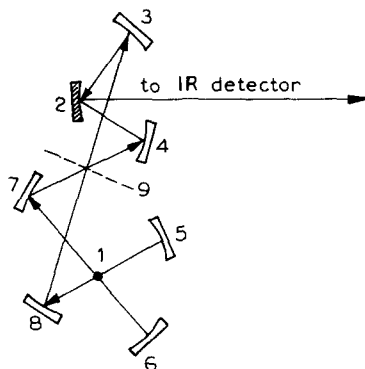


Fig. 3. Diagram of diffuse reflectance spectrometer: 1, emission source; 2, sample; 3–6, spherical mirrors; 7–8, plane mirrors; 9, auxiliary chopper.

where R is the portion of light reflected by the infinitely thick medium covered with an adsorbed layer, ϵ and C are the extinction coefficient and the concentration of an adsorbed substance, respectively. R and R_∞ can be determined from the spectrum (see Fig. 4).

The intensity of the band is determined by the formula

$$J = (R_\infty - R) / R_\infty \quad (2.5)$$

From (2.3), (2.4) and (2.5) one can obtain the relation between the intensity of the absorption band and the concentration of the substance in the adsorbed layer:

$$F(R) = J(1/R - R_\infty) = 2\epsilon c/S \quad (2.6)$$

This formula allows one to estimate the optical length in the catalyst. It is about 2–3 mm and is much more than the optical length in the transmission technique. Such a large value is one of the reasons underlying the high sensitivity of diffuse reflectance spectroscopy. Theoretically, for samples which scatter well diffuse reflectance spectroscopy is more than ten times as sensitive as traditional transmission spectroscopy. In reality, however this relation differs from the theoretical one, due to the different scattering ability of powders (used to record diffuse reflectance spectra) and pellets (transmission spectra). Furthermore, the devices used to record spectra are not ideal and cannot collect all the light scattered by the sample. With all these corrections, however, for well scattering substances (R ca. 1), the diffuse reflectance spectroscopy is more sensitive than the transmission mode (even if only a few percent of scattered light arrives at the detector).

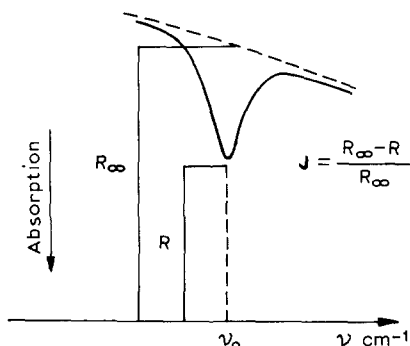


Fig. 4. Measurement of R and R_∞ in the diffuse reflectance spectra.

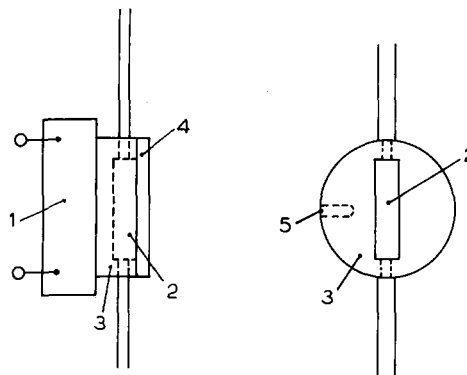


Fig. 5. Diagram of cell reactor for recording diffuse reflectance spectra: 1, heater; 2, sample position; 3, cell; 4, 'window' (Zn_2S); 5, thermocouple pocket.

In order to find the concentration of adsorbed substance one has to determine the scattering coefficient (according to the Kubelka–Munk formula). Some methods for its independent determination are given in Ref. [28]. However, for low intensity bands the concentration of the absorbing substance is related to the intensity of the appropriate band by a formula analogous to the Beer–Lambert law

$$-\epsilon c l_{\text{eff}} = \ln(R/R_{\infty}), \quad (2.7)$$

where l_{eff} is the optical length of the sample. Eq. (2.7) is valid at $(R_{\infty} - R)/R_{\infty} \ll 2(1 - R_{\infty})/R_{\infty}^{1/2}$.

The characteristic times of processes which can be studied by diffuse reflectance spectroscopy are the same as for the transmission mode.

Fig. 5 shows the construction of sample cell reactors for the simultaneous recording of the diffuse reflectance spectra and the catalytic reaction rate.

2.3. Emission spectroscopy

This method is used more rarely than the two presented above. The intensity of the emission is quite low, and it is quite difficult to measure it. With the development of the Fourier facilities the capabilities of emission spectroscopy have been fundamentally increased.

It is not possible to obtain information about the substance from the emission spectra of a black body, but real materials are not black. The distribution of energy emitted by a non-black body is governed by the Kirchhoff–Planck laws. The emission coefficient of a grey body at temperature T and frequency ν is determined as the relation of emissions of grey ($J(\nu, T)$) and black ($J_B(\nu, T)$) bodies at the same temperature [17,18]:

$$\epsilon_{\nu} = J(\nu, T) / J_B(\nu, T) \quad (2.8)$$

According to the Kirchhoff law, $\epsilon_{\nu} = a_{\nu}$, where a_{ν} is the absorption of the substance.

To calculate the emission of liquids and solids it is necessary to take account of the reflection of the emission radiated towards the substance boundary. Catalytic systems partially transmit IR radiation. The theory of semitransparent substances is presented in Refs. [17,18].

The basic expression for quantitative study is

$$\epsilon + r + t = 1 \quad (2.9)$$

where r and t are the reflection and transmission coefficients of the substance, respectively.

For low-reflectance samples

$$\epsilon(\nu) = 1 - t(\nu). \quad (2.10)$$

The absorption of the sample $a(\nu)$ is related to the absorbing sample concentration by the Beer–Lambert law:

$$a(\nu) = -\log t(\nu) = Kcl. \quad (2.11)$$

In this case from (2.10) and (2.11)

$$c = -\log(1 - \epsilon(\nu)) / Kl. \quad (2.12)$$

This expression is obeyed well by gases and semitransparent substances [18]. Analogous expressions exist for the emission of substances on metal surfaces.

Before dealing with an emission spectrum it is necessary to correct it for a given spectrometer. The correction factor ($J_b(\nu)$), which includes the efficiency of a slit group, detector and amplifier characteristics and so on, can be determined experimentally by recording a black body spectrum at the appropriate temperature. An emission spectrum $J_s(\nu)$ then has to be divided by this quantity $J_b(\nu)$. The resulting spectrum thus obtained $\epsilon(\nu)$ will be independent on the recording device.

For substances which have low absorbance but high diffusivity,

$$\epsilon(\nu) = 1 - r(\nu), \quad (2.13)$$

which follows from Eq. (2.9). In this case, for quantitative analysis of emission measurements the mathematical apparatus of diffuse reflectance spectroscopy is usually used (see 2.2).

Emission spectroscopy is at present used to study organic substances [19], gases [20] and, most widely, the structure of solid surfaces [21–26] (the formation of oxide films [27], for example). Recently, some papers have been published which describe the use of emission spectroscopy to study molecules adsorbed on surfaces of various substances [28–31]. Such studies are the last step towards recording emission spectra immediately in a catalytic reaction. This spectral technique is the only one where heating of a sample does not obstruct the measurement, but is necessary for it. Some approaches to the use of emission spectroscopy to study a catalytic reaction *in situ* have been presented in Refs. [32–35]. However, we are probably the first to perform the systematic investigation of the catalytic reaction mechanism by this method.

Fig. 6 shows the construction of a spectral cell, which is at the same time the catalytic reactor. The cell is made from stainless steel with a working part in the form of glass with an inside diameter of 40 mm

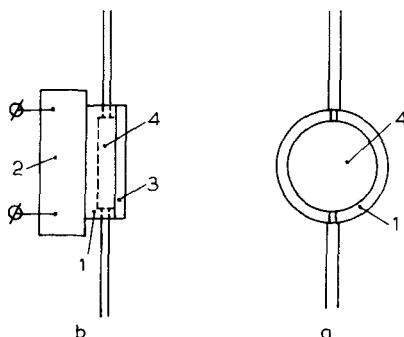


Fig. 6. Schematic diagram of cell-reactor for (a) recording emission spectra and (b) cell-reactor itself: 1, cell; 2, heater; 3, 'window'; 4, sample position.

Table 1
Optimum spectral ranges for various methods

Method subject of investigation	Transmission	Diffuse reflectance	Emission
Oxides	1100–2000 cm^{-1}	1600–5000 cm^{-1}	–
Supported metals	1100–2000 cm^{-1}	1600–5000 cm^{-1}	–
Bulk metals	–	–	400–2500 cm^{-1}

and thickness 1 mm. From the open side the cell is closed by a window of zinc sulfide. A heater is placed on the opposite side, thus allowing us to change temperature of the sample from 20 to 500°C. A reaction mixture is fed and removed through the orifices in side walls of the cell (see Fig. 6). In the traditional form of cell (large volume and cool ‘windows’), the spectra of surface compounds could be distorted because of absorption of some radiated energy by the cool ‘windows’, and by superimposition on the gas-phase spectrum. In our case these distortions are minimized by keeping the ‘windows’ practically at the sample temperature (the gap between the ‘window’ and the sample is very small: 1 mm).

2.4. Conclusions

This brief review of various methods of molecular spectroscopy shows that, used in combination, they allow one to study practically any catalytic system. Table 1 gives spectral ranges in which different methods of molecular spectroscopy give optimal results for various catalysts.

The molecular spectroscopy methods presented above can be used under both stationary and nonstationary catalytic conditions. It is known [36,37] that the characteristic times of catalytic heterogeneous reactions are in the range from 10^{-2} to 10^2 s. Reactions with characteristic times in excess of 1 s can be studied by nonstationary molecular spectroscopic methods.

It should be stressed once again that if one records only the spectra of surface compounds in a catalytic reaction *in situ* one cannot answer the question of whether these compounds are intermediates. The criterion for the observed surface compound to be an intermediate in the reaction is a coincidence between the rate of its conversion and the rate of formation of the reaction product.

Fig. 7 is the basic diagram of spectrokinetic measurements. The spectral cell, which is at the same time the gradientless catalytic reactor, allows one to perform the usual kinetic measurements. The construction of such a reactor cell has been described above. Its main features are a small volume and the absence of cold parts. The ‘windows’ are usually attached by the mechanical tightening of well-polished surfaces or by the use of glue. To check whether the cell is gradientless or not it is necessary to make some theoretical and experimental estimates for every individual catalytic system. The experimental conditions have to permit the process under study to proceed in the kinetic (non-diffusion) region.

The spectrokinetic experiment usually involves several steps:

- (1) the simultaneous recording of spectral and kinetic properties of the system;

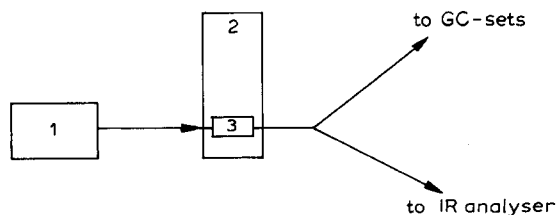


Fig. 7. Basic diagram of spectrokinetic measurements: 1, block of gas pretreatment; 2, IR spectrometer; 3, cell reactor.

(2) the assignment of bands in the spectra. This is done by the adsorption of molecules containing isotopes. The problems of assignment are not discussed in details in this review: necessary references are given throughout the discussion. Such an approach allows us to concentrate most of our attention on the study of surface compound properties;

(3) the quantitative analysis of the spectra. This step usually has two parts. Firstly, it is necessary to check the Beer–Lambert law. The reasons for its violation are discussed in Ref. [13]. It is valid if the extinction coefficient is constant for all coverages. If the form and position of a spectral band change when the coverage of the surface with the corresponding complex changes the Beer–Lambert law is violated. In our experiments the form of spectral bands and their position were checked constantly, and we consider that the Beer–Lambert law was not violated in all system studied. It should also be mentioned that the coverage of the surface with complexes studied does not essentially change. This also reduces the possibility that the extinction coefficient will change with coverage. We now have to determine the concentration of the absorbing substance (the intensity of the relevant absorption band is known). For this, following (2.2), one needs to know the extinction coefficients of the vibrations of surface complexes. Problems connected with their experimental determination are discussed in Refs. [11,38]. At present, the extinction coefficients of vibrations in a variety of surface complexes are estimated (among them are CO , CO_3^{2-} , C_nH_m , NH_4^+ , NH_3 , NCO , etc.). This estimate is based on the independent determination of surface coverage by one or another of the surface compounds. It is also possible to find the extinction coefficients using the balance equation if it can be shown independently that this surface compound is an intermediate in the reaction;

(4) the final step is the comparison of the reaction rate, calculated from surface coverage, with the rate measured in the experiment. The coincidence of these two values means that the surface compounds under study are the intermediates in the reaction.

This approach allows one to determine the role of surface compounds in the reaction and the quantitative characteristics of the elementary steps of the reaction. In other words, the spectrokinetic method is an experimental basis for the study of mechanisms of heterogeneous catalytic reaction.

3. Partial olefin oxidation

Hydrocarbon oxidation proceeds via two main routes: partial oxidation to oxygen-containing compounds, and total oxidation to CO_2 and H_2O . We consider here only those reactions of partial oxidation in which the basic carbon skeleton of the molecule is not destroyed and only one or two oxygen atoms are added to it, forming oxygen-containing compounds.

Our main concern in this section will be with the partial oxidation of propylene. The mechanism of this reaction was studied by the authors at the Institute of Chemical Physics, Russian Academy of Sciences, Moscow.

3.1. Partial oxidation of ethene

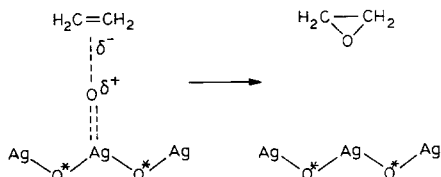
The partial oxidation of the simplest of olefins, ethene, gives ethene oxide: $\text{C}_2\text{H}_4\text{O}$. The best catalyst for this reaction is silver supported on γ -alumina. The reason for this phenomenon is not yet clear, which is why the mechanism of this reaction is being studied by many scientists.

FTIR diffuse reflectance spectroscopy, together with transient response kinetic measurements revealed the presence of weakly and strongly bound acetaldehyde and also $\text{CH}_3\text{CHO}_{\text{ads}}$ in the oxidation of C_2H_4 to $\text{C}_2\text{H}_4\text{O}$ on $\text{Ag}/\alpha\text{-Al}_2\text{O}_3$ [39]. Similar investigations over $\text{Ag}/\gamma\text{-Al}_2\text{O}_3$, which has a lower selectivity,

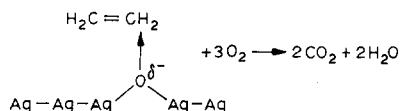
show that adsorbed ethene, carbonates and Ag–CO, which are possibly precursors of total oxidation [40], are present at the surface.

Mention has already been made of the problems associated with kinetic and spectral measurements at short characteristic times (less than 1 s) and of the need to perform such measurements when studying the intermediate compounds because the characteristic times in catalysis are 10^{-2} – 10^2 s. New possibilities for the study of intermediate compounds appeared when Gleaves et al. [41] reported the construction of a so-called TAP reactor (temporal analysis of products). This allows the analysis products immediately after their desorption from the surface, thereby avoiding their readsorption. As a result, it has become possible to study processes with characteristic times in the millisecond and even microsecond range, far below the limits of traditional contact time ranges.

Using the TAP reactor to study the mechanism of ethene oxidation over Ag powder, Gleaves and coworkers [42] showed that surface ethene complexes appear to be the same for total and partial oxidation. But the oxygen, which reacts with them, does not act in the same way. CO_2 is formed more quickly than $\text{C}_2\text{H}_4\text{O}$ mainly at the expense of the weakly bonded surface oxygen. Ethene oxide is formed with the help both of surface atomic oxygen and subsurface oxygen O^* , due to which the intermediate charge state of silver ($\text{Ag}^{\delta+}$) is possibly Ag^{3+} . The authors [42] suggested the Van Santen scheme [43] according to which ‘electrophilic’ oxygen, $\text{O}^{\delta+}$, forms a complex, giving rise to ethene oxide:

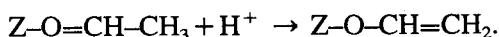
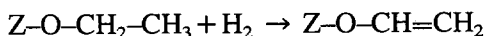
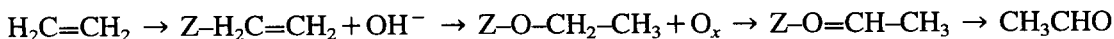


and a ‘nucleophilic’ oxygen, $\text{O}^{\delta-}$, forms a complex, giving rise to total oxidation:



Currently a vast amount of published data is available concerning the nature of oxygen which participates in the total oxidation and partial oxidation of ethene over an Ag surface. Recent data appear to support the Van Santen scheme (3.1). For example, three bands of Ag–O vibrations were recorded in the Raman spectra in situ during ethene oxidation on Ag(111) and Ag(110) [44] due to three forms of adsorbed oxygen. As the ethene is oxidized the subsurface oxygen disappears, quickly exchanging with $\text{O}^{\delta+}$. Ethene can also be oxidized to acetaldehyde. Investigation of this process on $\text{MoO}_3/\text{TiO}_2$ by FTIR spectroscopy [45] showed the presence of a π -complex of C_2H_4 , adsorbed acetaldehyde and also some weakly bound enol complexes. The catalytic reaction according to Ref. [44] proceeds via the following steps:

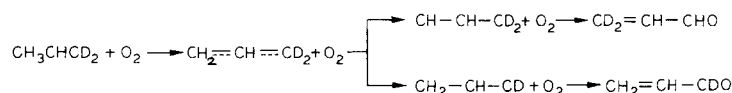
- (1) C_2H_4 adsorption on Lewis acid sites;
- (2) electrophilic attack of a weak acid proton from a Mo–OH group; and
- (3) oxidation to aldehyde without following oxidation to acetate:



3.2. Partial oxidation of propene to acrolein (general information)

The conversion of propene to acrolein is one of the most intensively studied catalytic processes of selective oxidation [46]. The first selective catalyst for this reaction was Cu_2O . But most attention is now being paid to bismuth molybdate and other systems containing Bi_2O_3 and MoO_3 . At present it can be taken as having been proved that the oxidation of propene to acrolein proceeds via a symmetrical π -allyl complex of propene with metal M (after splitting out of one hydrogen atom).

The assumption that π -allyl complexes are formed during the adsorption of propene over oxides was made on the basis of catalytic and isotope data well before the IR spectra of adsorbed propene were recorded. The initial stage of the oxidation of propene over Cu_2O , following the results of Adams and Jennings [47,48], is the removal of a hydrogen atom from the methyl group of the olefin together with formation of a symmetrical π -allyl complex. With the same probability, the second hydrogen atom splits out of the first (C_1) or third (C_3) carbon atom of the olefin, and the product of partial oxidation (acrolein) is then formed:



Similar results were obtained in experiments with propene labeled with radioactive ^{14}C . It turns out that, during C_3H_6 oxidation over bismuth molybdate, both carbon atoms (C_1 and C_3) have the same properties and are oxidized to the intermediate complex with the same probability [49].

It is worth noting that the formation of π -allyl complexes could follow the molecular adsorption of propene. Busca et al. [50] used FTIR spectroscopy to show that a molecular form of propene does exist on the surface of oxides at relatively low temperatures after propene adsorption. It may be supposed that this is just the form that is formed before the π -allyl complex.

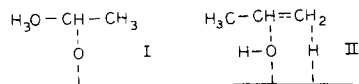
The results of TAP experiments show that weakly bound forms of adsorbed propene do take part in its oxidation to acrolein over $\text{Bi}_2\text{O}_3 \cdot \text{MoO}_3$ [51]. These experiments also found the existence of two forms of adsorbed oxygen. One of them takes part in the partial oxidation; the other does not, but easily exchanges with oxygen from the gas phase.

The sites at the oxides surfaces where olefin complex can be adsorbed as π -allyl, are not only metal ions, but also the surface acid Bronsted sites [52].

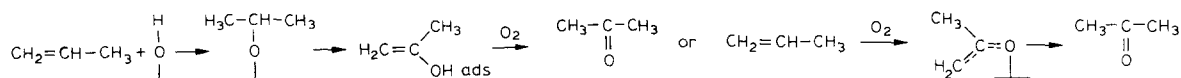
Trefiro et al. [53] studied the $\text{Bi}-\text{MO}-\text{O}$ system and found adsorption bands in the range of vibrations of $\text{R}-\text{C}=\text{O}$ and CH_2 bonds. Acetate-type and acrylate-type compounds were found over copper oxides [54]. These compounds do not appear to be initial forms in the adsorption of propene. Gorokhovatskii and Gerey detected π -olefin and π -allyl complexes on the Cu_2O surface [55].

Davydov et al. [56–58] used IR spectroscopy and the thermodesorption technique to investigate the adsorption of propene on a variety of oxide systems, among which were Cu_2O and Ga_2MoO_4 . They showed that propene interacting with a solid surface forms both complexes which are reversibly bound to the surface (π -allyl and σ -allyl) and destructively oxidized, strongly bound compounds. The former are responsible for the formation of acrolein (the product of partial oxidation), and the latter for the formation of CO_2 and H_2O . In their study of the transformation of surface complexes the authors of Refs. [56–58] found that π -allyl compounds can transform to σ -complexes. They suggested the following general scheme of C_3H_6 oxidation:

The following surface complexes were found in situ over the surface of Sn–Mo–O and Sn–V–O [69]:



The intensity of bands assigned to the first complex over Sn–V–O increases with increasing temperature up to 120°C, and then decreases. The yield of acetone also increases. Thus the conclusion was drawn that the complex (I) is an intermediate. When the reaction proceeds over Sn–Mo–O, some fraction of the acetone is formed via enolate complex (II). Thus the following mechanism was suggested for the reaction:



Closing this listing of papers in which the intermediates of the propene oxidation were studied, we conclude that:

- (1) in most of the stepwise schemes of propene conversion to acrolein, in spite of their variety, a π -allyl complex is present as one of the intermediates;
- (2) according to the isotope exchange and spectral data, π -allyl complexes convert to σ -complexes;
- (3) there is practically no spectral information presently available on the steps of oxygen insertion.

In order to clarify the way in which the surface steps proceed in this reaction it is absolutely necessary to obtain information about the further conversion of π -allyl complexes. Furthermore, information concerning the properties of the π -allyl complex and properties of other intermediate substances is also needed.

3.3. Propene oxidation over a Bi–Mo–Mg–O system

As was mentioned above, the oxidation of propene to acrolein is one of the best studied reactions of selective hydrocarbon oxidation. It is the ideal case for developing a new (spectrokinetic) approach to the investigation of a reaction mechanism. But it should be noted that this reaction is fast and some problems connected with time limitations of spectral techniques (Section 2) could arise. So we decided first to study it over a model Bi–Mo–Mg system.

The results are presented below. The kinetics of surface compound conversion during the oxidation of propene was studied in situ by high-temperature IR spectroscopy using the flow cell-reactor [70,71]. The reaction products were analyzed by gas chromatography. The conversion in the reactor did not exceed 1%, so the operating conditions of the cell-reactor were close to differential. Model $\text{Bi}_2\text{O}_3 \cdot \text{MgO}$ (5 at.-% Bi) and $\text{Bi}_2\text{O}_3 \cdot \text{MoO}_3 \cdot \text{MgO}$ (5 at.-% Bi and 5 at.-% Mo) catalysts with the same surface (150 m²/g) were investigated. According to X-ray data, the γ - Bi_2O_3 phase in the first catalyst is dispersed on MgO. It is known that γ - Bi_2O_3 is a typical catalyst for oxidative dimerization of propene to diallyl, $\text{CH}_2=\text{CH}-\text{CH}_2-\text{CH}_2-\text{CH}=\text{CH}_2$, and it does not allow propene oxidation to proceed to acrolein [45]. In our case, the total oxidation to CO_2 was the main route of the reaction. As was established in our previous study [72], some surface compounds are formed during the oxidation of propene over these catalysts. Among them are: π -allyl complex, with absorption band 1510 cm⁻¹ (antisymmetric stretching vibrations of C=C=C bond); polyene surface compound, with absorption band 1605–1590 cm⁻¹ (stretching vibrations of C=C bond in polyene molecule –C=C–C=C–) (the frequency of the absorption band changes with increasing temperature, possibly because of the lengthening of the polyene chain); surface carbox-

ylate (this has two absorption bands, at 1580 and 1430 cm^{-1} , which correspond, respectively, to anti-symmetric and symmetric stretching vibrations of the COO^- group [73]); and a surface complex with an absorption band at 1340 cm^{-1} . On the basis of spectral and kinetic data, together with some isotope exchange experiments, we assigned this band not to carboxylate, but to a surface complex, which we have arbitrarily called the ‘destruction product’ (DP) of propene.

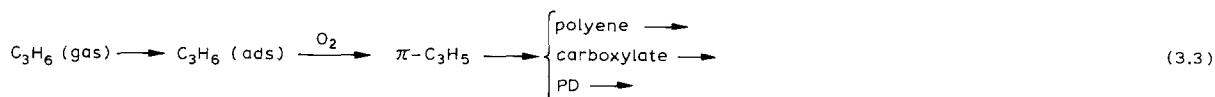
Fig. 8 presents the typical spectrum recorded in a flow cell at 290°C when a reaction mixture of $\text{C}_3\text{H}_6 + \text{O}_2$ was flowing over the 5% Bi–Mo–MgO catalyst. Before the experiment the catalyst pellets (45 mg/cm^2) were treated in flowing oxygen and then in helium at 475°C. The temperature was then decreased to a predetermined level, the reaction mixture was fed in and the IR spectrum was recorded in the range 1100–1800 cm^{-1} at regular time intervals. Thus the optical density of the absorption bands (determined at the band maximum) was obtained versus time. According to Eq. (2.2), these kinetic curves represent the surface compound concentration versus time. A typical kinetic curve of carboxylate formation at 310°C is shown in Fig. 9. The kinetic curves obtained were treated for first or for second order and (from the dependence of the effective rate constants on inverse temperature), and the effective activation energies, E_a , for formation and consumption of surface compounds were determined.

At temperatures in the range 150–300°C, it usually takes only a few minutes to obtain an equilibrium coverage of a surface, whereas the surface reaction achieves its stationary state in 60–200 min. This means that the adsorption and the external and internal diffusion are not limiting steps. The combined coverage in propene and oxygen is 1–5% of a monolayer. An irreversible part is 25–40% of the whole number of molecules adsorbed. The surface coverage under flow conditions is no more than 10–12% of a monolayer. The results of adsorption measurements were identical for both pellet and powder catalysts.

An increase of optical density with temperature points to the possible energy inhomogeneity (ΔE_a) of the sites where the surface compounds are formed. This interval was estimated on the basis of kinetic data and turned out to be 16–20 kJ/mol over the whole interval of measured optical densities. This value does not exceed $4RT$, the criterion of inhomogeneity published by Roginskii [74] (in our case $4RT = 20$ kJ/mol). It is thus possible to use the model of a quasihomogeneous surface as a first approximation for the calculation of the reaction orders and activation energies.

Table 2 lists reaction orders and activation energies for the formation and consumption of surface compounds in propene oxidation. The data were obtained by kinetic measurements.

The data presented allow us to suggest two possible schemes for the destruction of adsorbed propene:



All these surface compounds are assumed to be formed over different surface sites.

Let us consider these schemes. According Eq. (3.3), π -allyl has to be accumulated and consumed as an intermediate. If at t_1 the reaction mixture is replaced by oxygen the concentration of polyene, carboxylate and PD have to increase further, while the π -allyl concentration has to decrease. According Eq. (3.2), in turn, the concentration of all surface compounds has to be practically constant. The kinetic curves of the formation of all four surface compounds are shown in Fig. 10 and the validity of the scheme (3.2) is well demonstrated. We have also checked the scheme (3.2) in a subsequent experiment: the

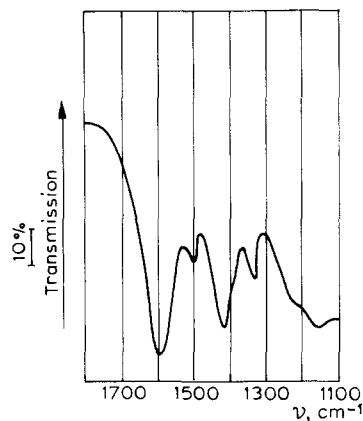


Fig. 8. IR spectrum of surface compounds formed on 5% Bi–Mo–Mg at $T = 290^\circ\text{C}$ in $\text{C}_3\text{H}_6 + \text{O}_2$ flow.

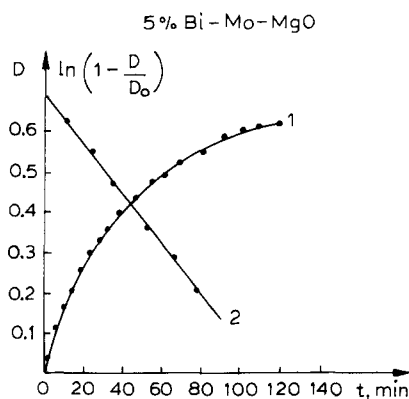


Fig. 9. Typical kinetic curve (1) and its treatment according to first-order equation (2). Curve (1) was obtained for 5% Bi–Mo–Mg at $T = 310^\circ\text{C}$ in $\text{C}_3\text{H}_6 + \text{O}_2$ flow.

Table 2

Reaction orders^a and activation energies^b for formation and consumption of surface compounds in propylene oxidation

Catalyst		Surface complex							
		π -allyl 1510 cm^{-1}		Polyene 1605 cm^{-1}		Carboxylate 1430 cm^{-1}		Product of destructive oxidation 1340 cm^{-1}	
		Form	Cons	Form	Cons	Form	Cons	Form	Cons
5% Bi–Mg	E (kJ/mol)	86	84	25	~	25	84	46	92
	order	1	1			1	1	1	1
5% Bi–Mg–Mo	E (kJ/mol)	25	58	25	79	21	117	33	109
	order	1	1	1	2	1	1	1	1

^a The order of equation which was used to treat kinetic curves.

^b The accuracy of E_a determination is ± 10 kJ/mol.

reaction mixture ($\text{C}_3\text{H}_6 + \text{O}_2$) was replaced by propene (in order to check the possibility of consecutive reaction of π -allyl with propene from the gas phase with polyene formation); in this case, the optical densities of polyene and π -allyl ceased to increase and did not change up to the next feed of the gas

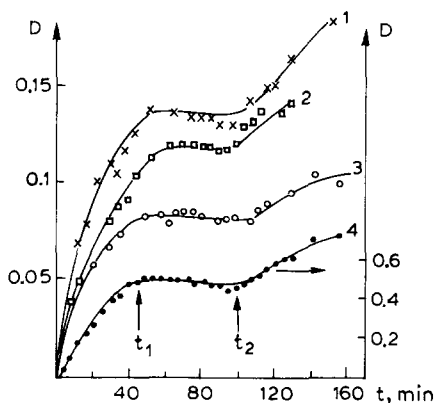
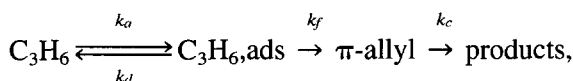


Fig. 10. Optical density of 1430 cm^{-1} (1), 1340 cm^{-1} (2), 1505 cm^{-1} (3), 1605 cm^{-1} (4) absorption bands versus time. $T=260^\circ\text{C}$. At t_1 the propene flow was turned off, at t_2 it was turned on again.

mixture. It is necessary to note that the carboxylate is formed even without oxygen in the reaction mixture. This means that surface oxygen of the oxide catalyst takes part in its formation. This conclusion could also be supported by the analysis of values (reaction orders and activation energies) presented in Table 2. If π -allyl transformation to the reaction products (CO_2 , diallyl) is taken to be a rate-determining step, the reaction will proceed the following way:



where k_a and k_d are the adsorption and desorption constants, and k_f and k_c are the effective constants of π -allyl formation and consumption. In this case the concentrations of π -allyl and adsorbed propene are

$$d\theta_{\text{al}}/dt = k_f\theta_{\text{C}_3\text{H}_6} - k_c\theta_{\text{al}} \quad (3.4)$$

$$d\theta_{\text{C}_3\text{H}_6}/dt = k_a P_{\text{C}_3\text{H}_6} P_{\text{O}_2} (1 - \theta_{\text{C}_3\text{H}_6} - \theta_{\text{al}}) - k_d \theta_{\text{C}_3\text{H}_6} - k_f \theta_{\text{C}_3\text{H}_6}.$$

Under stationary conditions, according to (3.2) and (3.3),

$$\theta_{\text{C}_3\text{H}_5} = \theta_{\text{al}} k_c / k_f \quad (3.5)$$

$$\theta_{\text{C}_3\text{H}_6} = (k_a P_{\text{C}_3\text{H}_6} P_{\text{O}_2} - k_d P_{\text{C}_3\text{H}_6} P_{\text{O}_2} \theta_{\text{al}}) / (k_a P_{\text{C}_3\text{H}_6} P_{\text{O}_2} + k_d + k_f). \quad (3.6)$$

Equating the right-hand sides of (3.5) and (3.6), we get

$$\theta_{\text{al}} = k_f k_a P_{\text{C}_3\text{H}_5} P_{\text{O}_2} / \{k_f k_a P_{\text{C}_3\text{H}_6} P_{\text{O}_2} + k_c (k_a P_{\text{C}_3\text{H}_6} P_{\text{O}_2} + k_d + k_f)\}. \quad (3.7)$$

As was mentioned above, the adsorption is many times more rapid than surface conversion of π -allyl. So, at $k_a P_{\text{C}_3\text{H}_3} P_{\text{O}_2} \gg k_d + k_f$, Eq. (3.7) becomes simplified to:

$$\theta_{\text{al}} = k_f / (k_f + k_c) = 1 / (1 + k_c / k_f). \quad (3.8)$$

Similar formulas can be obtained for other surface compounds: carboxylate (1430 cm^{-1} band) and PD of propene (1340 cm^{-1} band). For carboxylate, the consumption of which is first-order in oxygen, Eq. (3.8) is also valid, because the effective constant of consumption, obtained by spectrokinetic measurements, depends on oxygen pressure, i.e. $k_{\text{eff},c} = k_c \cdot P_{\text{O}_2}$.

One can use the values of effective constants, determined separately for the formation and consumption of surface compounds, coupled with Eq. (3.8) to calculate the stationary concentration of surface compounds in situ.

In our case spectrokinetic measurements allowed us to determine optical density, which is proportional to the surface concentration. So we calculate the surface coverage by the following formula:

$$\theta_{\text{exp}} = D_T^{\text{stat}} / D^{\text{max}},$$

where D^{max} is the maximum possible optical density for a given catalyst and surface compound under study, and D_T^{stat} is the ‘stationary’ optical density of this surface compound at temperature T .

For the band at 1510 cm^{-1} (π -allyl) at 357°C $\theta_{\text{exp}} = 0.46$, whereas $\theta_{\text{calc}} = 0.60$, and for the 1340 cm^{-1} band (‘PD’) $\theta_{\text{exp}} = 0.42$ and $\theta_{\text{calc}} = 0.44$. So it can be seen that in the temperature range of $290\text{--}380^\circ\text{C}$ the agreement between calculated and measured values is rather good. Thus, effective constants of formation and consumption of surface compounds, measured separately (when only one process (formation or consumption) proceeds) could give information about the conversion of surface compounds under stationary conditions (in a catalytic reaction in situ). It has been found in our experiments that the formation of all surface complexes is zero order in propene and oxygen. This shows once again that the adsorption of propene and oxygen is more rapid than surface reaction. Their concentrations on the surface are sufficiently high and practically constant (even when the concentration of C_3H_6 and O_2 in the flow changes from 10 to 100%). The consumption of π -allyl and ‘PD’ of propene is also zero order, while carboxylate and polyene are involved in a first-order reaction (the results are rather approximate), indicating a different mechanism of interaction with oxygen.

It was mentioned above that carboxylate can be formed with no oxygen in the gas mixture (oxygen is taken from the catalyst’s lattice), whereas for its consumption the presence of oxygen in the gas mixture is absolutely necessary. It was shown in Ref. [75] that the destruction of carboxylate structures with the formation of CO_2 in the presence of oxygen proceeds at temperatures $150\text{--}200^\circ\text{C}$ lower than in the absence of oxygen. According to these data, the complete oxidation of carboxylate and polyene is possible with participation of oxygen from the gas phase.

We now consider possible mechanisms by which surface complexes may be transformed on the basis of data presented in Table 2. Every surface compound has its own conversion route to the products of partial or complete oxidation, although generally the possibility of consecutive transformations cannot be ruled out. For example, in addition to conversion to acrolein, π -allyl can also be transformed to CO_2 via carboxylate or ‘PD’. Polyene conversion to CO_2 can be direct or can proceed via carboxylate. We can exclude some routes on the basis of kinetic data. Let us consider, for example, the following scheme (for a 5% Bi–Mo–MgO catalyst):



Comparison of the activation energies of polyene (79 kJ/mol) and carboxylate (117 kJ/mol) consumption shows that the limiting step of this reaction is the consumption of carboxylate ($k_2 \ll k_1$), and therefore, the reaction order observed is determined by this step only, and has to be about 1. However, it equals 2, which contradicts scheme (3.9).

Other possible mechanisms are:



Both these routes are possible over 5% Bi–MgO and 5% Bi–Mo–MgO catalysts, because of the coincidence (for 5% Bi–MgO) and rather close agreement (for 5% Bi–Mo–MgO) of E_a values and consumption orders of these surface compounds.

The coincidence of the reaction orders and agreement of E_a observed for π -allyl and polyene consumption over the $\text{Bi}_2\text{O}_3 \cdot \text{MoO}_3 \cdot \text{MgO}$ catalyst does not rule out the following route:



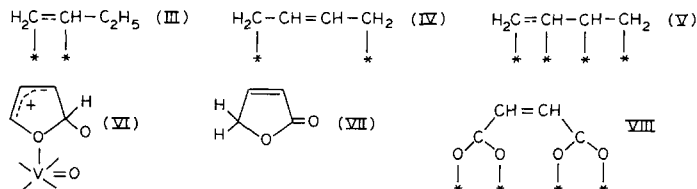
The kinetic curves for polyene formation over the $\text{Bi}_2\text{O}_3 \cdot \text{MgO}$ catalyst are rather intricate. Unfortunately, our experimental technique does not allow us to investigate the initial parts of these curves. Data presented in Table 2 show that at an addition of Mo ions to the $\text{Bi}_2\text{O}_3 \cdot \text{MgO}$ system causes the observed activation energy of π -allyl formation to decrease sharply (from 96 to 25 kJ/mol). Catalytic measurements in the pulse reactor over a 400–500°C temperature range (with the same gas mixture as in the spectrokinetic measurements) showed that nearly equal quantities of diallyl were formed over both catalysts, whereas the propene conversion was about 1.5 times higher on the $\text{Bi}_2\text{O}_3 \cdot \text{MoO}_3 \cdot \text{MgO}$ catalyst. The increase of conversion may be explained if one hypothesizes the formation of partial propene oxidation products (acrolein in particular, among others) which burn up completely over this catalyst. Our experiments showed that acrolein, acetaldehyde, acetic and acrylic acids really do burn completely over this catalyst.

The E_a values for the consumption of carboxylate and 'PD' over the 5% Bi–Mo–MgO catalyst are greater than those for the $\text{Bi}_2\text{O}_3 \cdot \text{MgO}$ catalyst, which means that the rates of formation of propene oxidation products (both total and partial) are decreased. The increase of propene conversion observed in this case is attributable to a greater contribution of propene conversion to acrolein via π -allyl. E_a for π -allyl consumption in this case is less than for the $\text{Bi}_2\text{O}_3 \cdot \text{MgO}$ catalyst (58 kJ/mol) (see Table 2).

It is known [76,77] that the activation energies of formation of acrolein, CO_2 , acetaldehyde, formaldehyde and CO are, respectively, 65–84, 70–92, 113, 105 and 113 kJ/mol. We see from Table 2 that these values are rather close to the values of activation energies of π -allyl, carboxylate and 'PD' consumption. Thus we can conclude that the observed surface complexes are formed from adsorbed propene by parallel routes. The improvement of catalyst properties by addition of Mo is accompanied by an essential decrease of the activation energy of surface π -allyl complex consumption.

3.4. Partial butene oxidation to acrolein over complex oxides

Partial oxidation of higher olefins has not been so well studied as the oxidation of ethene and propene. Butadiene, furan and maleic anhydride are formed from the partial oxidation of 1-butene. The oxidation of 1-butene over $\text{V}_2\text{O}_5\text{--P}_2\text{O}_5/\text{Al}_2\text{O}_3$ at 100–150°C (i.e., below the temperature of stationary catalysis) gives adsorbed 1- C_4H_8 (two forms of p -complexes), butadiene, furan, maleic anhydride, 2,5-n-furanone, according to the IR spectra. Butadiene forms two different complexes: π -complexes (III) are formed during the interaction of --C=C-- bonds, and 1–4 addition goes through the σ -bond (complex (IV)). Furan adsorbs through the second position of the ring (complex (VI)), 2,5-n-furanone forms the complex (VII) by splitting off the allyl hydrogen. Maleic anhydride forms the strong complex (VIII), but the physisorbed maleic anhydride is also observed. Among all observed complexes:



only complex (VII) (of 2,5-n-furanone) is able to react under catalysis conditions [78].

In oxidative dehydrogenation of butenes over ferrites MgFe_2O_4 , CoFe_2O_4 , CuFe_2O_4 π -allyl and adsorbed butadiene are observed in the IR spectra [79]. The rupture of a C–H bond with subsequent formation of π -allyl is possibly the limiting step. Formates, carboxylates and carbonates, which are found as adsorbates, are precursors of complete oxidation [79]. The π -allyl complex is also thought to be an intermediate in the oxidative dehydrogenation of 1-butene over Bi–Mo–V catalysts [80].

The product of partial oxidation of isobutene is methacrolein. The most selective catalysts for this process are multicomponent Bi–Mo–Fe–Co-oxide catalysts, which have been studied in detail at the Institute of Chemical Physics in Moscow [81].

In Ref. [82] the conversion of the surface compounds formed in selective oxidation of propene and isobutene over industrial oxide catalysts $[\text{Co}(\text{Mg})_6\text{Mo}_{12}\text{Bi}_{0.5}\text{Fe}_{0.75}\text{O}_x]$ was studied by FTIR spectroscopy. The surface area of the samples was $6 \text{ m}^2/\text{g}$. Spectral measurements were carried on by the UR-20W and FTS-15 devices with the use of the gradientless IR reactor cell (see Figs. 1 and 2). Under optimum conditions ($T = 340\text{--}350^\circ\text{C}$, $t = 1 \text{ s}$) the yields of acrolein (from propene) and methacrolein (from isobutene) were 70% (selectivity 90%) and 55% (selectivity 70%), respectively.

IR spectra recorded by the UR-20W in situ in the catalytic oxidation of isobutene exhibit broad absorption bands with maxima at 1610 , 1790 and 1850 cm^{-1} (Fig. 11). The maxima positions and the intensities of these bands at constant temperature were practically unchanged when the concentrations of isobutene (2–10%) and oxygen (5–30%) were changed.

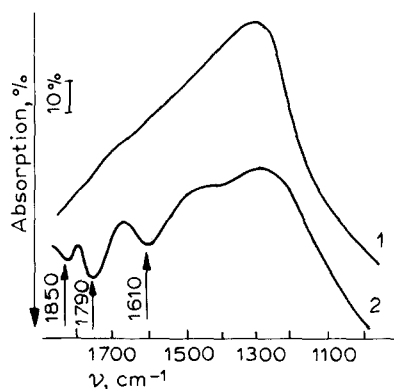


Fig. 11. IR spectrum of surface compounds on Co–Mo–Bi–Fe–O during propene oxidation in situ (2) (1 — background).

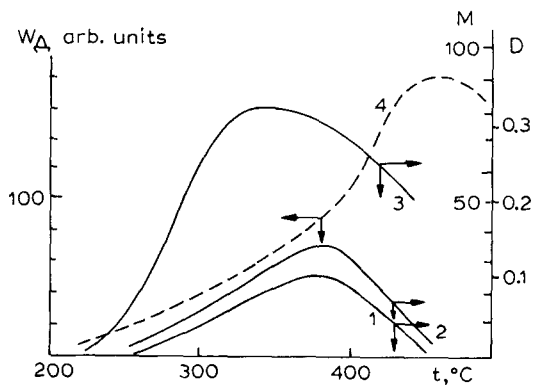


Fig. 12. Optical density (D) of 1610 cm^{-1} (1) and of 1790 cm^{-1} (2) absorption bands, as well as acrolein yield (3) and CO_2 desorption rate (4) versus temperature.

The temperature dependence of optical densities of the 1610 and 1790 cm^{-1} bands (the exposure at each temperature and constant composition of the reaction mixture was 30 min) is shown in Fig. 12. It can be seen that these two bands are in the same temperature range and the relationship between their intensities is constant. Thus they seem to be due to the same surface compound (intermediate I-1).

Treatment of the catalyst surface with the mixture of air with aldehydes, acids or aromatic hydrocarbons (reaction products) caused no pronounced absorption bands to appear in the range 100–500°C. Therefore, intermediate I-1 is not formed by reaction products. As can be seen from Fig. 12, I-1 is formed in parallel with the selective oxidation products.

Additional experiments were performed in order to discover how I-1 is formed. Flowing isobutene was used for adsorption at 120°C. After adsorption the sample was heated in flowing air up to 500°C. IR spectra were recorded every 25°C, and the exposure at every given temperature was no less than 10 min. At 260°C, bands at 1610, 1790 cm^{-1} and a weak band at 1850 cm^{-1} appeared. The temperature of appearance and the intensity of the bands are practically the same for experiments in flowing air and in the reaction mixture. At temperatures higher than 380–420°C, the optical density of bands drops markedly; in this case only CO_2 , H_2O and some traces of low-molecular-weight organic acids are yielded to the gas phase.

As was reported in Ref. [83], the 1610 cm^{-1} absorption band can be assigned to the vibration of conjugated double bonds $-\text{C}=\text{C}=\text{C}=\text{C}-$, and the 1790 and 1850 cm^{-1} bands to $\text{C}=\text{O}$ vibrations in cyclic anhydrides of organic acids. Therefore, the compounds observed represent cyclic di- or polyenes, containing carbonyl groups similar to the anhydride- and salt-types.

The absence of absorption bands of isobutene adsorbed at low temperature could be reasonably explained by the low values of extinction coefficients of bonds in its molecules: they are much less than these of double and conjugated bonds. These bands appear as a result of the interaction of adsorbed isobutene with oxygen of the catalyst.

As was stated previously, [84], the concentration of isobutene adsorbed irreversibly over this catalyst at 350°C is $4 \cdot 10^{-10}$ mol/ cm^2 . The fact that both absorption bands in the IR spectra belong to the same compound enables to find an independent evaluation of the extinction coefficients for $\text{C}=\text{O}$ and $-\text{C}=\text{C}-$ bonds in adsorbed molecules. The extinction coefficients were calculated from the following formula: $\epsilon = Dc^{-1}l^{-1}$. In our experiments: $D_{1790} = 0.11$, $D_{1610} = 0.085$, $c = 4 \cdot 10^{-10}$ mol/ cm^2 , the conventional thickness of the sample, $l = P \cdot S_{\text{exp}} = 9 \cdot 10^{-2}$ (P (g/ cm^2), is the thickness of the pellet, and S_{sp} (cm^2/g), is the surface area of the sample). Thus, $\epsilon_{1790} = 3 \cdot 10^5$ cm^2/mol or 300 l/mol·cm, and $\epsilon_{1610} = 100$ l/mol·cm. The value of the extinction coefficient obtained for the $\text{C}=\text{O}$ band (ϵ_{1790}) coincides with published data for carbonyl-containing molecules, while for conjugated bonds (ϵ_{1610}) it is at least twice that for conjugate dienes [83].

The rate of conversion of I-1 to products of total oxidation at 350°C (according to the IR spectroscopy and desorption data) does not exceed $1 \cdot 10^{15}$ molecules/s/ m^2 , which is three orders of magnitude lower than the rate of stationary isobutene oxidation to methacrolein under the same conditions. Thus, strong complexes like I-1 are practically unreactable at the temperature of selective oxidation.

A catalyst in which Co ions were replaced by Mg ions, with the formation of isostructural molybdate [85], was studied in a similar way. After this replacement, catalytic activity and selectivity does not change, with an accuracy of 5%; the irreversible adsorption of olefins at reaction temperature is not detectable and IR spectra in situ exhibit only low intensity absorption bands.

Fig. 13 presents the spectra of surface compounds obtained after treatment of the Mg–Mo–Bi–FeO catalyst with a reaction mixture (isobutene:air = 8:92) at 340°C. These spectra did not practically change if the reaction flow was replaced by the flowing helium at 300°C. Only an additional absorption band appears due to gaseous reaction products.

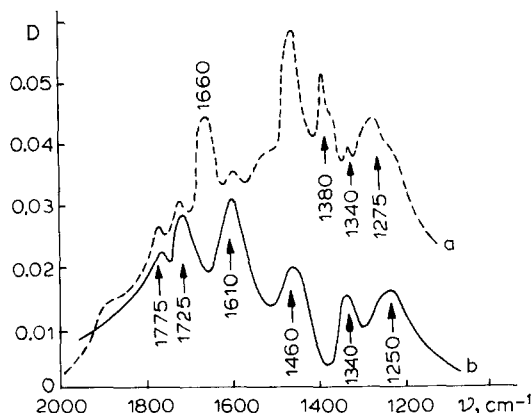
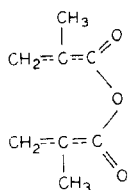


Fig. 13. IR spectra of surface compounds on Mg–Mo–Bi–Fe after treatment with the reaction mixture (see text): a, cooling in the reaction mixture; b, cooling in He flow. Spectra were recorded by FTS-15; number of scans = 800; resolution = 4 cm^{-1} .

The absorption bands at 1775 , 1725 , 1610 , 1460 , 1350 , 1250 cm^{-1} in both spectra can be assigned to $\nu_{\text{C=O}}$, $\nu_{\text{C}\equiv\text{C}\equiv\text{C}}$, δ_{CH} in CH_3 , δ_{CH} in CH_2 , $\nu_{\text{C-O}}$ vibrations in the complex of a methacrylic anhydride type.



(I. 2)

The 1610 cm^{-1} absorption band (not observed in the intrinsic spectrum of methacrylic anhydride) pointed to additional conjugated double bonds, possibly due to interaction with the catalytic surface.

Although the spectra presented in Fig. 13b and Fig. 11 show a similar general character, they also exhibit a number of noticeable distinctions: $\nu_{\text{C=O}}$ of anhydride-like compounds are shifted by 50 cm^{-1} to the short-wave range (this is due to carbonyl bonds of a linear anhydride), and their band intensity is markedly less that of the 1610 cm^{-1} band.

Additional bands at 1680 , 1450 , 1380 and 1275 cm^{-1} , appearing after cooling the sample in the reaction mixture, can be assigned to the weakly bound ethene. According to adsorption measurements, this covers about 10–12% of the surface [84]. The ratio of optical densities of the bands at 1680 cm^{-1} (weakly bound isobutene) and 1775 cm^{-1} (carbonyl-containing surface complex I-2) is 1.5 (Fig. 13a). The ratio of the extinction coefficient for C–C vibrations in isobutene [83] to that of the carbonyl group (see above) is 1:10. Simple calculations show that surface compound I-2 covers less than 1% of the surface.

The rate of isobutene conversion to methacrolein over this catalyst at 350°C is 10^{18} molecules/s/m². According spectral measurements taking after replacing the reaction mixture by oxygen, the absorption bands of complex I-2 disappeared in a time less than one scan (about 1 s). So we can evaluate the conversion rate of complex I-2 and compare it with the methacrolein formation rate. Actually, as was mentioned above, there are 10^{17} complexes /m² on the surface. The characteristic time of their conversion is about 0.1 s. If methacrolein is formed via this complex, its formation rate has to be about 10^{18} complexes/s/m². This value agrees well with that obtained by catalytic measurements.

Thus, surface complex I-2 may be stated to be an active compound in the selective oxidation of isobutene. Its structure, according to the IR spectroscopy data, is just that proposed previously [84]. To prove with certainty that this complex is an intermediate, one needs spectrokinetic measurements.

It is possible that a similar complex is formed over a Co–Mo catalyst. However, it could not be observed because of the simultaneous presence of a great amount of inactive complexes having similar structure.

It should be noted that there are no absorption bands which could be assigned to a methallyl complex in the spectra (Fig. 13a,b). Probably, the steady-state concentration of such complexes over active multicomponent catalysts is quite small. A hydrogen atom, abstracted from the olefin molecule on chemisorption, goes quickly to the desorbing molecule of unsaturated aldehyde. This mechanism can explain the observed kinetic isotope effect in the replacement of hydrogen by deuterium in the olefin [47].

3.5. Conclusions

The majority of the data presented above shows that in the field of partial olefin oxidation there are no investigations which satisfy the strict requirements of spectrokinetics (see Section 2). The best ones in this respect are possibly our own works [70–72,82], but they also give only estimates of surface compound conversion rates. In some cases these values have been compared with the reaction rates.

Nevertheless, we can see that the spectrokinetic method is an efficient one for studying surface processes in a catalytic reaction *in situ*. It can be used to obtain kinetic parameters of the rates of formation and consumption of surface complexes, as well as their surface coverage. These data allow the calculation of the reaction rate (suggesting that the compound observed is an intermediate) and its comparison with the experimentally determined rates. This comparison is fundamental for the determination of the role of observed surface compound.

If there are several complexes at the surface, spectrokinetic measurements could give an answer to the question of whether the reaction product is a result of stepwise conversion of these complexes or whether there are several parallel surface reactions. The maximum amount of such information can be obtained by means of nonsteady-state spectrokinetic experiments. In other words, the spectrokinetic method is an experimental basis for the investigation of processes on the catalytic surfaces.

A summary of data on intermediates in partial olefin oxidation is presented in Table 3. Here and below, the letters ‘H’, ‘M’ and ‘L’ are used to characterize the degree of reliability of the data.

— ‘H’ is the highest degree of reliability. These are investigations where the formation rate of surface compounds obtained by spectral data *in situ* was compared with the catalytic reaction rate.

— ‘M’ is a medium degree. These are works where intermediate compounds were studied under catalytic conditions *in situ*, but kinetic measurements were either not performed or were scarce.

— ‘L’ is a low degree of reliability. Here the reaction mechanism is suggested on the base of spectral data obtained before or after the reaction.

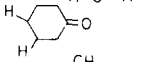
It can be seen from Table 3 that all the works on intermediates in partial olefin oxidation are graded ‘L’ or ‘M’.

4. Interaction of nitric and carbon oxides over metal surfaces

4.1. Introduction

The heterogeneous catalytic reactions of total oxidation of CO and hydrocarbons in the presence of oxygen and nitric oxide underlie many currently developed processes connected with the cleaning of exhaust gases from industry, power stations and car engines.

Table 3
Intermediates in reactions of partial olefin oxidation

Reaction, catalyst	Intermediates	Degree of reliability	Ref.
$C_2H_4 + O_2$ on Ag/ Al_2O_3	CH_3CHO ads	L	[39]
$C_2H_4 + O_2$ on Ag	C_2H_4 ads	L	[40]
$C_2H_4 + O_2$ on MoO_3/TiO_2	$Ag-O-\overset{\overset{O}{\parallel}}{Ag^{6+}}-O-Ag$	M	[42,44]
$C_2H_4 + O_2$ on MoO_3/TiO_2	$H_2C=CH_2$, CH_3CHO ads, $CH_2=CHO-M$	M	[51]
$C_3H_6 + O_2$ on Ag/ SiO_2	CH_2CHCHO ads	M	[65]
$C_3H_6 + O_2$ on $Bi_2O_3-MoO_3$, Cu_2O , $Ga_2(MoO_4)_3$	$CH_2=CHCH_3$, $CH_2-\overset{\overset{CH}{\parallel}}{M}-CH_2$	L	[52,54]
$C_3H_6 + O_2$ on Bi-Mg-O, Bi-Mo-Mg-O	$\pi-C_3H_5$, $RCOO^-$, $[C_3H_6]_n$ ads M	M	[70–72]
$C_3H_6 + O_2$ on Ti(Fe)-Sb-O	$CH_2=CH-CH_3 \cdots O^{2-}$	L	[62,63]
$C_3H_6 + O_2$ on Sn-Mo-O	$CH_3-\overset{\overset{O}{\parallel}}{CH}-CH_3$	L	[66–68]
$C_3H_6 + O_2$ on Sn-V-O	$CH_3-\overset{\overset{O}{\parallel}}{CH}-CH_2$	M	[69]
i-Butene + O_2 on $V_2O_5-P_2O_5/Al_2O_3$		L	[78]
Oxidative dehydrogenation of butene on $Mg(Co,Cu)Fe_2O_4$	$H_2C-\overset{\overset{CH}{\parallel}}{M}-CH-CH_3$, C_4H_6 ads	L	[79]
The same on Bi-Mo-V-O	$H_2C-\overset{\overset{CH}{\parallel}}{M}-CH-CH_3$	L	[80]
i- $C_4H_8 + O_2$ on Mg-Mo-Bi-Fe-O	$CH_2=\overset{\overset{CH_3}{\parallel}}{C}=\overset{\overset{O}{\parallel}}{C}-O-\overset{\overset{O}{\parallel}}{C}-CH_2$	M	[82]

One of the most important lines of ecological investigation is the three-way cleaning of exhaust gases (i.e., the simultaneous neutralization on the catalyst of all three toxic components: CO , C_nH_m and NO). Two of these three basic reactions ($CO + O_2$ and $C_nH_m + O_2$) are oxidative and proceed more readily in gas mixtures enriched with oxygen (so called lean mixtures). The third reaction (NO reduction) proceeds more easily in gas mixtures enriched with organic fuel (rich mixtures). The extent of conversion of NO to N_2 decreases in the lean mixtures, whereas that of CO and C_nH_m to CO_2 decreases in rich ones. Only within narrow limits of concentration near stoichiometry there is a 'window' where it is possible to carry out both the oxidation of CO and hydrocarbons and the reduction of nitric oxides.

The best catalysts for NO and CO interaction are platinum group metals. It is known [86–88] that the activity of metals in the reduction of NO by CO decreases in the following sequence:

$Ru > Rh > Pd > Pt$.

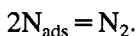
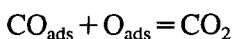
The best catalyst for the process is rhodium [89,90]. Its activity is higher than that of Pt and Pd at low temperatures and in the presence of oxygen in the reaction mixture. However, Rh , as well as Ir , is rather expensive and not readily available, which is why only a small amount of Rh (about 0.002%) is usually added to Pt and Pd catalysts to carry out the three-way cleaning of exhaust gases [89]. Pt and Pd in this

case improve the activity of three-component catalysts in the oxidation of CO and hydrocarbons.

Despite a great number of investigations of the activity of Pt-group metals in the reactions in automotive catalytic converters, the mechanism and kinetics of CO and NO interaction over these catalysts have not been sufficiently well studied, because of the rather complex nature of the changes of kinetic relationships with varying reaction mixture composition and temperature. The products of CO and NO interaction on noble metals are CO₂, N₂ and N₂O. It has been shown that N₂ and N₂O are formed via parallel reactions. The selectivity depends on the catalyst, reaction mixture and temperature.

A variety of methods are in widespread use to elucidate the mechanism of NO and CO interaction over metals; investigations of particular metal planes are performed.

Over Rh(100) this reaction was studied by TPD, LEED and AES spectroscopy [92]. The following mechanism was suggested: dissociative adsorption of NO resulting in N_{ads} and O_{ads} and stepwise inter-actions:



Somorjai et al. [93] have studied the interaction of CO and NO over Rh(331). By recording in situ the 520 cm⁻¹ absorption band, which is due to adsorbed oxygen, they proved that oxygen atoms formed by NO dissociation immediately leave the surface to interact with adsorbed CO. It has also been shown that this oxygen is less active in the interaction with adsorbed CO than oxygen resulting from dissociative adsorption of oxygen.

Different Pt planes were shown [94–96] to have different activity in the CO + NO reaction, this activity correlating with ability to dissociate NO (Pt(111) < Pt(100) < Pt(410)).

The reaction over Pt foil was studied [97] by absorption–reflection IR spectroscopy. Below 150°C the surface is covered by CO and the activation energy for desorption is 14.2 kJ/mol. Above 150°C desorption is dissociative, with an activation energy of 36 kJ/mol. The following dissociative mechanism was suggested for the reaction:

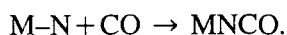
- (1) $\text{CO} + \text{Z} \rightleftharpoons \text{CO-Z}$
- (2) $\text{NO} + \text{Z} \rightleftharpoons \text{NO-Z}$
- (3) $\text{NO-Z} + \text{Z} \rightarrow \text{N-Z} + \text{O-Z}$ (the rate-determining step)
- (4) $\text{CO-Z} + \text{NO-Z} \rightarrow \text{N-Z} + \text{Z} + \text{CO}_2$
- (5) $2\text{N-Z} \rightarrow \text{N}_2 + 2\text{Z}$
- (6) $\text{CO-Z} + \text{O-Z} \rightarrow \text{CO}_2 + 2\text{Z}.$

The rate of CO removal (according to the IR spectra) correlates well with the kinetics of step (4). Conrad et al. [98] use photoelectron spectroscopy (PES) to study the substitution of molecular NO adsorbed on Pd(110) and polycrystalline Pd by molecular CO from the gas phase. Such a mechanism of substitutive adsorption of NO and CO was also found for Ru(001) [99]. Rh(331) [100], however — as opposed to Pt, Pd and Ru — can adsorb NO even if its surface is covered by CO molecules. In addition, CO desorbs from a Rh surface at lower temperatures than from other metal surfaces [101]. This difference in adsorption properties is probably the reason for the high activity of Rh in the CO and NO reaction.

The presence of CO has no effect on the rate of CO and NO interaction over Rh catalysts. On Pt, Pd and Ir, however, strongly bound CO molecules can suppress the sites which are active in the NO dissociation and, as a result, the reaction rate decreases in the presence of CO. According to Ref. [102], the reason for the lower activity of Pt compared with Rh lies in the difference of NO and CO coverages.

Most spectral investigations of the NO + CO reaction were performed using supported Pt-group metals [101–140]. All of them showed the presence of the isocyanate (NCO) complex together with adsorbed NO and CO molecules on the surface.

The NCO complex has attracted considerable interest, because it is a result of the interaction of reactants on the surface. The mechanism of its formation, place of localization and role in the reaction have been widely discussed in the last few years. This complex was first found by IR spectroscopy by Unland et al. [101,103] and London and Bell [104]. Unland [103] has studied the interaction of CO and NO at 400°C over Pt, Pd, Rh, Ir, and Ru supported on alumina oxide. For all metals except Ru, an intense and very stable absorption band was found at 2260–2270 cm⁻¹. This was assigned to the isocyanate complex bound to the metal atom. Solymosi et al. [105] showed that a mixture of CO and NO has a greater rate of adsorption than the rates of separate adsorption of these gases. According to the authors, preadsorption of NO accelerates CO adsorption by generating the isocyanate complex ($\nu_{\text{NCO}} = 2267 \text{ cm}^{-1}$):



The coverage of the surface by isocyanate complex depends on the temperature, reaction mixture composition and state of the surface. Over an oxidized surface the intensity of the NCO absorption band is low [106].

The influence of the support on the formation and stability of the isocyanate complex on platinum has been reported in Ref. [106]. The supports studied were SiO₂, MgO, Al₂O₃ and TiO₂. Under similar experimental conditions the following NCO absorption bands were recorded: Pt/TiO₂ 2210 cm⁻¹, Pt/MgO 2241 cm⁻¹, Pt/Al₂O₃ 2272 cm⁻¹ and Pt/SiO₂ 2318 cm⁻¹. The most stable isocyanate complex is that on Pt/SiO₂. The assignment of bands in this frequency region to the isocyanate complex was based on at least three facts:

- (1) they appear only after coadsorption of CO and NO;
- (2) the shift of band on the adsorption of isotope molecules is consistent with that calculated for NCO;
- (3) NCO complex could also be formed after adsorption and dissociation of HNCO on the surface, and its vibration frequency is in good agreement with the above values.

Summing up these results [108–111], we can assign the 2265 cm⁻¹ absorption band observed upon NO and CO interaction over Al₂O₃ supported metals to the vibrations of an Al–NCO complex.

The absorption bands in the region of 2180–2200 cm⁻¹ found after the CO + NO reaction on SiO₂ supported Ru and Ni were assigned to the vibrations of Ru–NCO and Ni–NCO complexes [112,113]. No bands were recorded near 2300 cm⁻¹.

Lorimer and Bell [91] recorded IR spectra of the CO + NO reaction in situ at 300°C over Pt/SiO₂. Two absorption bands were observed: one, stable, at 2300 cm⁻¹ and another, weak, at about 2190 cm⁻¹. They were assigned to the vibrations of the SiNCO and SiCN complexes, respectively.

Over Rh/Al₂O₃ [114] in the CO + NO reaction a weak band at 2270 cm⁻¹, and a very weak band at 2195 cm⁻¹ were observed. These were assigned to the vibrations in Al–NCO and Rh–NCO, respectively.

To refine the assignment of observed bands, a spectral investigation of NCO formation over unsupported metals was carried out [115]. The samples were prepared by precipitation of metal salts from solution over an NaCl disk. The catalyst was then reduced and treated in the reactor cell. Under similar experimental conditions the following absorption bands were observed: Pt 2180 cm⁻¹, Ir, Ru, Rh 2176–2183 cm⁻¹. Using isotope CO and NO molecules, as well as HNCO adsorption, the authors showed that these bands could be assigned to M–NCO vibrations.

Upon HNCO adsorption over monocrystalline Pt [116], a 2160 cm⁻¹ band was observed. The complex to which this band is related is very unstable and decomposes even at 0°C, giving a nitrogen-containing surface fragment and CO.

Hecker and Bell [117,118] studied the formation of NCO over Rh/SiO₂ using IR spectroscopy in situ. The band observed at 2300 cm⁻¹ was assigned to the vibrations in the Si–NCO complex. Based on a comparison with the spectra of the isocyanate complex over transition metals, the authors assigned the band observed at 2190–2170 cm⁻¹ to the vibrations in the Rh–NCO complex.

A good consensus thus exists among scientists on the assignment of 2265 cm⁻¹ and 2300 cm⁻¹ bands to the vibrations of Al–NCO and Si–NCO, respectively. However, the assignment of bands in the 2170–2200 cm⁻¹ range is not so simple. Most of the investigators believe that these bands are due to an isocyanate complex associated with a metal atom. In this case, from the data presented, it follows that the vibration frequency of isocyanate complex on the support depends strongly on the nature of the support (2210–2300 cm⁻¹) [119] and only weakly on the nature of the metal (2170–2200 cm⁻¹) [115]. Moreover, NCO associated with oxides (these investigations will be discussed below) also has frequencies within these narrow limits. In other words, the vibration frequency of isocyanate complex depends weakly on the nature of the metal and its valence state. More problems arose when it was reported that cyanides adsorbed on Pt and Pd surfaces have absorption bands in the range of 1980–2200 cm⁻¹ [120,121]. Moreover, it was shown via isotope exchange experiments [122] that there could be two different isocyanate complexes on Pt-group metal surfaces: Rh–NCO (2172 cm⁻¹) and Rh–OCN (2225 cm⁻¹).

The fact that isocyanate complexes can be localized both on the support and on the metal, but cannot be formed on the support alone, suggests either spillover of NCO complex or migration of N atom to the support with stepwise interaction with CO molecules from the gas phase. Spillover of NCO on Pt/SiO₂ has been investigated by IR spectroscopy, as reported in Ref. [123]. NCO was formed by HNCO adsorption. For comparison, the HNCO adsorption on the support alone was also studied. It was found that dissociative adsorption of HNCO on Pt results in a strong Pt–NCO band (2180 cm⁻¹) even at –80°C. As the temperature increases, a new Si–NCO band arises (at 2310 cm⁻¹), pointing to the migration of NCO from Pt to SiO₂. Preadsorbed oxygen was shown to stabilize NCO on Pt, accelerating the migration of NCO. With increasing temperature the intensity of the Rh–NCO adsorption band remains practically unchanged, while the intensity of Si–NCO band increases further.

The Si–NCO complex was shown to be very stable. Treatment of the catalyst with various gases (100% H₂, 2% NO, 3% O₂, 3% H₂O) at 330°C did not cause the disappearance of the Si–NCO band. Only during treatment in air at 25°C does it slowly disappear.

The Rh–NCO absorption band is very unstable and disappears quickly from spectra, even when one of the reagent flows is turned off.

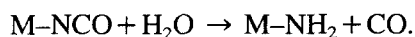
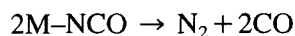
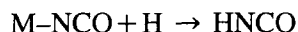
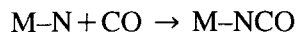
It was shown that the migration rate of NCO from Pt to the support and its further stability (on the support) depends strongly on the support [114,119,124,125]. NCO complex on the support was not destructed when the reaction mixture flow was turned off and the sample was cooled. Only an increase in temperature and the addition of water vapour causes its destruction [114,125]. Rh–NCO complex, observed on Rh foil and Rh monocrystalline surfaces, is very unstable: it is destroyed forming adsorbed N atoms and CO upon heating to only –120°C.

The data concerned the stability of isocyanate complex on Rh surface have also been presented by Rasco et al. [127]. Preadsorbed oxygen causes the increase of both the stability of Rh–NCO complex and the intensity of its absorption band. If the quantity of preadsorbed oxygen increases, the intensity of the Rh–NCO absorption band decreases, whereas its stability increases further, and the position of the Rh–NCO band shifts on 10 cm⁻¹ towards high frequencies. These things are due to the more ionic character of the Rh–NCO bond in the presence of oxygen on the surface.

Preadsorbed CO has no effect on the stability of NCO, but causes decrease in its absorption band intensity.

The role of isocyanate complex in the reduction of NO by CO is the subject of considerable debate. We have already mentioned that Unland [103] assigned the $2260\text{--}2270\text{ cm}^{-1}$ band on Al_2O_3 -supported Pt, Pd, Ir, Ru and Rh to the Al–NCO vibrations. The absence of this band in the case of Ru/ Al_2O_3 correlates well with the lower activity of Ru (in comparison with other metals listed above) in the reaction of ammonia formation. This correlation allows one to consider the observed isocyanate complex as an intermediate in ammonia formation during the catalytic cleaning of exhaust automotive gases.

Voorhoeve et al. [128–130] studied the reduction of NO by CO and hydrogen. The data obtained are explained on the basis of the hypothesis that isocyanate complex is an intermediate in the reaction. It possibly takes part in the following reaction steps:



Chang and Hegedus [131] studied the reaction of NO + CO on a Pt/ Al_2O_3 surface. The 2250 cm^{-1} band of the isocyanate complex was observed in IR spectra recorded in situ. Fig. 14 shows the intensity of this band as well as NO conversion and the 2170 cm^{-1} band intensity versus CO concentration. There is no correlation between the intensity of NCO complex absorption band and NO conversion. Thus, the authors concluded that NCO complex takes no part in the reaction. The intensity of the 2110 cm^{-1} band (CO over oxidized Pt) changes inversely to the NO conversion. On the basis of this fact the authors concluded that CO adsorbed on the reduced Pt inhibited the reaction.

Some authors [132–134] have suggested that the presence of stable isocyanate groups on the surface causes deactivation of the catalyst by blockage of active sites at the surface or by changing the electronic state of the metal due to the accumulation of NCO on the surface [135]. If this were so, the activity of the catalyst should be restored after removal of NCO from the surface. Both points of view came under criticism in Ref. [127], where it was shown that NCO is localized on the support and, therefore, cannot block the active catalyst sites; besides, its removal from the surface did not cause any restoration of the catalyst's activity.

The surface of the binary catalyst Pt–Rh/ SiO_2 was found to possess several forms of adsorbed CO, $\text{Pt}_{\text{Rh}}\text{>C=O}$ (1875 cm^{-1}) among others. NCO groups were recorded only on Rh [136].

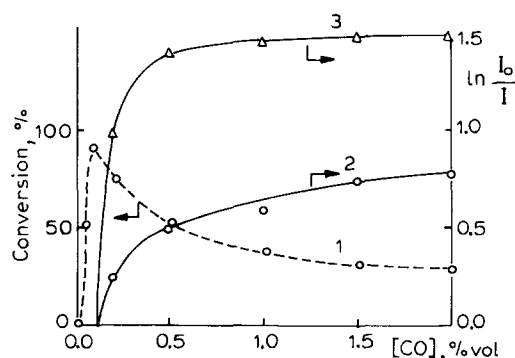


Fig. 14. Intensity of 2170 cm^{-1} (2) and 2250 cm^{-1} (3) absorption bands as well as NO conversion versus CO concentration (1) [134].

The reaction of $\text{NO} + \text{CO}$ on $\text{Pt-WO}_3/\text{SiO}_2$ was investigated in situ at 280°C by Regalbuto and Wolf [137]. The rate-limiting step was found to be NO dissociation. Pt-CO groups were changed quickly into Pt-NO groups which then dominated in the spectra. CO bands on Pt and WO_3 , as well as NCO , NO_3^- and NO_2^- bands were observed only in situ, being accumulated during poisoning by CO. So, the authors believe [137], these bands are not due to intermediates but rather to reaction side products. The active catalyst sites are suggested to be localized on the boundary of Pt and WO_3 .

Alikina et al. [138] found no Rh-NCO complex on $\text{Rh/Al}_2\text{O}_3$ but only $\text{Rh} \xrightarrow{\text{NO}} \text{CO}$ groups, which are thought to be responsible for NO reduction. Dicarboxyl formation prevents the reaction proceeding. However, Dictor [139] did not manage to observe the formation of $\text{Rh}(\text{CO})(\text{NO})$ under reaction conditions but only $\text{Rh}(\text{CO})_2$, Rh-NO^+ , Rh-NO , Rh-NO^- , Rh-CO , Rh_2CO , RhCN groups and a great variety of NCO -groups, mainly on Al_2O_3 , were also recorded. In the authors opinion [139], NO dissociates on the reduced Rh and easily oxidizes the catalyst. NCO is possibly formed on the Rh-support boundary (but not on the Rh^+).

NO/Ru^{2+} and NO_2/ZnO were found on the Ru/ZnO surface. CO adsorbed at the surface of Ru reacts with NO after its dissociation, resulting in the formation of NCO and CO_3 . These NCO and CO_3 species then spill over from the metal into the support and remain there, stable up to temperatures higher than the catalyst's [140].

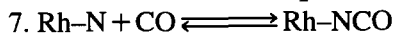
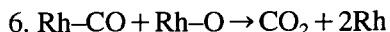
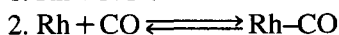
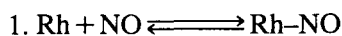
The presence of nitrogen on the surface of a Pt catalyst under reaction conditions has been demonstrated by Yamada et al. [141]. It is stabilized in the structure (2×2) and desorbs as N_2 at 420°C .

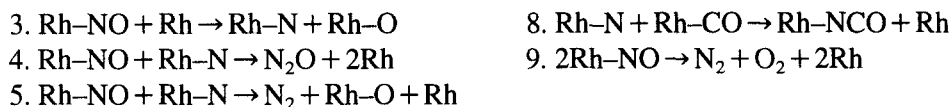
The bulk of the data presented above shows that there are a great variety of stepwise schemes for the description of the interaction of NO and CO on Pt-group metals. The set of surface compounds observed is not very large: CO_{ads} , NO_{ads} , NCO , $(\text{CO} \cdot \text{NO})$, O_{ads} , N_{ads} . Two forms of CO and NO adsorption are possible: linear and bridge.

It is reasonable to suggest that the variety of schemes used, is connected not with different reaction mechanisms, but rather with different rates of steps of the same mechanism. In reality, the change of rate relations causes the change of measured kinetic regularities. But this is traditionally treated as a change of reaction mechanism. All the schemes used are constructed on a lack of information, which is why the role of NCO complex in the $\text{NO} + \text{CO}$ reaction has not yet been determined definitely.

Let us now state the basic problems of the investigation of the role of isocyanate complex in the reaction. According to the data [117,142,143], the absorption band of a M-NCO complex can shift from 2180 to 2240 cm^{-1} depending on its charge. In addition, the position of this band also depends on the NO pressure in the reactor, temperature [118], and pretreatment of the surface [127]. Isocyanate complex can exist both on the metal and on the support surfaces and sometimes it may be difficult to distinguish these varieties under reaction conditions because of the rather small intensity of the M-NCO absorption band in comparison with the Al-NCO band. Also, the possible existence of the M-OCN complex [122], the adsorption band of which is very close to that of Al-NCO , has to be taken into account. It should be noted, too, that most of the investigations were carried out at low pressure, low temperature, under stationary conditions, which is to say, far from real catalytic conditions.

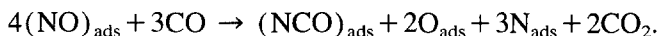
Measurements of IR spectra in a catalytic reaction in situ without simultaneous measurement of a reaction rate do not allow the determination of a uniquely kinetic scheme for the reaction. For example, Hecker and Bell [117] studied the dependence of optical density of absorption bands of surface compounds on Rh/SiO on CO and NO pressure in the reaction mixture and suggested the following reaction mechanism:



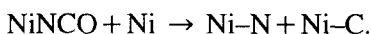


This scheme allows one to obtain equations for the dependence of surface coverage on CO and NO pressure in the gas phase which are in qualitative agreement with the observed dependence on optical density. It is not, however difficult to show that similar dependencies could be also obtained on the basis of another reaction mechanism (see below, Section 4). In the scheme suggested in Ref. [117], the NCO complex was not treated as an intermediate, although there is some indirect evidence for this. The intensity of the M–NCO absorption band depends on temperature and composition of the reaction mixture. N and CO were shown to be formed upon M–NCO decomposition and this reaction can proceed in the presence of the gas phase. The main reason for the ambiguity is the failure to compare the surface compounds' conversion rate with the rate of formation of reaction products.

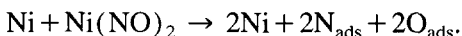
For completeness we list here the results of spectral studies of the NO + CO reaction on non-noble transition metals. The reaction of NO + CO on Ni/SiO₂ was studied by means of IR spectroscopy and microbalance methods [144]. Adsorbed NO (mainly Ni(NO)₂) reacts with CO resulting in NiNCO + CO₂. After the reaction the stoichiometry corresponds to the following equation:



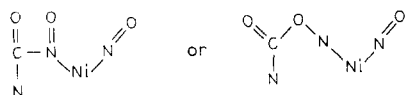
The weak form of the adsorbed CO is generated in the reaction through the interaction of NiNCO with Ni:



In the absence of CO the following process takes place:

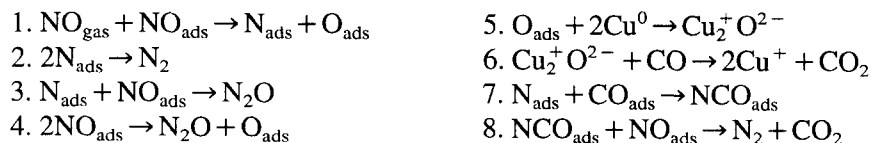


Within ten minutes after the start of the reaction a correlation between NO decomposition and NCO generation was observed. The formation of associative intermediate complexes presented below is thought to be possible:



The reaction of surface nitride NiN (formed after the dissociation of NiNO) with CO resulting in the NCO formation was not observed.

The NO + CO reaction on a reduced copper catalyst was studied in situ using IR spectroscopy and TPD techniques [145]. It was shown that CO₂ and N₂ were formed in the same elementary step. CO groups were observed on Cu⁰ and Cu⁺. The presence of NO on the reduced surface results in the reoxidation of Cu (→ Cu–O + Cu⁺–CO) with further formation of NCO, possibly on the support. The following reaction mechanism is proposed:



The last step is the limiting one. Spillover of nitrogen atoms from copper onto the support and their further interaction with CO are thought to be possible.

IR spectra recorded in situ on the surface of a Cu–Cr/Al₂O₃ catalyst exhibited absorption bands due to Cu²⁺–NCO, Cu⁺–NCO, Cu⁺–NO, Cr²⁺–NO, Cu²⁺–CO, and Cu⁺–CO complexes, as well as those of carbonates, carboxylates, nitrites, and nitrates [146]. An NCO complex is formed both under reaction conditions (NO + CO) and after stepwise input of gases (first NO, then CO). The formation and decomposition of NCO on Cu may possibly occur as:



We have performed a systematic spectrokinetic investigation of the NO + CO interaction over Pt-group metals [147–156]. Our results are the subject of the following section.

4.2. Reaction of carbon monoxide and nitric oxide in the presence of oxygen on a supported rhodium catalyst

The reaction of CO + NO on supported Rh catalyst was studied in a heated, flowing IR cell reactor [147–152] (see Fig. 1) with the reagents and reaction products being analyzed. The mathematical model of the reactor was close to the model of a reactor of an ideal mixing. Catalyst powder (1.0% Rh/γ-Al₂O₃, ('Rhône-Poulenc')) pressed into pellets (25 mg, 2 cm²) was used as a sample. The surface area of support and pressed catalyst was 80 m²/g.

We shall start with the data obtained under stationary conditions. The temperature dependence of the CO + NO interaction was studied for a reaction mixture containing 1.2% CO, 0.6% NO and 0.2% O₂ in nitrogen. At low temperatures 2030 cm^{−1} and 2100 cm^{−1} absorption bands were recorded in the IR spectra. These were assigned to the stretching vibrations of CO in the dicarbonyl complex of Rh: Rh<sup>CO₂ [157]. Increasing the temperature results in the decrease of optical density of these bands, the reaction rate thereupon increases and the 2240–2260, 1635, 1580 and 1480 cm^{−1} bands appear in the IR spectra. The 1480 cm^{−1} absorption band could be assigned to the surface complex CO₂^{2−} vibrations [158].

Fig. 15a shows the temperature dependencies of the nitric oxide (*W*_{NO}) and carbon monoxide (*W*_{CO}) consumption rates. It can be seen that the reaction rate increases with increasing temperature up to 320°C and is independent on temperature over 320°C. The optical densities of the 2260, 1635, 1580 and 1480 cm^{−1} absorption bands pass a maximum at 270°C (Fig. 15b) This is possible if the reaction rate is determined by the rate of reagent diffusion to the catalyst surface.

The dependencies of the reaction rate at 250°C (in kinetic region) and of the 2240–2260 cm^{−1} band's optical density (*D*₂₂₄₀) on the CO concentration in the reactor are shown in Fig. 16. NO concentration was 0.6%. It can be seen that, if CO concentration increases up to 0.3%, the reaction rate and *D*₂₂₄₀ increase, too. At CO concentration higher than 0.3%, a sharp increase of *D*₂₂₄₀ with the displacement of the band's maximum was observed. *W*_{CO} and *W*_{NO} have achieved their maximum values and then ceased to depend on CO concentration. Similar behavior is exhibited by the intensity of the 2260 cm^{−1} absorption band. The consumption rate of CO under stationary conditions is more than that of NO, because of CO oxidation.

Fig. 17 shows the dependencies of *W*_{CO}, *W*_{NO} and *D*₂₂₆₀ on the NO concentration in the reactor. CO concentration was 1.2%. It can be seen that even at low NO concentration *D*₂₂₆₀, *W*_{CO} and *W*_{NO} pass through their maximum values. When the NO concentration in the reactor changes, the relation between

W_{CO} and W_{NO} changes, too. At low NO concentration W_{CO} is higher than W_{NO} , whereas the reverse is true for NO concentrations higher than 0.3%. Displacements of the 2240–2260 cm^{-1} band upon the

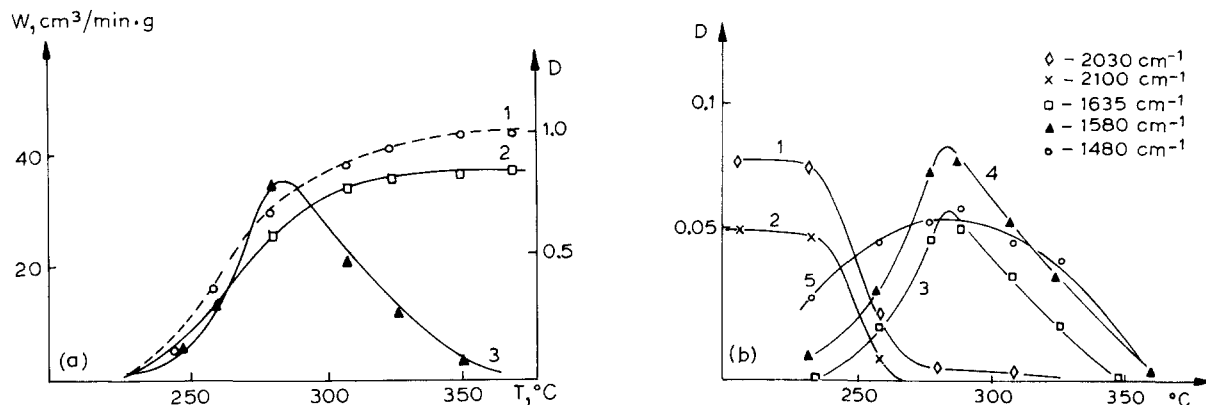


Fig. 15. (a) Temperature dependencies of CO (1) and NO (2) consumption rate, as well as of optical density of 2260 cm^{-1} absorption band. (b) Optical density of 2030 cm^{-1} (1), 2100 cm^{-1} (2), 1635 cm^{-1} (3), 1580 cm^{-1} (4) and 1480 cm^{-1} (5) absorption bands versus temperature.

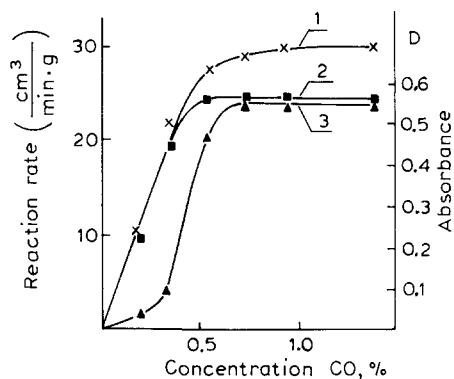


Fig. 16. Dependencies of CO (1) and NO (2) consumption rates and of optical density of 2240–2260 cm^{-1} absorption band (3) on CO concentration in reactor at 250 $^{\circ}\text{C}$.

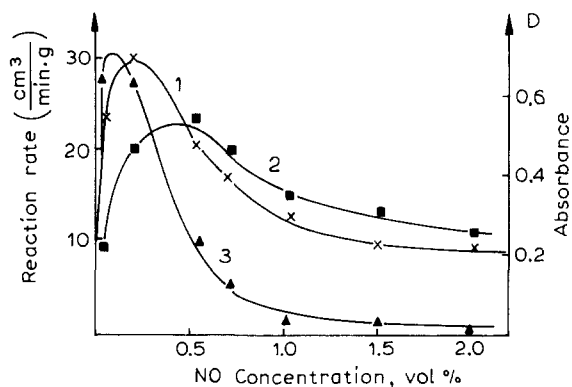


Fig. 17. Dependencies of CO (1) and NO (2) consumption rates and of optical density of 2240–2260 cm^{-1} absorption band (3) on NO concentration in reactor at 250 $^{\circ}\text{C}$.

adsorption of CO and NO isotopes correspond to the values calculated for isocyanate complex.

The optical density of the 1480 cm^{-1} absorption band as the concentration of reagents in the reactor changes increases with increasing consumption rate (Fig. 19). It is notable that both the 1480 and the $2240\text{--}2260\text{ cm}^{-1}$ bands are observed only under reaction conditions: if the feed of reagents is switched off or the temperature of the reaction mixture is decreased these bands disappear from the spectra. In the presence of excess NO, the IR spectra exhibited the 1680 and 1560 cm^{-1} absorption bands assigned to the $\text{Rh}\text{--}\text{NO}^{\delta-}$ vibrations [114] and $\text{N}\text{--}\text{O}$ vibrations in the NO_3^- complex adsorbed on Al_2O_3 , respectively.

The data presented above show that CO_{ads} , NO_{ads} , isocyanate ($2240\text{--}2260\text{ cm}^{-1}$) and carbonate (1480 cm^{-1}) complexes exist on the $\text{Rh}/\text{Al}_2\text{O}_3$ surface under reaction conditions. The complex form of the 2260 cm^{-1} absorption band, the variability of its half-width with catalyst temperature and its shifting position with the reaction mixture composition point to the existence of two forms of the isocyanate complex. It is possible to state that the low frequency absorption band (2240 cm^{-1}) is due to isocyanate complex on Rh, whereas that at 2260 cm^{-1} is due to the complex on Al_2O_3 . It can be seen from Fig. 16 that at low CO concentration in the reactor (oxidizing mixture) the optical density of the NCO absorption band is low and its position is at 2240 cm^{-1} . In this case NCO is localized at the metal atom. When CO concentration increases the intensity of the 2240 cm^{-1} absorption band increases too, together with its displacement up to 2260 cm^{-1} . I.e., in the reducing mixture spillover of NCO from metal to support becomes possible. When the reaction mixture flow is turned off, the isocyanate complex decomposes. This process can very possibly occur on the Rh surface.

At low CO concentrations in the initial mixture, the rate of nitrogen formation is proportional to the concentration of NCO localized at metal atoms (2240 cm^{-1}), both at 0.6% NO concentration (Fig. 16) and in the presence of excess NO (Fig. 17). Data obtained show that isocyanate complex may be an intermediate in the N_2 formation. This point of view is also supported by the instability of NCO in the absence of reaction mixture and by the decrease of its concentration at the surface at the transfer to the external diffusion region.

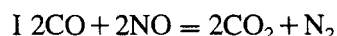
The independence of D_{2260} on the CO concentration in the presence of excess CO (Fig. 16) points to the fact that the NCO complex concentration is kept constant both for complexes localized at metal and at support surfaces.

The independence of W_{CO} on the CO concentration in the gas phase could arise from the fact that CO and NO are adsorbed on different sites, determined by the method of sample preparation. In reality, Rh supported over Al_2O_3 from $\text{RhCl}_2 \cdot 3\text{H}_2\text{O}$ solution with subsequent drying in hydrogen at 400°C is not completely reduced. Together with Rh^0 , Rh^+ is formed which is stabilized by Cl ions [159]. CO, being adsorbed on Rh^+ , results in Rh dicarbonyl formation [159]. Because of this, the 2030 and 2100 cm^{-1} absorption bands which are observed in the system demonstrate the presence of Rh^+ ions.

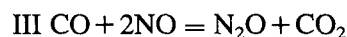
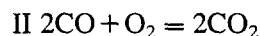
More probably, the NCO complex is formed during the interaction of an adsorbed nitrogen atom and an adsorbed CO molecule, and decomposed by reacting with an adsorbed NO molecule. The carbonate complex CO_3^{2-} is formed on the Rh catalyst surface in the absence of NO in the gas phase. The optical density of the 1480 cm^{-1} absorption band changes parallel to the CO consumption rate when the reagent concentrations change. This points to the possibility of the carbonate complex formation during CO interaction with both oxygen and nitric oxide. This complex most probably precedes the formation of CO_2 in the gas phase. It is likely to be localized at Rh atoms, because its concentration is at a maximum when practically all the carrier is covered by NCO complex.

The $\text{CO} + \text{NO}$ interaction in the presence of oxygen may proceed according to the following mechanism:

	I	II	III
$\text{CO} + \text{M}_1 \xrightleftharpoons[k_{-1}]{k_1} \text{M}_1\text{-CO}$	2	2	1
$\text{NO} + \text{M}_2 \xrightleftharpoons[k_{-2}]{k_2} \text{M}_2\text{-NO}$	2	0	2
$\text{M}_2\text{-NO} + \text{M}_2 \xrightarrow{k_3} \text{M}_2\text{-N} + \text{M}_2\text{-O}$	1	0	1
$\text{M}_2\text{-N} + \text{M}_1\text{-CO} \xrightarrow{k_4} \text{M}_2\text{-NCO} + \text{M}_1$	1	0	0
$\text{M}_2\text{-NCO} + \text{M}_2\text{-NO} \xrightarrow{k_5} \text{M}_2\text{-CO} + \text{M}_2 + \text{N}_2$	1	0	0
$\text{M}_1\text{-CO} + \text{M}_2\text{-O} \xrightarrow{k_6} \text{M}_2\text{-CO}_2 + \text{M}_1$	1	2	1
$\text{M}_2\text{-CO}_2 \xrightarrow{k_7} \text{M}_2 + \text{CO}_2$	2	2	1
$\text{M}_2\text{-N} + \text{M}_2\text{-NO} \xrightarrow{k_8} \text{N}_2\text{O} + 2\text{M}_2$	0	0	1
$\text{O}_2 + 2\text{M}_2 \xrightarrow{k_9} 2\text{M}_2\text{-O}$	0	1	0



(4.1)



where M_1 and M_2 are different kinds of active sites on the catalyst surface, and numbers on the right are the stoichiometric numbers of the steps.

Assuming that the course of the reaction does not perturb the adsorption–desorption equilibrium for CO and NO, and using the stationary reaction theory, we can obtain the rate equations for reaction routes (I)–(III) (these rates are denoted as r^{I} , r^{II} , r^{III}). Analysis of the r^i dependencies on the CO and NO concentration showed that they can be qualitatively described by the mechanism presented above. We have also analyzed other schemes, among which were the mechanisms:

- with irreversible NO adsorption;
- with N_2 formation after recombination of nitrogen atoms;
- without the influence of oxygen, and so on.

Practically all schemes studied can qualitatively describe the observed dependence of the reaction rate on the composition of the reaction mixture. However, the dependence of the reaction rate and selectivity on the composition of the reaction mixture can be described only by the scheme presented above.

As measure of selectivity we use the ratio of N_2O and N_2 formation rates ($r_{\text{N}_2\text{O}}$ and r_{N_2} , respectively):

$$S = r_{\text{N}_2\text{O}} / r_{\text{N}_2}.$$

Then from the scheme presented above it follows that

$$S = k_8 \theta_{\text{NO}} / k_4 \theta_{\text{CO}}. \quad (4.2)$$

It can be seen that a change in the ratio of coverages (θ) of the surface by CO and NO molecules with reaction conditions will determine the change in S . We will consider the change of θ_i with changing of reaction conditions.

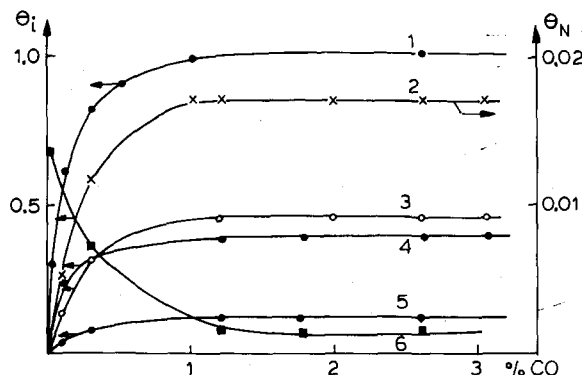


Fig. 18. Surface coverage of CO (1), N (2), NCO (3), NO (4), O (6) and free surface area (5) as functions of CO content in the reaction mixture.

Analyzing the scheme (4.1), we evaluated the values of k_4 , k_5 and k_8 independently by spectroscopic measurements in the nonstationary region. Other rate constants were selected from Ref. [151].

Assuming that the course of the reaction does not perturb the adsorption–desorption equilibrium for CO and NO, and using the steady-state approximation, for the values of the reaction rates W_{CO} and W_{NO} on the basis of mechanism (4.1) we obtain the following equations:

$$W_{NO} = 2\beta\theta_{NO}(k_5\theta_{NCO} + k_4\theta_N) \quad (4.3)$$

$$W_{CO} = \beta\theta_{CO}(k_6\theta_O + k_4\theta_N).$$

Here, β ca. 0.1 cm^3 is the capacity of the monolayer, evaluated from spectroscopic measurements in the nonsteady-state region.

Calculated values of θ for increasing CO content in the reaction mixture are presented in Fig. 18. It can be seen that the occupation of the surface by CO molecules approaches unity quite rapidly (curve 1). The rapid decrease in the coverage of the surface by oxygen atoms (curve 6) should also be noted.

The values of S , W_{NO} and W_{CO} calculated on the basis of Eq. (4.3) and the values of measured rate constants and coverages are presented in Fig. 19 together with the experimental data (points are calculated and curves are experimental). The agreement is rather good. The physical meaning of this can be

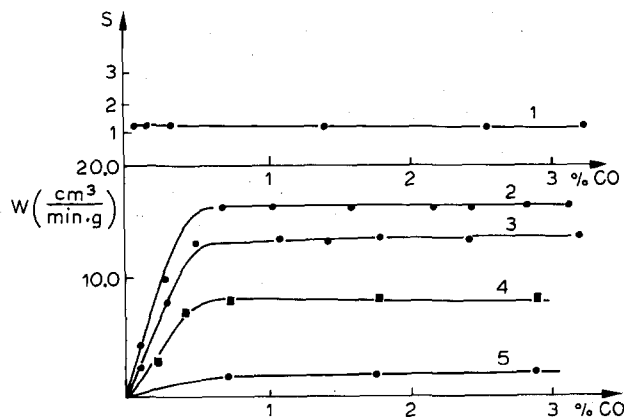
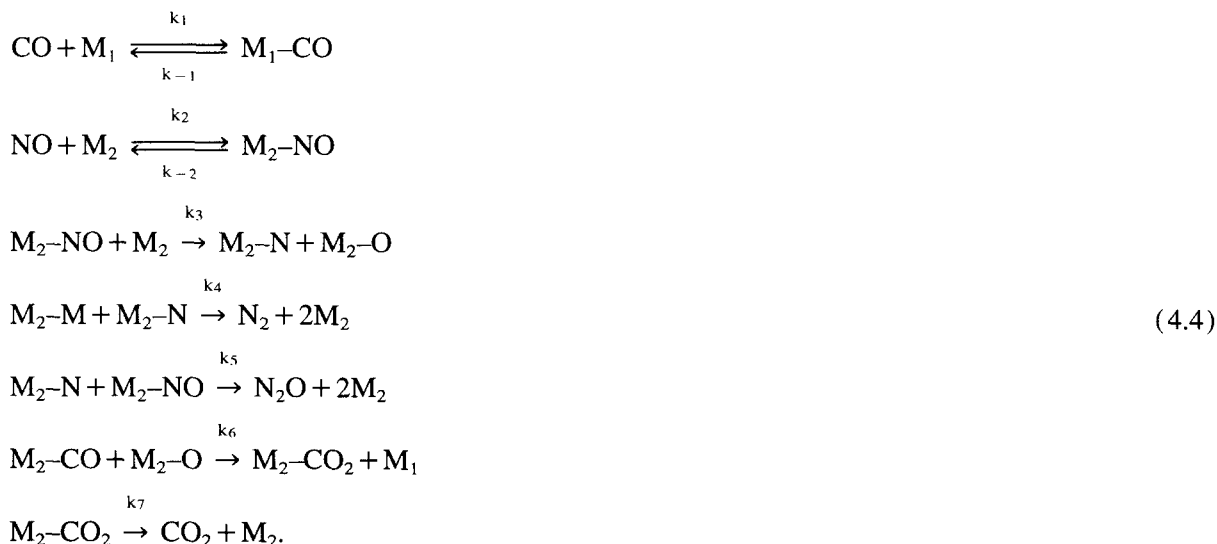


Fig. 19. Experimental and calculated values of selectivity (1), W_{CO} (2), W_{NO} (3), as well as of optical density of 1480 cm^{-1} absorption band (4) and of surface coverage by CO complexes (5) versus CO concentration in the reaction mixture.

interpreted as follows. In the absence of CO in the gas phase, sites of the first kind are free, and sites of the second kind are completely occupied by oxygen atoms. In fact, an adsorbed NO molecule can dissociate into N and O atoms at the temperature of the experiment. A nitrogen atom reacts with an adsorbed NO molecule, resulting in formation of N_2O . An oxygen atom remains on the surface. Oxygen atoms are also formed during O_2 adsorption. As a result of these processes under steady-state conditions the surface is covered with oxygen atoms. CO, interacting with oxygen, frees the surface for the adsorption of NO molecules. After that, the reaction between CO and NO becomes possible. If the CO concentration in the reaction mixture increases, the free surface (because of the acceleration of the $CO + O$ reaction) and, consequently, the θ_{NO} increase, too. Thus, when the coverage of the surface by CO molecules increases there is an increase in the coverage of the surface by NO molecules. The ratio of θ_{NO} and θ_{CO} is then kept constant. In agreement with (4.2), this implies that selectivity is independent on the CO concentration. The foregoing applies to the region of low CO concentration. At high concentration (Fig. 18), θ_{CO} is about 1. Increase of the CO concentration in this case does not lead to any change in the surface coverage, nor in the reaction rate (Figs. 18 and 19). Oxygen present in the reaction mixture in this region of CO concentration is completely consumed in the $CO + O_2$ reaction.

The correlation in the changes of optical density of the 1480 cm^{-1} absorption band (D_{1480}) and θ_{CO_2} (Fig. 19, curves 4 and 5) should be noted. Such a correlation supports the conclusion that the surface compound absorbing at 1480 cm^{-1} is a CO_2^{2-} complex. When NO is absent in the gas phase, O_2 is completely consumed in the reaction with CO. NO will effect the reaction of CO and O_2 only at high NO pressures when, because of the decrease of free surface, the rate of the reaction will drop to zero. At the same time the $CO + O_2$ reaction has virtually no effects on the interaction of CO and NO. The fact that NO inhibits the $CO + O_2$ reaction was also noted by Oh and Carpenter [160].

We now consider one of the possible reaction mechanisms in which nitrogen is formed by the recombination of nitrogen atoms [151,154].



Analysis of this scheme under steady-state conditions showed that selectivity is equal to

$$S = k_5 \theta_{NO} / k_4 \theta_N$$

and increases linearly with increasing P_{NO} . This result contradicts the experimental data.

As was indicated by Hecker and Bell [91], the selectivity does not depend on the composition of the reaction mixture. On this basis, they proposed the following scheme:

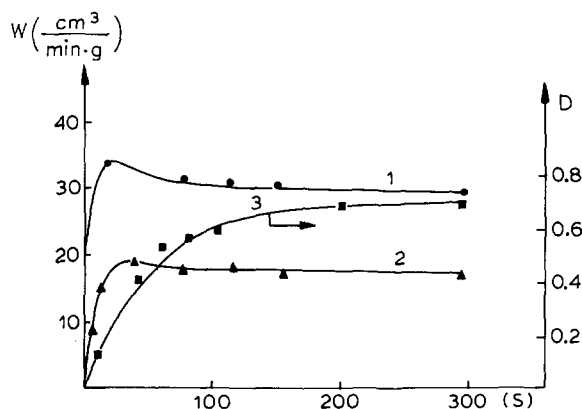
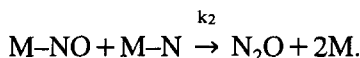
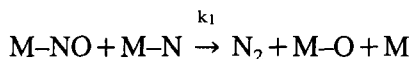


Fig. 20. Time dependencies of W_{CO} (1), W_{NO} (2) and D_{NCO} (3) during the transition to the steady state. The reaction mixture 1.2% CO + 0.39% NO.



Apparently, they [91] have measured the selectivity in a relatively narrow range of reactant concentrations. Over a wider range of concentrations the selectivity depends on P_{NO} . Therefore one may express doubts concerning the validity of the mechanism proposed in Ref. [91].

As was noted above, the isocyanate complex found on the surface of the Rh catalyst in the majority of studies is a stable surface compound. It should be noted, too, that these studies were carried out in the absence of O_2 . In our investigations, the absorption band corresponding to the isocyanate complex disappeared from the spectrum practically at once after the reaction ceased (decrease of temperature, turning off the flow of reactants). Analysis of the scheme (4.1) afford an explanation for this difference. It follows from (4.1) that the steady-state occupation of the surface by isocyanate complex is determined by the formula [147,151]:

$$\theta_{\text{NCO}} = \frac{k_4 \theta_{\text{CO}}}{k_5} \cdot \frac{k_3 (k_6 \theta_{\text{CO}} \theta_{\text{O}} / (k_3 K_2 P_{\text{NO}} + k_9 P_{\text{O}_2}))^{1/2}}{k_4 \theta_{\text{CO}} + k_8 K_2 P_{\text{NO}} \{k_6 \theta_{\text{CO}} \theta_{\text{O}} / (k_3 K_2 P_{\text{NO}} + k_9 P_{\text{O}_2})\}^{1/2}}. \quad (4.5)$$

If O_2 is now absent in the gas phase, (4.5) reduces to the following:

$$\theta_{\text{NCO}} = \frac{k_4 k_6 \theta_{\text{CO}}^2 \theta_{\text{O}}}{k_5 (K_2 k_6 \theta_{\text{CO}} \theta_{\text{O}} P_{\text{NO}} / k_3)^{1/2} \{k_4 \theta_{\text{CO}} + k_8 (K_2 k_6 \theta_{\text{CO}} \theta_{\text{O}} P_{\text{NO}} / k_3)^{1/2}\}}.$$

Calculation shows that in the absence of O in the gas phase $\theta_{\text{NCO}} \rightarrow 1$ as $P_{\text{NO}} \rightarrow 0$ (quasi-steady-state approximation). In the presence of O_2 , θ_{NCO} is substantially less than unity.

Further development of the reaction mechanism was based on a spectrokinetic study under nonsteady-state conditions [152]. All measurements were carried out at 250°C, where there are no complications from diffusion. The reaction mixture was fed to the cell reactor. Adjusting the device at a fixed frequency, associated with the absorption of one or another surface complex, we followed the transition to a steady state.

The process of transition to a steady state depends substantially on the reaction mixture. Consumption rates of carbon monoxide (W_{CO}), of nitric oxide (W_{NO}) and the optical density of the isocyanate complex

absorption band (D_{NCO}) versus time during the transition to a steady state of the reaction mixture with an excess of CO (reducing region) are shown in Fig. 20. It can be seen that the NCO absorption band is at 2260 cm^{-1} and the steady state value of D_{NCO} is rather large (ca. 0.8). As was explained above, this absorption band arises from the vibrations in an isocyanate complex, localized on the support. In other words, isocyanate complex in the excess of CO migrates from the metal surface onto the carrier. It can also be seen from Fig. 20 that the W_{CO} and W_{NO} values reach their steady states more rapidly than D_{NCO} . In the presence of excess NO, the steady-state value of D_{NCO} is small (about 0.1), and the corresponding absorption band is placed at 2240 cm^{-1} . In this case it arises from the vibrations of NCO, localized on metal atoms. This means that in the oxidizing region the NCO complex does not migrate onto the support.

Let us consider in greater detail the migration of isocyanate complex in the reducing (excess of CO) and oxidizing (excess of NO) regions. The migration of isocyanate complex from Rh to SiO_2 in the reducing region was studied by Hyde and Rudman [124]. They showed that isocyanate complex migrates onto the support after its concentration on the metal becomes constant. According to our data, this migration starts after a certain NCO concentration has been reached on the metal. One of the possible reasons for the spillover could be the marked increase of the diffusion coefficient with increasing NCO concentration on the metal surface.

In the view of the fact that the time for W_{CO} and W_{NO} to become steady is less than that for $D_{\text{Al-NCO}}$, it is possible to state that spillover of NCO complex in the reducing region occurs under conditions of the steady-state interaction between CO and NO. Kinetic analysis [151] shows that under such conditions the free surface of metal is small. This fact allows us to hypothesize that the reverse spillover (from support to metal) is negligibly small. In such a case, the accumulation of isocyanate complex on the carrier can be described by the following equation:

$$\frac{d\theta_{\text{Al-NCO}}}{dt} = k\theta_{\text{NCO}}(1 - \theta_{\text{Al-NCO}}). \quad (4.6)$$

Experimental curves of D_{NCO} transition to the steady state in the reducing region are described by the following equation

$$\frac{dD}{dt} = A - BD, \quad (4.7)$$

where A and B are constants.

Comparing (4.6) and (4.7) and taking into account that $D = \beta\theta\epsilon/S$, we obtain

$$A = k\theta_{\text{NCO}}D_{\text{Al-NCO}}^{\text{max}}, \quad B = k\theta_{\text{NCO}}. \quad (4.8)$$

Here S is the geometrical surface of the pellet (cm^2); ϵ is the extinction coefficient ($\text{cm}^2/\text{molecule}$); $D_{\text{Al-NCO}}^{\text{max}}$ is the maximum possible value of the isocyanate absorption band optical density, when it is localized on the surface; β is the capacity of the monolayer (cm^3), and k is the rate constant of spillover of NCO.

Thus, by performing nonsteady-state spectrokinetic measurements in the reducing region, we managed to determine the nature of the dependence of the steady-state coverage of the metal by isocyanate complex on the composition of the mixture.

Isocyanate complex on the metal was observed spectroscopically in the oxidizing region. The steady-state value of the coverage of the metal surface by this complex is less than $\theta_{\text{NCO}}^{\text{r}}$, consequently its migration onto the carrier does not take place in this region. In accord with (4.4), the establishment of the steady-state concentration of isocyanate complex on the metal is described by the equation

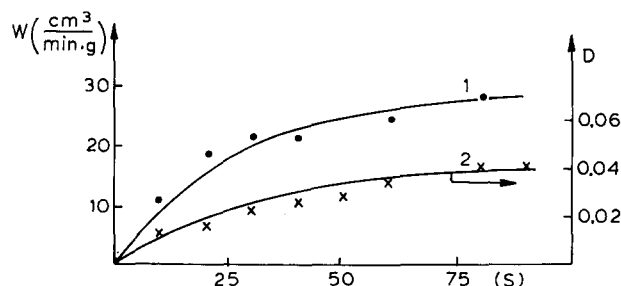


Fig. 21. Time dependencies of W_{CO_2} (1) and D_{1480} (2) for 1.2% CO + 0.18% NO reaction mixture.

$$\frac{d\theta_{\text{MNCO}}}{dt} = k_4\theta_{\text{N}}\theta_{\text{CO}} - k_5\theta_{\text{NO}}\theta_{\text{MNCO}}. \quad (4.9)$$

The experimental curves for the establishment of steady-state values of D_{MNCO} in this region are also described by Eq. (4.7). A comparison of (4.9) and (4.7) shows that in the oxidizing region the values A and B equal:

$$A = \beta k_4\theta_{\text{N}}\theta_{\text{CO}}\epsilon/S, \quad B = k_5\theta_{\text{NO}}. \quad (4.10)$$

The constancy of A and B means, obviously, that during the establishment of a steady-state value of θ_{MNCO} the values θ_{N} , θ_{CO} and θ_{NO} vary very little. Thus, nonsteady-state spectrokinetic measurements in the oxidizing region give information about the steady-state coverage of the surface by N atoms and CO and NO molecules.

The results of the steady-state and nonsteady-state spectrokinetic measurements, when compared, are in good agreement. This allows one to assert that the proposed mechanism of the CO + NO reaction is correct.

A comparison of the steady-state and nonsteady-state spectrokinetic data allows one to estimate the rate constant of NCO migration from the metal onto the support. The dependencies of θ_{NCO} and $k\theta_{\text{NCO}}$ on the NO content in the reaction mixture are presented in Refs. [151] and [152]. Comparison of these dependencies shows that $k = 0.025 \text{ s}^{-1}$.

Spectrokinetic measurements under nonsteady-state conditions also allow one to obtain additional information about the structure and properties of the intermediate complex. It was mentioned above that under the reaction conditions, absorption bands were also observed in the spectra at 1635 and 1580 cm^{-1} . The values of A and B determined from the change of optical density of these absorption bands are the same as those given above. This, together with the data from the steady-state measurements (the similar changes in the optical density of the 2260, 1635 and 1580 absorption bands with temperature and concentration of reagents), shows that all of the absorption bands named belong to the isocyanate complex.

It was shown previously that as a result of the reaction of CO and NO in the presence of O_2 at the surface of the Rh catalyst, an intermediate CO_2^{2-} complex is formed. Fig. 21 shows the curves of CO_2 formation rate (W_{CO_2}) and of the 1480 cm^{-1} absorption band optical density (D_{1480}) belonging to the CO_2^{2-} complex on Rh. The experimental data show that the ratio of the W_{CO_2} values, determined at different times, equals the ratio of the corresponding values of D_{1480} ; i.e., the CO formation rate is linear with respect to the concentration of carbonate complex at the surface, which confirms the hypothesis stated above that the surface carbonate complex precedes the formation of CO_2 in the gas phase.

The results of studying of the reaction of CO and NO under steady-state and nonsteady-state conditions show that the isocyanate complex is an intermediate in the reaction of N_2 formation. According to the

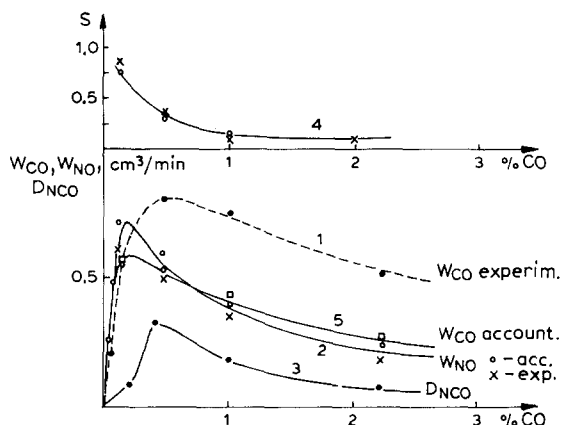


Fig. 22. Experimental and calculated values of selectivity (4), W_{NO} (2), W_{CO} (5 — calc. and 1 — exp.) and D_{NCO} (3) versus CO concentration at 360°C.

mechanism proposed the rate of formation of nitrogen (W_{N_2}) is determined by the following formula, taking into account that $D_{NCO} = \beta \theta_{NCO} \epsilon / S$:

$$W_{N_2} = k_5 \theta_{NO} D_{NCO} S / \epsilon. \quad (4.11)$$

Using numerical values for $\beta = k_5 \theta_{NO}$ calculated from the time curves of D_{NCO} in an oxidizing medium and experimentally measured values of W_{N_2} , we were able to use Eq. (4.11) to evaluate the extinction coefficient of asymmetric vibrations in the isocyanate complex (2240 cm^{-1}) [152]. We note that the value of B can also be determined from the data presented in Figs. 16–19. According to the experimental data, the maximum coverage of the metal surface by isocyanate complex corresponds to the D_{NCO} value of 0.2. Simple calculations show the quantity of NCO complexes in this case to be ca. $1.7 \cdot 10^{18}$. In view of the fact that the area of the sample used was 1.8 m^2 , we find an active sites concentration of $1.0 \cdot 10^{14}$ sites/ cm^2 , which is somewhat less than the number of Rh atoms in the sample.

Thus, the spectrokinetic study of the CO + NO reaction on a Rh surface, together with the reaction mechanism proposed, allow us:

- (1) to give a quantitative description of the activity and selectivity under steady-state and nonsteady-state conditions;
- (2) to explain literature data on the stability of isocyanate complex;
- (3) to estimate the extinction coefficient of isocyanate complex;
- (4) to give a quantitative description of the migration of NCO; and
- (5) to estimate the number of active sites.

4.3. Interaction of CO and NO in the presence of oxygen on supported Pt

In the spectra obtained in situ in the CO + NO reaction over a supported Pt catalyst (1 wt.-% Pt/ Al_2O_3) absorption bands at 2245–2260, 1635, 1580, 1480 cm^{-1} were found [153,155,156]. Similar to the case of the Rh catalyst, the 1480 cm^{-1} absorption band could be assigned to the vibrations of surface carbonate complex CO_2^{2-} , and the others to vibrations of a surface isocyanate complex [114,117,122,147–152]. Fig. 22 shows the rate of consumption of CO (W_{CO}) and NO (W_{NO}), and the optical density of the isocyanate band (D_{NCO}) as functions of the concentration of CO at 360°C. The NO concentration was 0.6%. In the oxidizing region ($[\text{CO}] < 0.6\%$), the rates of consumption of CO and NO are similar and increase linearly with increasing CO concentration. With a low concentration of CO in the reaction

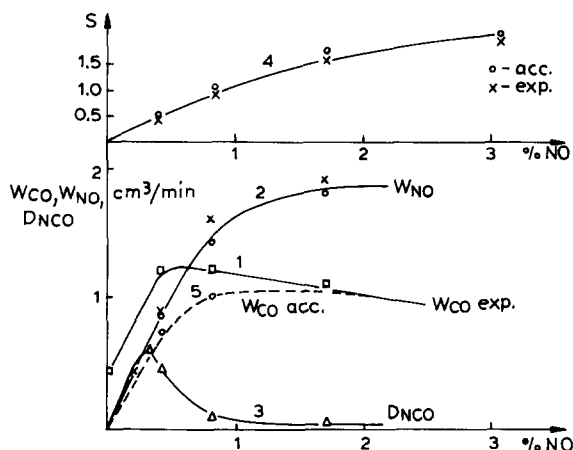


Fig. 23. Experimental and calculated values of selectivity (4), W_{NO} (2), W_{CO} (5 — calc. and 1 — exp.) and D_{NCO} (3) versus NO concentration at 360°C.

mixture the absorption band of the isocyanate complex is placed at 2240 cm^{-1} and its optical density is low. When D_{NCO} increases, the position of the absorption band shifts to 2260 cm^{-1} . Further increase of CO concentration leads to a decrease of D_{NCO} as well as of W_{CO} and W_{NO} . It should be noted that in the reducing region (excess CO) W_{CO} is larger than W_{NO} . This excess is due to the oxidation of CO by oxygen present in the reaction mixture as an impurity (0.2%). In the oxidizing region, the rate of reaction of CO with the oxygen impurity is substantially lower. The dependence of the selectivity of the reaction (S) on the CO content in the reaction mixture is shown in Fig. 22 (curve 4). We define the quantity S as the ratio of the rates of formation of N_2O (W_{N_2O}) and of N_2 (W_{N_2})

$$S = W_{N_2O} / W_{N_2}.$$

It can be seen that the selectivity to N_2O falls as the CO content in the reaction mixture increases.

The dependencies of W_{CO} , W_{NO} , S and $D_{2240-2260}$ on NO concentration in the initial mixture at 360°C (CO concentration is 1.2%) are shown in Fig. 23. It can be seen that at low concentrations W_{CO} , W_{NO} and D_{NCO} increase practically linearly.

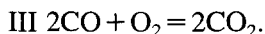
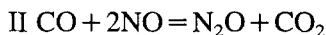
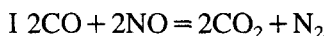
A further increase in the percentage of NO leads to a decrease of D_{NCO} and W_{CO} . W_{NO} is kept practically constant. It should be noted, that at low NO concentration, $W_{CO} > W_{NO}$, while at high NO concentration, $W_{NO} > W_{CO}$. Such a rate relationship is probably determined by the predominance of the oxidation of CO by oxygen in the reducing region. It can also be seen that selectivity increases with increasing NO concentration in the reaction mixture. The results presented show similar relationships between spectral and kinetic values on platinum and rhodium catalysts. Under reaction conditions there are CO_{ads} , NO_{ads} as well as isocyanate and carbonate complexes on the catalyst surface. Lowering the temperature or turning off the reactant flow causes the disappearance of these complexes. The optical density of the isocyanate band changes in parallel with the CO consumption rate when the concentration of reagents changes. Two forms of the isocyanate complex exist on the surface. One (2240 cm^{-1} band), localized on metal atoms, is active; the other (2260 cm^{-1} band), localized on the carrier atoms, is inactive. Since NCO complex cannot be formed on the support, its existence there can be explained only by spillover. As was mentioned previously, NCO complexes start their migration after their concentration at the surface of metal has reached a certain value. The steady-state value of D_{NCO} for NCO complex on the support depends on the experimental conditions (temperature in particular). This implies the existence of a

reverse spillover (from support to metal). Experiments carried on under nonsteady-state conditions showed that there is no decomposition of NCO complex on the support.

The bulk of experimental data obtained for Pt catalysts (Figs. 22 and 23) can be described by the scheme proposed for Rh (see Section 4.2). The main difference is that here all steps occur on one single kind of site. The scheme of the NO + CO interaction on Pt is presented below.

	I	II	III
$\text{CO} + \text{Pt} \xrightleftharpoons[k_{-1}]{k_1} \text{Pt-CO}$	2	1	2
$\text{NO} + \text{Pt} \xrightleftharpoons[k_{-2}]{k_2} \text{Pt-NO}$	2	2	0
$\text{Pt-NO} + \text{Pt} \xrightarrow{k_3} \text{Pt-N} + \text{Pt-O}$	1	1	0
$\text{Pt-N} + \text{Pt-CO} \xrightarrow{k_4} \text{Pt}_{\text{MNCO}} + \text{Pt}$	1	0	0
$\text{Pt-NCO} + \text{Pt-NO} \xrightarrow{k_5} \text{Pt-CO}_2 + \text{Pt} + \text{N}_2$	1	0	0
$\text{Pt-O} + \text{Pt-CO} \xrightarrow{k_6} \text{Pt-CO}_2 + \text{Pt}$	1	1	2
$\text{Pt-CO}_2 \xrightarrow{k_7} \text{CO}_2 + \text{Pt}$	2	1	2
$\text{Pt-N} + \text{Pt-NO} \xrightarrow{k_8} \text{N}_2\text{O} + 2\text{Pt}$	0	1	0
$\text{O}_2 + 2\text{Pt} \xrightarrow{k_9} 2\text{Pt-O}$	0	0	1

(4.12)



Here M is an active catalyst site.

Assuming that the occurrence of the reaction does not perturb the adsorption/desorption equilibrium, and using the steady-state condition for scheme (4.12), we obtain the relationships between surface coverage and the composition of the reaction mixture. It then becomes possible to calculate W_{CO} , W_{NO} and S

$$W_{\text{CO}} = \beta \theta_{\text{CO}} (k_6 \theta_{\text{O}} + k_4 \theta_{\text{N}}) \quad (4.13)$$

$$W_{\text{NO}} = 2\beta \theta_{\text{NO}} (k_5 \theta_{\text{NCO}} + k_8 \theta_{\text{N}}).$$

Figs. 22 and 23 present a comparison of the calculated and experimental dependencies of the reaction rates and selectivity on the reaction mixture composition. It can be seen that for W_{NO} (curve 2) and S (curve 4) the agreement is rather good. The W_{CO} dependencies coincide only in the oxidizing region (curves 1 and 5).

In the reducing region, the difference between calculated and experimental values is constant and equals the rate of CO reaction with admixed oxygen at complete conversion. This is due to the minor effect of small amounts of oxygen on the CO + NO reaction under steady-state conditions. Thus, the

results presented show the correctness of the reaction mechanism, in which nitrogen is formed via isocyanate complex.

As in the case of the Rh catalyst, we have also studied the transition to a steady state for the CO + NO reaction on a Pt catalyst. Here, as for Rh, we find two kinds of dependencies between W_{CO} , W_{NO} , W_{CO_2} , D_{NCO} and time: with and without a maximum. A maximum is found when the reducing region is studied. As the temperature is lowered, the concentration region, in which the maximum is found, is broadened. This maximum is possibly due to the competition of CO, NO and O₂ for surface sites. In the oxidizing region the dependencies of W_{CO} , W_{NO} , W_{CO_2} and D_{NCO} have no maxima.

We now consider the transfer of surface NCO concentration to a steady-state. In these conditions, the 2240 cm⁻¹ absorption band is assigned to the vibrations in the isocyanate complex localized on metal. The $D_{\text{NCO}} = f(t)$ dependence in this case reflects the change of NCO concentration on the metal (θ_{MNCO}), which, in agreement with (4.12), is described by

$$d\theta_{\text{MNCO}}/dt = k_4\theta_{\text{N}}\theta_{\text{CO}} - k_5\theta_{\text{NO}}\theta_{\text{MNCO}}. \quad (4.14)$$

We treated the experimental $D_{\text{MNCO}} = f(t)$ dependencies according to Eq. (4.7). Comparison of Eq. (4.14) and (4.7) shows that

$$A = \beta k_4 \epsilon \theta_{\text{N}} \theta_{\text{CO}} / S, \quad B = k_5 \theta_{\text{NO}}. \quad (4.15)$$

The comparison takes into account that $D_{\text{MNCO}} = \beta \epsilon \theta_{\text{MNCO}} / S$. The constancy of A and B values in the transfer of NCO concentration to the steady state apparently means that the surface coverages θ_{N} , θ_{CO} , θ_{NO} change very insignificantly. This conclusion is also confirmed by spectral measurements. In particular, it was shown that time of transfer of the CO absorption band optical density to the steady-state is an order of magnitude less than that for isocyanate complex.

It follows from (4.15) that the A and B values could also be estimated via kinetic analysis of the steady-state scheme (4.12). It turned out that when they are so defined they are in good agreement with the values determined from nonsteady-state spectrokinetic measurements. This also points to the correctness of the proposed mechanism. The extinction coefficient was determined from the comparison of A values [155].

From the reaction mechanism it follows that

$$W_{\text{N}_2} = \beta k_5 \theta_{\text{NO}} \theta_{\text{NCO}} \quad \text{or} \quad W_{\text{N}_2} = k_5 \theta_{\text{NO}} D_{\text{NCO}} S / \epsilon.$$

$$\text{Therefore, } \epsilon = k_5 \theta_{\text{NO}} D_{\text{NCO}} S / W_{\text{N}_2}.$$

Experimental data for various reaction mixtures resulted in ϵ values of $2.1\text{--}2.6 \cdot 10^{-19}$ cm²/molecule or on average, $\epsilon = 2.3 \cdot 10^{-19}$ cm²/molecule. This value is virtually the same as that for the isocyanate complex on Rh. Note also that ϵ is kept constant, when the optical density of NCO band changes from 0 to 0.2. This fact proves the validity of the Beer–Lambert law, at least for this region of coverage.

We can now estimate the number (N) of active sites in the sample. In fact, the maximum value $D_{\text{MNCO}}^{\text{max}} = 0.20$, so that

$$N = D_{\text{MNCO}}^{\text{max}} S / \epsilon \sim 10^{18} \text{ sites.}$$

The surface of the sample is ca. 2 m², therefore the concentration of active sites is 10^{14} sites/cm².

The values obtained are similar to those for the Rh catalyst. It seems likely that the metal concentration is determined mainly by the capacity of the support surface layer ($\gamma\text{-Al}_2\text{O}_3$) and depends slightly on the nature of the supported metal. Thus, on the basis of steady- and nonsteady-state spectrokinetic measurements we have managed to show that the mechanisms of CO + NO reaction over supported Pt and Rh

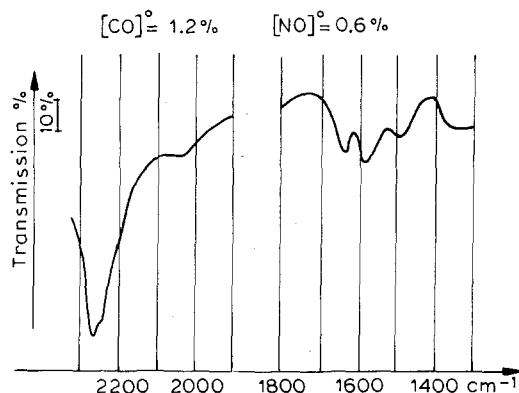


Fig. 24. Typical spectrum of surface compounds during CO + NO interaction over platinum group metals.

catalysts are very similar. The basic feature for both catalysts is the formation of nitrogen from the isocyanate complex, together with N_2O formation from the $\text{NO}_{\text{ads}} + \text{N}_{\text{ads}}$ reaction.

4.4. Interaction of CO and NO on supported Pd and Ru

We have studied 1 wt.-% Pd and Ru catalysts supported on Al_2O_3 . Under reaction conditions all catalysts show very similar spectra for the surface compounds (Fig. 24). Absorption bands at 1480, 1580, 1635, 2260–2270 cm^{-1} and a shoulder at 2240–2230 cm^{-1} are recorded in the spectra. At low temperatures, absorption bands of CO are also recorded. At high NO pressure the NO absorption band is observed. The 1580, 1635, 2260–2270 cm^{-1} absorption bands were assigned (above) to the isocyanate complex, localized on the support, and the 2240–2230 cm^{-1} absorption band to the same complex localized on the metal. The 1480 cm^{-1} absorption band is assigned to the vibrations of the surface carbonate complex CO_3^{2-} .

The reaction rates and NCO concentrations versus the reaction mixture composition are presented on Figs. 25 and 26 for all catalysts studied. It can be seen that for Pd and Ru catalysts these dependencies are intermediate between those for Pt and Rh catalysts. The relationship between concentration of surface compounds and reaction rate is also similar to that obtained for Pt and Rh. There is also a similarity in the parallel change of optical density of the carbonate complex absorption band with the rate of CO_2 formation. Some features in the behavior of the CO + NO reaction on Pd and Ru catalysts are very similar to those on Pt and Rh. Among them are: the relationship between concentration of surface compounds and the reaction rate; the parallel change of optical density of carbonate complex absorption band with the CO_2 formation rate; the presence of NCO localized on metal (2240 cm^{-1}); and NCO localized on the support (2260 cm^{-1}). On the basis of all these facts we conclude that the reaction mechanism over supported Pd and Ru is the same as over Pt and Rh.

4.5. The influence of oxygen on the CO + NO interaction over supported platinum-group metals

The majority of known catalysts for the CO + NO reaction lose their activity in the presence of oxygen. This is due to the competition between two reactions:



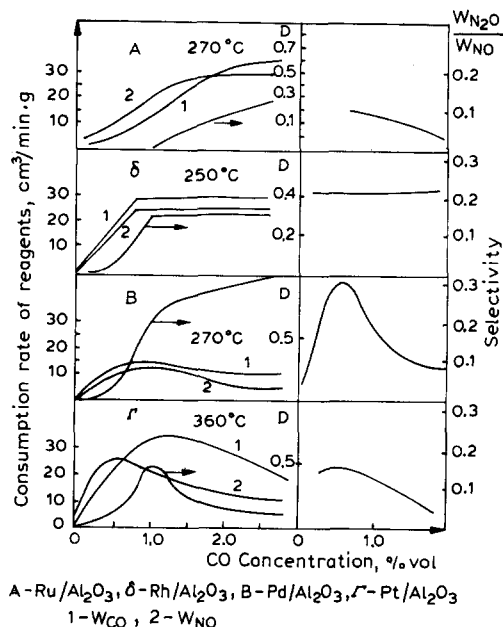


Fig. 25. Effect of CO concentration on activity (1 — W_{CO} , 2 — W_{NO}), isocyanate complex concentration (D) and selectivity in CO+NO reaction.

At 230°C on Pt, reaction (I) proceeds more rapidly than reaction (II). However, when a mixture of NO and O₂ with $P_{O_2}/P_{NO}=0.5$ is used, only 30% of CO is oxidized by NO, the rest reacting with O₂ [161]. The CO + O₂ reaction predominates over all metals of the platinum group, with the exception of Ir [162,163]. Shelef et al. [164] showed that CO is oxidized mainly by oxygen over practically all oxides of transition metals in a CO + NO + O₂ mixture. The loss of activity of oxide catalysts is likely to be due to oxygen adsorption on the sites where NO could be adsorbed. Witner [165] is of the opinion that in the presence of oxygen the rate of NO decomposition on the surface of metal oxides decreases due to NO and O₂ competition for the same sites.

We have studied the mechanism of the CO + NO reaction in the presence of oxygen on 1.0% Pt/Al₂O₃, 1% Rh/Al₂O₃ and 1% Pt–0.5% Rh/Al₂O₃ catalysts [153]. The effect of oxygen on the reaction rate and on the concentration of surface complexes on an Rh catalyst was studied at 250°C. Oxygen was added to a reaction mixture of 1.2% CO with various amounts of NO. Fig. 27 shows the selectivity (S), the consumption rates of CO (W_{CO}), NO (W_{NO}) and O₂ (W_{O_2}) as well as optical densities of NCO complex absorption band (D_{NCO}) and of carbonate complex absorption band (D_{1480}) versus oxygen concentration in the mixture with 1.8% NO. It can be seen that W_{NO} , D_{NCO} , D_{1480} decrease and W_{CO} and W_{O_2} increase with increasing content of oxygen in the mixture. Selectivity, $S = W_{N_2O}/W_{NO}$, does not depend on the oxygen concentration (curve 6). The optical density of the isocyanate absorption band (2240 cm⁻¹) is low (curve 3). As was mentioned above, this means that NCO complex is localized on the metal. According to the mechanism proposed here, this work, isocyanate complex, localized on metal is an intermediate in the nitrogen formation and N₂O is formed by the reaction $NO_{ads} + N_{ads} = N_2O$.

In Ref. [151] the constants of elementary steps for this mechanism were determined and on this basis the coverages of surface by intermediates were calculated. These coverages, plotted against content of oxygen in the mixture, are presented in Fig. 28. It can be seen that θ_{CO} and θ_{NO} do not depend on the oxygen content. The physical meaning of this is as follows. All the steps of the interaction between CO,

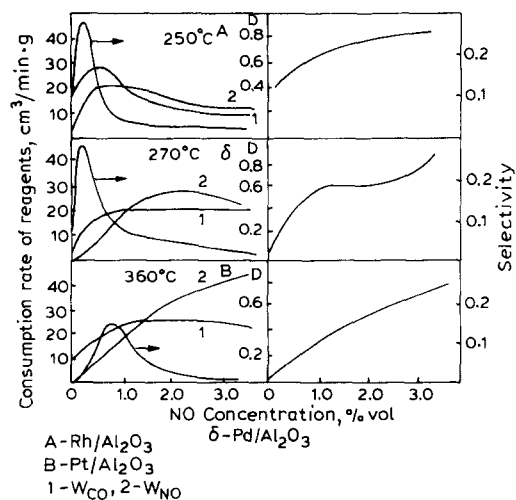


Fig. 26. Effect of NO concentration on activity (1 — W_{CO} , 2 — W_{NO}), isocyanate complex concentration (D) and selectivity in CO + NO reaction.

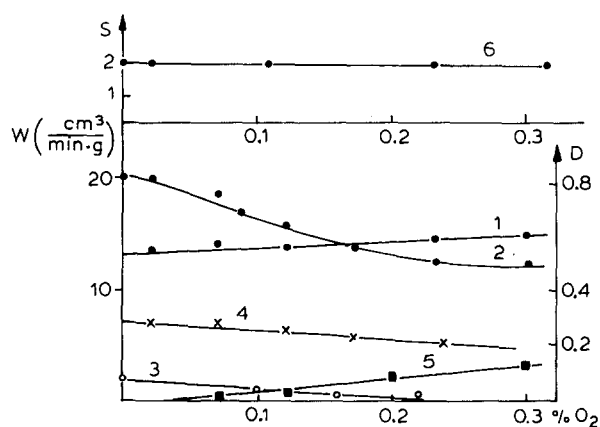


Fig. 27. Effect of oxygen content on W_{CO} (1), W_{NO} (2), D_{NCO} (3), D_{1480} (4), W_{O_2} (5) and S (6) over 1% $\text{Rh}/\text{Al}_2\text{O}_3$.

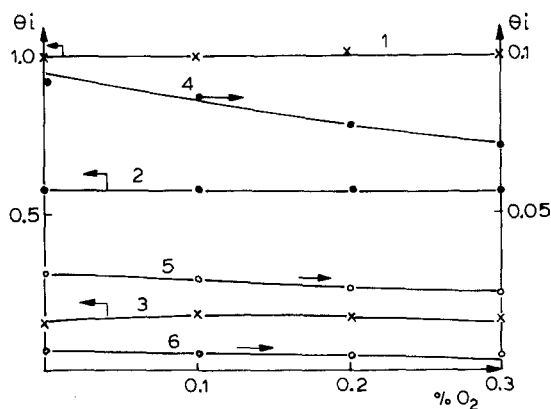


Fig. 28. Surface coverage of CO (1), NO (2), O (3), NCO (4), N (6) and free surface area (5) as functions of oxygen content in the reaction mixture over 1% $\text{Rh}/\text{Al}_2\text{O}_3$.

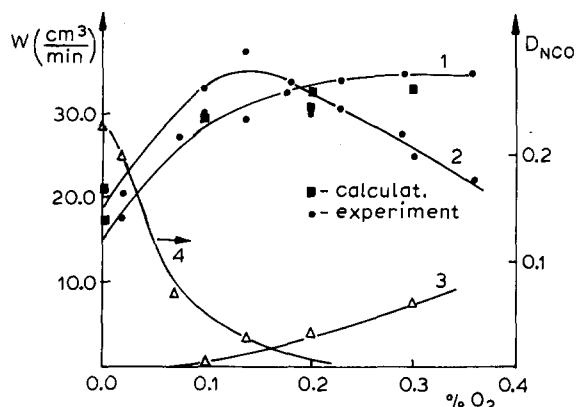


Fig. 29. Experimental and calculated values of W_{CO} (1), W_{NO} (2), W_{O_2} (3) and D_{NCO} (4) versus oxygen concentration over 1% Pt/ Al_2O_3 ($[\text{CO}] = 1.2\%$, $[\text{NO}] = 1.8\%$).

NO and O_2 take place on two different kinds of sites. On one of them only CO is adsorbed. At the CO pressure used all these sites are occupied and the reaction's proceeding does not change the value of θ_{CO} . Thus it will not depend on the content of oxygen in the reaction mixture. The coverage of the surface by NO molecules is determined by the ratio of NO pressure in the reaction mixture and the free surface area (since it is assumed that there is an adsorption-desorption equilibrium between NO molecules on the surface and in the gas phase). An increase of oxygen pressure leads, on the one hand, to a decrease in the free surface and, on the other, to an increase in the pressure of NO in the reaction mixture (at the expense of NO) (Fig. 27, curve 2). The combination of these two processes is likely to underlie the independence of θ_{NO} on the concentration of oxygen. The independence of θ_{NO} and θ_{CO} on the concentration of oxygen explains the independence of selectivity on O_2 content in the reaction mixture (Fig. 27, curve 6).

Using the rate constants presented in Ref. [151] and surface coverages (Fig. 28) we can calculate W_{CO} and W_{NO} on Rh/ Al_2O_3 on the basis of equations similar to (4.3). The values of reaction rates calculated in such a manner are presented in Fig. 27 (solid lines) together with the experimental results (points). It can be seen that the agreement is rather good. Fig. 29 shows similar data for Pt/ Al_2O_3 .

We have studied the effect of O_2 on the reaction rate over a Pt catalyst at 360°C . Fig. 29 shows the dependencies of W_{CO} , W_{NO} , W_{O_2} and D_{NCO} obtained with the addition of O_2 to the mixture containing 1.2% CO and 1.8% NO. It can be seen that W_{CO} and W_{O_2} increase continuously (curves 1,3), that W_{NO} (curve 2) passes through a maximum, and that D_{NCO} constantly decreases (curve 4), which is evidence for the decrease in the concentration of isocyanate complex on the metal.

The mechanism of the CO + NO reaction in the presence of O_2 on a Pt catalyst was described in Ref. [155]. Using the values given in that paper for the rate constants of the stages one can calculate the values of W_{CO} and W_{NO} . It can be seen (Fig. 29, curves 1 and 2) that the calculated and experimental data are in good agreement. The physical meaning of such a result is as follows. Addition of O_2 leads to an acceleration of the reaction of CO and O_2 . Because of this reaction, θ_{CO} is decreased, freeing sites for the adsorption and dissociation of NO and increasing θ_{N} and θ_{NO} . Calculations show that W_{NO} decreases because of the decreased coverage of the surface by CO molecules, and not because of a decreased rate of NO dissociation.

On the Pd catalyst the relationships under discussion are of the same character, and therefore the same explanation can be used for them. The results obtained for Pt–Rh catalysts can be explained by the set of properties of Pt and Rh catalysts.

Thus there exist two ways for oxygen to influence on the CO + NO reaction. The first is by freeing active sites on the surface through the interaction of CO and O₂. This is apparently characteristic of the catalysts on which all steps of the process occur on a single kind of site. On such catalysts, the drop in the rate of neutralization of NO with increasing oxygen concentration is due to the decreased coverage of the surface by CO molecules.

The second way is due to a decrease of the free surface and, as a result, a decrease in the rate of NO dissociation. Such an effect of oxygen is characteristic of catalysts on which the reaction of CO and NO occurs on two kinds of sites. The decrease in W_{NO} in this case is due to the decreased coverage of the surface by N atoms. Therefore, the catalyst that operates steadily in the presence of oxygen must be characterized by large values of the coverage of the surface by CO molecules and a rapid rate of NO dissociation. In view of what has been said above, it would seem useful in this context to create a Pt–Rh composite catalyst.

It was mentioned above that W_{CO_2} and the optical density of the carbonate complex absorption band change in parallel. According to the reaction scheme (4.1) $W_{\text{CO}_2} = k_7 S D_{1480} / \epsilon$. The data presented show that the increase of W_{CO_2} on the addition of oxygen is accompanied by a decrease of D_{1480} . This is possible if oxygen takes part in the process of CO₂ desorption. It was also noted that the observed carbonate complex is a charged molecule CO₂²⁻. It is quite probable that the transfer of charge from CO₂²⁻ to an oxygen molecule with the subsequent desorption of the neutral CO₂ molecule takes place via an associative substitution reaction. The results and their discussion show that the effect of oxygen on the CO + NO reaction on the supported Pt group metals is also described quite well on the basis of the isocyanate mechanism.

4.6. Regularities of the CO + NO interaction on supported metals

The bulk of IR data on the CO and NO interaction reveals that in all cases the isocyanate complex is formed on the surface of supported metals. The 2260 cm⁻¹ absorption band is assigned to the isocyanate complex localized on the support (Al₂O₃). Isocyanate complex cannot be formed on the support alone. It is formed on the metal atoms and then migrates to the support. The less intensive absorption band at 2240 cm⁻¹ is assigned to the vibrations of isocyanate complex localized on metal atoms. The appropriate absorption band of NCO on metals is in the 2180–2240 range [117].

It should be noted that surface isocyanate compounds recorded under reaction conditions have a range of reactivity. Fig. 30 shows the dependence of the reaction rate on the optical density (D_{NCO}) of the

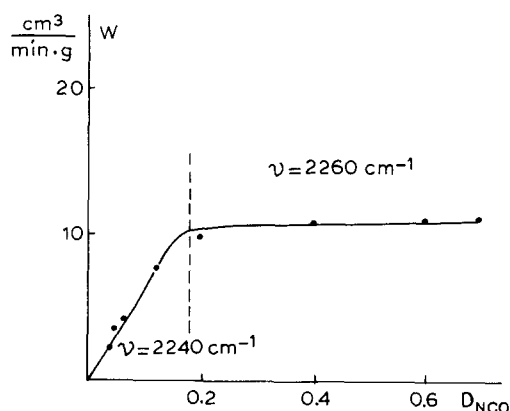


Fig. 30. Effect of optical density of isocyanate complex absorption band on NO consumption rate.

isocyanate absorption band. The data were obtained on the surface of supported platinum. The reaction rate changes in parallel with D_{NCO} when the low-frequency form of NCO (on metal) is observed in situ. Following the change of the intensities of absorption bands of NCO on metal and on support, we find that the migration of NCO complex to the support starts after its concentration on the metal surface reaches a steady value. This value depends on the experimental conditions, pointing to the existence of reversed spillover (from the support to the metal). Then, on the metal surface, NCO interacts with NO molecules, giving N_2 and CO_2 . We used these facts to determine the extinction coefficient of NCO which turned out to be $2.3 \cdot 10^{-19} \text{ cm}^2/\text{molecule}$.

The carbonate complex (1480 cm^{-1}) is also observed on the catalyst surface in situ. The optical density of its absorption band changes in parallel with the rate of the CO consumption when the concentration of reactants in the reactor changes. This band disappears if the reaction mixture flow is turned off.

Thus we conclude that there are two reactive complexes at the catalyst surface: the isocyanate and the carbonate, and we suggest a reaction mechanism (Sections 4.2–4.5) for the CO and NO interaction in which both of these complexes are intermediates. It is shown that the dependence of the reaction rates and selectivity on the reaction mixture composition can be quantitatively described only on the base of this mechanism.

However the question arises of why, in a complex system (CO , NO , O_2), nitrogen atoms formed after NO dissociation do not recombine but react with a CO molecule, resulting in the formation of NCO. One possible reason is that nitrogen atoms cannot migrate along the surface if there are other molecules on it. For example, the temperature of recombinative nitrogen desorption from a Pt surface increases by about 300°C in the presence of CO.

In addition, there are some published data concerning the existence of the $\text{Me} \begin{smallmatrix} \text{CO} \\ \diagup \text{NO} \end{smallmatrix}$ complex on the surface of platinum-group metals, which, after NO dissociation, can form the NCO complex. Further transformation of NCO results in molecular nitrogen.

Thus, our complex spectrokinetic study enables us to establish the sequence of elementary steps in the CO + NO reaction on the surface of supported platinum-group metals. This sequence turns out to be the same for all catalysts studied.

In conclusion, we present Table 4, which lists intermediates observed in the CO + NO reaction on metals. The degree of confidence in the cited data is also presented.

5. CO and NO interaction on oxide systems

5.1. CO and NO reaction on simple oxides

Systematic study [166–168] of the reaction of CO and NO on a variety of oxide catalysts reveals the following sequence of activity: $\text{CuO} > \text{Co}_3\text{O}_4 > \text{Mn}_3\text{O}_4 > \text{Fe}_2\text{O}_3 > \text{NiO} > \text{Cr}_2\text{O}_3 > \text{ZnO} (\text{V}_2\text{O}_5, \text{TiO}_2)$. The reaction starts below 100°C . The main reaction products are N_2O and CO_2 . The fraction of N_2O in the reaction products decreases with concurrent increase of N_2 concentration as the temperature increases. At constant temperature the relation between N_2 and N_2O in the reaction products depends on the contact time.

Sazonova et al. [169], in their study of the change of electric conductivity and of electron work function at NO and N_2O adsorption on oxides with electron (SnO_2 , TiO_2 , Fe_2O_3) and hole (NiO) conductivity, found that NO is adsorbed as NO^- and NO^+ . The relation between these adsorbed forms is defined by the nature of the oxide and by temperature. The conductivity in a reaction process ($\text{NO} + \text{CO}$) points to the fact that the negatively charged form NO^- takes part in the reaction.

Table 4
Intermediates in CO + NO reaction on metals

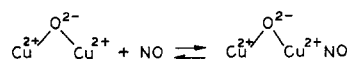
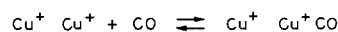
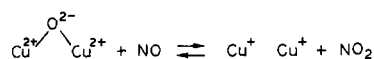
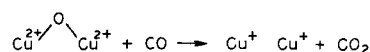
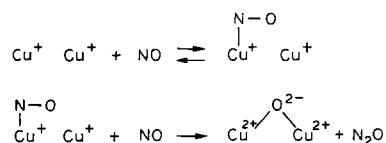
Catalyst	Intermediates	Degree of reliability	References
Pt-foil	CO _{ads} , NO _{ads}	H	[97]
Rh(100)	CO _{ads} , NO _{ads}	H	[92]
Rh(331)	CO _{ads} , NO _{ads} , O _{ads}	M	[93]
Pd(110)	NO _{ads} , CO _{ads}	M	[98,99]
Pt, Pd, Rh, Ir/Al ₂ O ₃	M–NCO	L	[103–105]
Pt/SiO ₂ , MgO, Al ₂ O ₃ , TiO ₂ , Ru, Ni/SiO	Pt–NCO, Support–NCO	L	[106]
	M–NCO	L	[112,113]
Pt/SiO ₂	NO _{ads}	L	[91]
Rh/SiO ₂	Rh–NCO, SiO ₂ –NCO, NO [–] , NO ^{δ–} , Rh–CO	M	[117]
Rh/Al ₂ O ₃	Rh–NCO, Al ₂ O ₃ –NCO	L	[114]
	Rh(NO)(CO)	L	[138]
	Rh(CO) ₂ , Rh–NO ⁺ , Rh–NO, Rh–NO [–] , Rh–CO, Rh ₂ –CO, Rh–CN, Al ₂ O ₃ –NCO	L	[130,139]
Pt–Rh/SiO ₂	Pt ⁺ _{Rh} –C=O, Rh–NCO	M	[135]
Pt–WO ₃ /SiO ₂	Pt–CO, Pt–NO, WO _x –CO, NCO, NO ₃ [–] , NO ₂ [–]	L	[137]
Ru/ZnO	Ru ²⁺ –NO, ZnO–NO, Ru–CO, Ru ²⁺ –CO, NCO, CO ₃ [–]	L	[140]
Pt, Pd, Ru, Rh, Pt–Rh/Al ₂ O ₃	M–NCO, M–CO, M–CO ₃ [–]	H	[147]
Ni/SiO ₂	Ni(NO) ₂ , Ni–CO, Ni–NO ₂	M	[144]
Cu/Al ₂ O ₃	Cu–CO, Cu ⁺ –CO, NCO	L	[145]
Cu–Cr/Al ₂ O ₃	Cu ²⁺ –NCO, Cu ⁺ –NCO, Cu ⁺ –NO, Cr ²⁺ –NO, Cu ²⁺ –CO, Cu ⁺ –CO	L	[146]

Glazneva et al. have studied compounds on Fe₂O₃ using IR spectroscopy during the CO + NO reaction [170]. A group of absorption bands in the 1200–1700 cm^{–1} range appears in the IR spectra. According to the authors, these surface complexes (carbonate–carboxylate, nitrate and nitrite) do not take part in the reaction. Only the adsorbed NO (1810 cm^{–1}) is active. Low intensity bands at 2210 and 2240 cm^{–1} were also recorded in the spectra. These were assigned to the vibration of the N₂O molecule. In fact, the intensity of these bands increases both upon N₂O addition to the cell and N₂O feed to the initial reaction mixture.

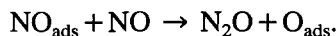
Solimosi and Rasco [173,174] have carried out a comparative study of supported and unsupported chromium oxide. The NCO complex was found on the catalyst supported on Al₂O₃, with simultaneous adsorption of CO and NO. The position of the NCO absorption bands (2262–2242 cm^{–1}) agrees very closely with that for metal supported on Al₂O₃. On this basis those bands were assigned to the vibrations in NCO localized over the support. One more strong band (2210 cm^{–1}) is observed in the spectra. This band has the following features. The band is formed at 350°C, and its intensity increases up to 450°C. The intensity of the band depends on the gas phase composition. It can be observed only in the presence of excess CO. It is stable below 200°C and quickly disappears from the spectrum above this temperature. The addition of a small amount of water causes its disappearance. The adsorption of CO and NO isotopes as well as HNCO adsorption were used by the authors to prove that the 2210 cm^{–1} band belongs to the vibrations of the surface isocyanate complex Cr–NCO. Thus, for oxide systems migration of NCO complex from metal ions to support is also possible. The migration rate depends on the nature of the support.

Lochov et al. [171,172] have studied the interaction of NO and CO over copper oxide supported on Al₂O₃ and SiO₂. Upon CO adsorption, carbonate–carboxylate complexes (1200–1650 cm^{–1}, CO_{2ads} (2350, 2370 cm^{–1}) and CO, bound to reduced ions (Cu⁺–CO, 2130 cm^{–1}) are recorded in the spectra. NO adsorption results in the formation of nitrite–nitrate structures (1200–1660 cm^{–1}) and NO complexes bound to Cu²⁺ ions (1880 cm^{–1}). The formation of Cu⁺–NO complexes (1740–1780 cm^{–1}) is also

possible. Upon the adsorption of a mixture of CO and NO, absorption bands at 2130 cm^{-1} (Cu^+-CO), 1880 and 1780 cm^{-1} ($\text{Cu}^{2+}-\text{NO}$ and Cu^+-NO) are recorded, as well as bands at 2270 , 2240 and 2140 cm^{-1} , which are assigned to the vibration of isocyanate complex. Its role in the reaction is not discussed. On the basis of the spectral data, the authors suggested a scheme for the CO–NO reaction in which the Cu^+-NO complex is an intermediate.



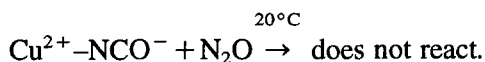
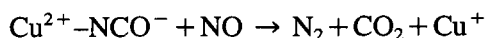
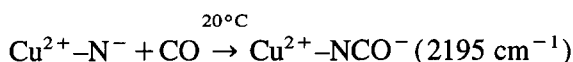
By following the change of the 1780 cm^{-1} absorption band intensity with NO pressure the authors [171,172] show that N_2O is formed by the interaction of adsorbed and gaseous NO:



London and Bell [175] have studied CO, CO_2 , NO, N_2O , NO_2 and N_2 adsorption on CuO/SiO_2 . The data obtained are used in the assignment of bands in spectra observed in the CO–NO reaction. The infrared study of Osmanov et al. [176] showed that on a Cu–Cr catalyst the CO + NO reaction proceeds via the following steps:



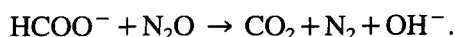
$$1775, 1710\text{ cm}^{-1}$$



This scheme can explain the observed poisoning of the CO– NO_2 reaction on the addition of NO.

The NCO complex was also observed in the CO–NO reaction on LaMO , where $\text{M} = \text{Cr}, \text{Mn}, \text{Fe}, \text{Co}, \text{Ni}$ [177].

The $\text{N}_2\text{O} + \text{CO}$ reaction on MgO was studied by IR emission spectroscopy and the response method [178]. An intermediate formate complex, formed with the help of OH group was observed. This transforms further according to the reaction:

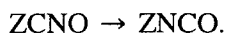
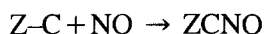
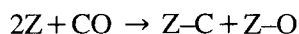


On the surface of redox catalysts, the $\text{N}_2\text{O} + \text{CO}$ reaction proceeds by surface oxidation followed by reduction.

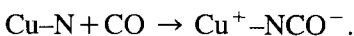
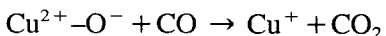
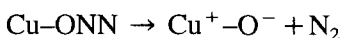
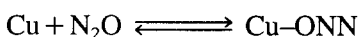
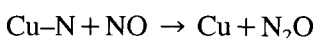
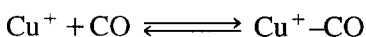
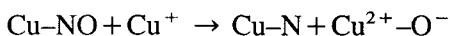
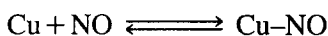
It should be noted that all the studies cited were performed under conditions far away from that of a real catalytic reaction. Nevertheless their results are in a good agreement with the suggestion about an intermediate character of adsorbed NO in $\text{N}_2\text{O} + \text{CO}$ reaction that was made in catalytic studies.

The formation of NCO complex on oxide systems is not regular. According published data, it has very weak absorption bands (if it is observed at all). It should be noted that most of the studies were performed under vacuum conditions. In this case some part of the oxide surface may be reduced. For example, Solymosi and Rasco [174] treated the sample under vacuum conditions and in hydrogen. It is natural to expect that the oxide surface is reduced after such a treatment. In fact, the observed NCO absorption bands (2210 cm^{-1}) practically coincide with that of NCO on metals. Thus NCO formation on oxides appears to be due their partial reduction. NO dissociation on metal atoms is much more probable than on ions.

Morrison and Thornton [179] have studied the mechanism of NCO formation on a $\text{SnO}_2\text{--CuO}$ catalyst. Using the isotope exchange technique they showed that oxygen in NCO came rather from the NO molecule than from CO. In other words, there is a dissociative CO adsorption on oxides:



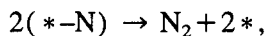
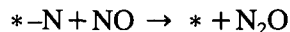
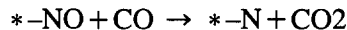
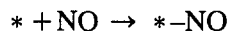
It should be noted that there are not so many studies in which the reaction rate and the rate of surface compounds transformation were measured at the same time. Among them, for example, is the investigation on a CuO/SiO_2 catalyst carried out by London and Bell [180]. Comparing spectral and kinetic data, authors suggested the reaction mechanism where adsorbed NO was an intermediate in the formation of N_2 . Under reaction conditions weak absorption bands of isocyanate complex were observed, pointing to dissociative NO adsorption:



As can be seen from the scheme, several different adsorption sites exist on the surface: Cu, Cu^+ , Cu^{2+} . NO dissociates and NCO forms on the reduced surface sites.

A very similar investigation was performed by Shin et al. [181] on a $\text{Cr}_2\text{O}_3/\text{SiO}_2$ catalyst. They measured catalytic activity simultaneously with recording IR spectra in a gradientless cell reactor. A correlation was found between CO_2 formation rate and the 1735 cm^{-1} absorption band intensity. This

band is due to vibrations of the NO molecule adsorbed as nitrosyl. The following scheme was suggested:

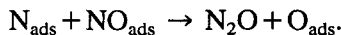
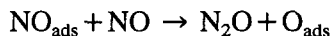


where * is an active surface site.

NCO complex was not observed under reaction conditions. The formed N_2O does not decompose and, hence, the catalyst has a great selectivity for N_2O formation.

Garrone et al. [182] showed that N_2 and CO_2 formation can proceed via an intermediate ($\text{CO} * \text{NO}$) complex.

Thus it can be seen that a consensus exists among all authors mentioned above on at least two conclusions: NO_{ads} is an intermediate in N_2O formation and $\text{N}_2\text{O}_{\text{ads}}$ is an intermediate in N_2 formation. However, several opinions exist on the way in which NO_{ads} transforms to N_2O . The most popular of them are:



Also, there is no consensus on how N_2O transforms to N_2 . The following routes are usually mentioned as possible ones: $\text{N}_2\text{O}_{\text{ads}} + \text{CO} \rightarrow \text{N}_2 + \text{CO}_2$, $\text{N}_2\text{O}_{\text{ads}} \rightarrow \text{N}_2 + \text{O}_{\text{ads}}$.

5.2. Spectrokinetic study of CO + NO interaction on spinel systems

The CO + NO reaction on the surface of CuCo_2O_4 , both supported on alumina and unsupported, was investigated by the spectrokinetic method [183]. The cell reactor shown in Fig. 2 was used. Adsorption of NO + CO at room temperature caused no changes in the region of stretching vibrations of NO and CO. In the low-frequency region, broad bands at $1330\text{--}1350\text{ cm}^{-1}$ and 1420 cm^{-1} appeared at the beginning of adsorption. Initially, they increased in intensity with time, the low frequency band becoming broader and shifting its maximum to $1320\text{--}1330\text{ cm}^{-1}$; a barely discernible band appeared at 1520 cm^{-1} . After about 90 min the band intensities reached their maxima and remained constant. Similar results were obtained when the catalyst was treated with the same mixture at 55 and 90°C. However, in this case the $1330\text{--}1350\text{ cm}^{-1}$ band underwent an earlier shift. The spectral changes recorded at 55°C are shown in Fig. 31. After the band intensities had reached their maxima at 25°C (Fig. 31), a further increase of temperature up to 450°C caused the following changes in spectra:

— at 50°C the 1330 cm^{-1} absorption band is shifted to 1320 cm^{-1} , its intensity and the intensity of 1420 cm^{-1} band decrease;

— at 130°C the band at 1420 cm^{-1} disappears;

— at 200°C the band at 1320 cm^{-1} is shifted to 1300 cm^{-1} , that at 1520 cm^{-1} disappears, after which a new band at 1560 cm^{-1} appears. The bands at 1300 and 1560 cm^{-1} disappear simultaneously at temperatures above 360°C.

Fig. 32 presents the consumption and evolution of NO and CO and spectral changes versus time for a stepwise heating of the catalyst in a CO + NO mixture. As can be seen from Fig. 32, introduction of the reaction mixture leads to consumption of both CO and NO from the gas phase, followed by an increase

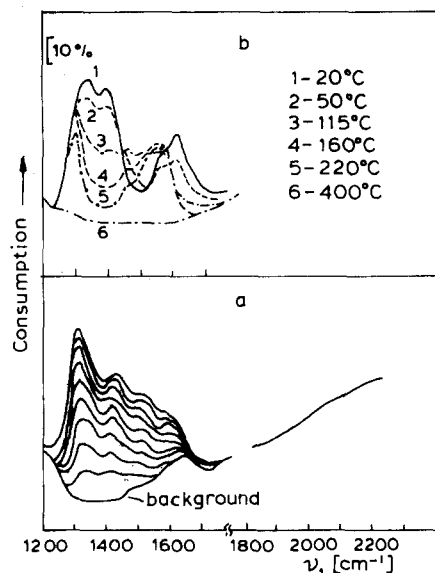


Fig. 31. IR spectra after CO + NO adsorption on $\text{CuCo}_2\text{O}_4/\text{Al}_2\text{O}_3$ (flow reactor) at (a) $T = 55^\circ\text{C}$, time interval = 10 min; (b) temperature increase.

in band intensities in the $1300\text{--}1600\text{ cm}^{-1}$ region. When the temperature is abruptly increased to 190°C , NO evolves into the gas phase. After a maximum rate of NO evolution is reached, the catalyst begins to consume CO. Simultaneously, the 1420 cm^{-1} band intensity decreases gradually until a constant value is reached after evolution of the main part of the NO. Further step-wise increases in temperature result in an additional consumption of CO. Above 250°C , consumption of NO occurs once again. It should be noted that in all cases when the catalyst was heated in a mixture of NO + CO, no bands were observed in the high-frequency region, which probably indicates the absence of any high concentration of adsorbed NO and CO, as well as of isocyanate complexes.

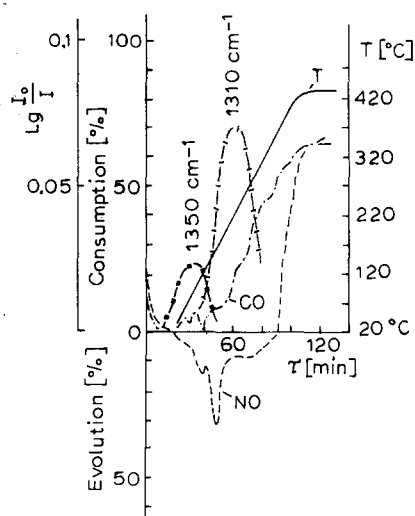
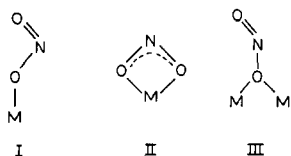


Fig. 32. IR spectra after CO + NO adsorption on $\text{CuCo}_2\text{O}_4/\text{Al}_2\text{O}_3$ (flow reactor) with a linear temperature increase.

We consider the structure of the adsorbed complexes we have been observed. Regardless of whether the high-temperature pretreatment of the catalyst was accompanied by an oxidation in a flow of NO or by a reduction in a flow of CO, the IR spectra show no absorption bands at above 1700 cm^{-1} . This indicates that complexes of the type $M^{n+}\text{-NO}$ are not formed. The fact that the bands at 1350 and 1420 cm^{-1} appear indicates that a bond is formed between NO and a surface oxygen atom. The absence of bands in the region of $1500\text{--}1600\text{ cm}^{-1}$, where NO_3^- groups absorb, shows that NO is not oxidized to nitrate structures during adsorption. In addition, the absence of N_2 , N_2O and NO_2 peaks in the TPD spectra indicates that NO does not dissociate during adsorption and catalyst heating. London and Bell [175] observed similar IR bands during NO adsorption and assigned them to surface nitro- and nitrite groups. On this basis, it can be assumed that NO (also in our experiment) is observed as nitro- and nitrite species, which are decomposed at high temperature, resulting in NO evolution to the gas phase. We have assumed these surface structures to be of the types 1–111 described by Nakamoto [12]:



It is interesting that the 2130 cm^{-1} band appeared during CO adsorption at temperatures below 230°C only after high-temperature (450°C) treatment of the catalyst in a CO atmosphere. As noted by Lokhov and Davydov [171], no bands corresponding to $\text{Cu}^{2+}\text{-CO}$ complexes were observed during adsorption of CO over CuY zeolites, $\text{CuO}/\text{Al}_2\text{O}_3$, CuCr_2O_4 and CuCl_2 at $> 20^\circ\text{C}$. The 2130 cm^{-1} band was attributed by these authors to CO adsorbed on partially reduced surface centers, resulting in the formation of $\text{Cu}^+\text{-CO}$ complexes. London and Bell [175] ascribed the 2130 cm^{-1} band which appeared after adsorption of CO on CuO/SiO_2 to CO attached to the copper sites present in a nonstoichiometric CuO phase. Thus, in our case the 2130 cm^{-1} band can be associated with $\text{Cu}^+\text{-CO}$ complexes appearing during CO adsorption on partially reduced sites.

The low-temperature bands appearing during cooling of the catalyst in a CO atmosphere after high-temperature treatment, can be due to bicarbonate and formate ions, formed from the interaction between CO and hydroxyl groups. The 1320 and 1540 cm^{-1} bands which were observed during admission of CO_2 at temperatures above 140°C can be assigned to surface carboxylate ions. The difference between the IR spectrum obtained for a mixture of $\text{CO}_2 + \text{O}_2$ and those for the individual adsorption of CO and CO_2 shows that a catalytic process occurs on the catalyst surface, even at room temperature. The 1360 and 1440 cm^{-1} bands may be assigned to carbonate structures formed during the course of CO oxidation. The changes observed in a $\text{CO} + \text{O}_2$ atmosphere with increasing temperature may be due to decomposition of a part of these surface structures. The bands at 1330 and 1570 cm^{-1} found in spectra above 100°C are associated with carboxylate complexes formed in the catalytic reaction.

The intense bands which appear in the low-frequency region at $1300\text{--}1700\text{ cm}^{-1}$ after adsorption of a mixture of NO + CO may be due either to surface structures formed as a result of a catalytic reaction and accumulated on the surface, or to surface intermediate complexes.

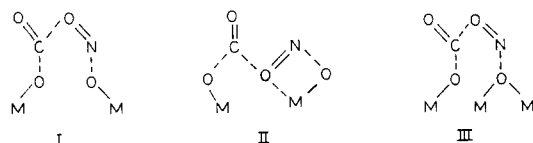
We follow the latter point of view, because:

(1) the bands observed differ considerably in position, intensity and behavior from those obtained during the adsorption of CO_2 and $\text{CO} + \text{O}_2$. This indicates that the surface species corresponding to these bands are not the products of CO auto-oxidation;

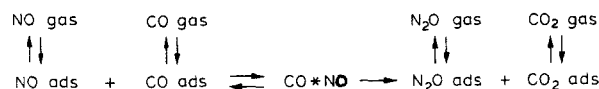
(2) the evolution of NO in the gas phase is accompanied by a decrease in intensity of the bands at 1350 and 1420 cm^{-1} , and no bands are observed for $M^{n+}\text{-NO}$ structures;

(3) the characteristics of the TPD spectra for the individual adsorption of NO and CO and for the adsorption of a NO + CO mixture are substantially different. There are at least three types of sites on the surface, two of them adsorbing only NO or CO. Competitive CO + NO adsorption and, hence, their interaction can proceed on the third one.

Thus the bands at 1330 and 1420 cm^{-1} which appeared initially at low temperatures can be attributed to CO*NO complexes formed in the mutually promoted adsorption of CO and NO. We propose the following structures for these complexes:



The interaction in the CO*NO complexes leads to breakage of the nitrogen–oxygen bond in NO and the formation of carbonate structures at room temperature. CO_2 evolves from the carbonate species upon decomposition and the bands at 1320 and 1520 cm^{-1} appear. This is confirmed by the fact that the temperature range in which these structures exist (20–200°C) corresponds to the temperature range in which CO_2 and N_2 are evolved in TPR spectra. An increase in temperature leads to an increase in the interaction in the CO*NO complexes: the intensity of the bands at 1330–1350 and 1420 cm^{-1} rapidly decreases while that of the bands at 1320 and 1520 cm^{-1} increases. The fact that the TPR spectra indicate simultaneous evolution of both reaction products and reagents in the temperature range 20–200°C, and that these processes end simultaneously, suggest that: (i) part of the surface CO*NO complexes are decomposed to CO and NO, and (ii) the desorption of products cannot be the rate-limiting step. We suppose that the interaction between CO and NO at low temperature (20–200°C) proceeds according to the following scheme:



It should be noted that there were no bands indicating the existence of isocyanate complex in the IR spectra in spite of the favorable CO:NO ratio. It is possible that surface isocyanate, formed from CO*NO complex, transforms quickly into N_2 . Its stationary concentration at the surface is small and it cannot be observed by the spectral method. The reaction of N_2 formation through the isocyanate complex is likely to be dominant at high temperatures.

5.3. NO + CO interaction over supported copper oxide

We have studied the CO + NO reaction over a alumina-supported 10 wt.-% CuO catalyst [184,185] (surface area 80 m^2/g). The Cu-containing systems could not be investigated by the spectrokinetic method using traditional absorption IR spectroscopy because of the low sample transmission. That is why diffuse reflectance spectroscopy was used (Section 2). We measured the consumption rates of CO and NO and the formation rate of N_2O simultaneously with optical densities of IR bands of surface structures versus CO and NO concentration and temperature. The results are presented in Figs. 33–37. Intense IR bands at 2130 and 2250 cm^{-1} are observed in the spectra obtained under reaction conditions. According to Ref. [172] the 2130 cm^{-1} band may be assigned to the absorption of CO bound with reduced copper ions $\text{Cu}^+ - \text{CO}$ (carbonyl structure), while that at 2250 cm^{-1} is assigned to the absorption

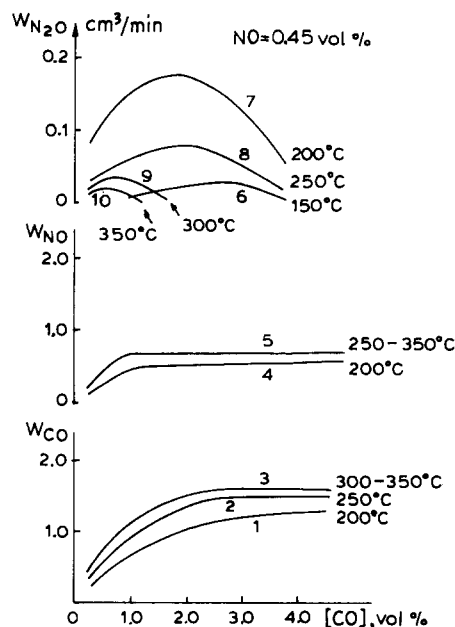


Fig. 33. CO (1–3) and NO (4,5) consumption rate, N_2O formation rate (7–10) versus CO concentration at various temperatures (0.45 vol.-% NO).

of isocyanate complex localized on the support [103]. Furthermore, carboxylate (1600 and 1380 cm^{-1}) and nitrate (1550 and 1300 cm^{-1}) complexes were observed on the catalytic surface.

To elucidate the reactivity of surface compounds observed in CO oxidation and in the reaction of CO and NO, the catalyst was treated with flowing of reaction mixture (CO + NO) at a predetermined temperature. Carbonyl, carboxylate and nitrate complexes thereby accumulated on its surface. After a steady state was reached, the flowing reaction mixture was replaced by a flow containing NO or CO. The intensity of the IR bands of the surface complexes thereby decreased, and the time dependencies of optical density (D) of surface complexes and of CO_2 formation rate were obtained at the given temperature. A typical result for a copper-containing catalyst is shown in Fig. 34. Linearizing the spectral curve in

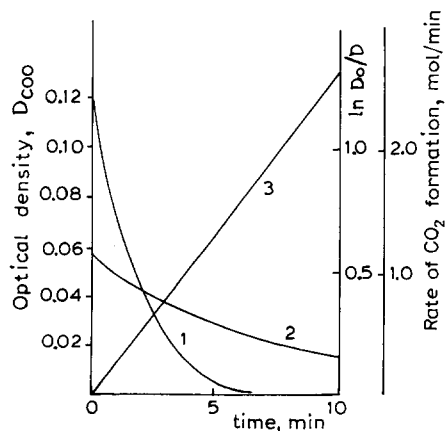


Fig. 34. Time dependencies of CO_2 formation rate (1) and of optical density of carboxylate absorption band (2), as well as treatment of (2) according to first-order equation after turning off CO from the reaction mixture over 10% Cu/ Al_2O_3 at 340°C .

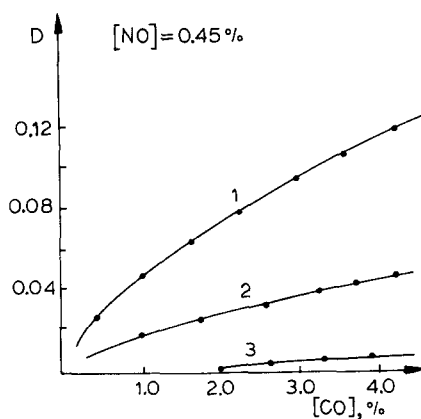


Fig. 35. Effect of CO concentration on optical density of carbonyl complex absorption band at various temperatures: 1, 200°C; 2, 250°C; 3, 300°C.

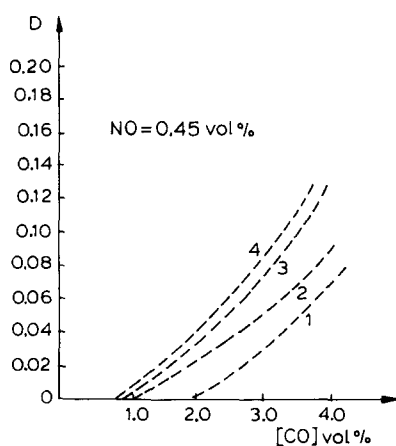


Fig. 36. Effect of CO concentration on optical density of isocyanate complex absorption band at various temperatures: 1, 200°C; 2, 250°C; 3, 300°C; 4, 350°C.

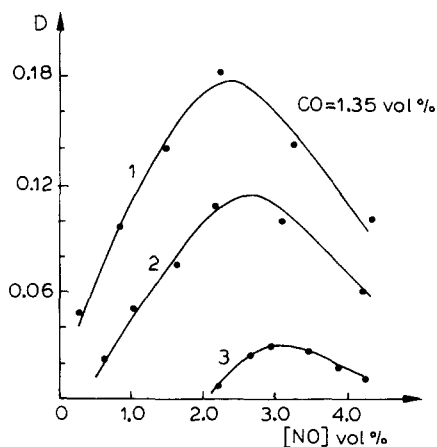


Fig. 37. Effect of NO concentration on optical density of carbonyl complex absorption band at various temperatures: 1, 200°C; 2, 250°C; 3, 300°C.

accordance with the first-order kinetic equation we obtain the effective rate constants for the reaction of surface complexes with O_2 or NO . Knowing the rate constants at various temperatures, we calculate the activation energy. Carbonyl reactivity was studied in the range 50–200°C, and carboxylate and nitrate reactivity at 300–450°C. Carbonyl complexes were found to be highly reactive. They disappear from the spectra very quickly and have a rather small activation energy (< 8 kJ/mol).

Carboxylate complexes do not react with NO . In flowing NO the relevant band (1600 cm^{-1}) hardly changes, while simultaneously intense nitrate absorption bands appear. Evidently, carboxylate complexes do not react with CO and NO over the test catalyst.

A similar conclusion could be drawn concerning nitrate complexes. The IR bands practically do not change when the sample is in a CO atmosphere, which is why attention in further investigations was paid to carbonyl and isocyanate complexes and their role in the reaction. Figs. 35 and 36 present the optical density of carbonyl and isocyanate absorption bands versus temperature and CO concentration (at constant NO concentration of 0.45 vol.-%). It can be seen from Fig. 36 that the D value of isocyanate complex increases with increasing temperature. Another relationship was observed for the carbonyl structure: D decreases with increasing temperature and at 300°C the band practically disappears from the spectra (Fig. 35). These relationships were typical for the ratio $[CO]:[NO] > 1$.

It can be seen from Figs. 33, 35 and 36 that when CO concentration in the reaction mixture increases:

- (1) the rates of CO and NO consumption increase up to some value, and then practically stop changing;
- (2) the rate of N_2O formation passes through a maximum;
- (3) the intensity of IR bands of carbonyl and isocyanate complexes increases.

At constant CO concentration in the gas phase ($[CO] = 1.35$ vol.-%), the intensity of carbonyl bands decreases with increasing temperature (Fig. 37). No IR bands of isocyanate complex are observed in this case. It can also be seen that when the NO concentration in gas mixture increases:

- (1) the NO consumption rate passes through its maximum value, reaching this value at about 1.4–1.5% of NO in the gas mixture;
- (2) the CO consumption rate increases and remains constant after $[NO] > 1.5\%$ when temperature $> 350^\circ\text{C}$ and begins to fall at temperatures $< 350^\circ\text{C}$;
- (3) the N_2O formation rate passes through its maximum value, reaching it at lesser NO concentrations and at lower temperatures;
- (4) the optical density of bands due to carbonyl complexes passes through its maximum, the value of which decreases and the position shifts to higher NO concentration at higher temperatures (Fig. 37).

We failed to observe bands attributed to nitrosyl complexes (Cu^+-NO , $Cu^{2+}-NO$, $Cu-NO$) in the spectra of these catalysts, although the existence of isocyanate complexes at the surface as well as the measurement of NO adsorption showed that NO adsorption occurs, the amount of adsorbed NO being quite large. These facts could be explained by assuming the formation of surface complexes without any characteristic $N-O$ vibration. The structure of such complexes has been presented above (Section 5.2). CO and NO molecules participate in redox processes on the catalytic surface. When the surface is oxidized by NO molecules, the conversion of Cu^+ ions into Cu^{2+} ions may occur. NO molecules are bound to surface oxygen ions, leaving Cu^{2+} ions free. However, at reaction temperature CO molecules are not adsorbed on Cu^{2+} ions. Formally, such a process can be explained by competitive adsorption of CO and NO on the surface sites. Notice that the oxidation of CO by oxygen occurs concurrently with an interaction between CO and NO . There are at least two sources of oxygen in the reaction system: O_2 as an impurity in the reaction flow and surface oxygen of the catalyst. At elevated temperature, the catalyst readily loses oxygen, the Cu^{2+} ions being converted into Cu^+ and Cu^0 .

Copper ions in different states exist on the surface under reaction conditions. The presence of an isocyanate complex band in the IR spectra of samples confirms the existence of Cu^0 (the dissociation of

NO proceeds effectively over them). The presence of Cu^+ ions is evident from the appearance of a $\text{Cu}^+ - \text{CO}$ complex band in the spectra. Cu^{2+} ions in the catalyst were observed by diffuse reflectance spectroscopy in the visible region. It appears that the distribution of copper ions in different states changes depending on temperature and CO and NO concentration in the gas phase. The degree of sample reduction was checked by reference to the optical density of the 2130 cm^{-1} band of carbonyl complex (D_{2130}). This value was determined in the following way: after spectrokinetic measurement, the sample was cooled to room temperature in flowing inert gas, then CO was adsorbed. The D_{2130} value obtained was indicative of the fraction of copper ions in the Cu^+ state. It turns out that D_{2130} value passes through maximum with increasing temperature in a reaction mixture of constant composition or with increasing CO content in the mixture. This means that Cu^{2+} ions can be quite easily reduced to Cu^+ and then to Cu^0 . This is just the process that can explain the dependence of D_{2130} on NO concentration in the gas phase. The data presented allow us to conclude that at high temperatures and CO concentrations, copper ions on the catalyst surface exist mainly in the Cu^0 and Cu^+ states, whereas at low temperatures and high NO concentrations the Cu^{2+} and Cu^+ predominate.

The data obtained indicate the occurrence of two reactions between CO and NO. At relatively low temperatures and CO concentration ($[\text{CO}]/[\text{NO}] < 1$) the interaction between adsorbed NO molecules results in the formation of N_2O in the gas phase and oxygen atoms on the surface. These atoms react with adsorbed CO molecules giving CO_2 in the gas phase.

At high temperatures and CO concentrations ($[\text{CO}]/[\text{NO}] > 1$) the degree of reduction of the surface increases; i.e. the NO dissociation rate increases. By interacting with adsorbed CO molecules, nitrogen atoms form isocyanate complexes, which react with adsorbed NO, giving N_2 . It should be noted that a similar mechanism was proposed for the CO + NO reaction on Cu–Co spinel (Section 5.2).

The above discussion can be summarized in the following scheme, describing the main features of the interaction between CO and NO on supported Cu-containing catalysts:

- | | |
|--|---|
| 1. $\text{Cu}^+ + \text{CO} \rightarrow \text{Cu}^+ - \text{CO}$ | 6. $\text{Cu} + \text{Z-NO} \rightarrow \text{Cu-N} + \text{Z-O}$ |
| 2. $\text{Z} + \text{NO} \rightarrow \text{Z-NO}$ | 7. $\text{Cu-N} + \text{Cu}^+ - \text{CO} \rightarrow \text{Cu-NCO} + \text{Cu}^+$ |
| 3. $2\text{Z-NO} \rightarrow \text{Z-N}_2\text{O} + \text{Z-O}$ | 8. $\text{Cu-NCO} + \text{Z-NO} \rightarrow \text{N}_2 + \text{CO}_2 + \text{Cu} + \text{Z}$ |
| 4. $\text{Z-N}_2\text{O} \rightarrow \text{N}_2\text{O} + \text{Z}$ | 9. $\text{Z-N}_2\text{O} + \text{Cu}^+ - \text{CO} \rightarrow \text{N}_2 + \text{CO}_2 + \text{Cu}^+ + \text{Z}$ |
| 5. $\text{Z-O} + \text{Cu}^+ - \text{CO} \rightarrow \text{CO}_2 + \text{Z} + \text{Cu}^+$ | |

Here Z denotes center of NO adsorption.

The scheme takes account of NO adsorption in a form that is inactive in the IR region, as well as the fact that various reactions occur at the surface at various degrees of reduction. On the catalyst surfaces with a high degree of reduction (large fraction of copper metal atoms at the surface) CO and NO interact effectively, giving molecular nitrogen. In this case, as for Pt group metals, isocyanate complex is an intermediate.

To support this scheme we can compare the conversion rate of surface compounds with the formation rate of CO oxidation products. If CO_2 is formed via carboxylate, the CO_2 formation rate in an excess of O_2 can be described by $W_{\text{CO}_2} = kN_{\text{COO}^-}$, where k is the effective rate constant of carboxylate conversion and N_{COO^-} is the amount of carboxylate complex on the surface. The k and N_{COO^-} values can be determined from spectrokinetic measurement. Indeed, from the known ratio $D = \epsilon N/S$, it follows that $N = DS/\epsilon$. Here D is the optical density of the respective band, ϵ is the extinction coefficient, and S is the geometrical sample surface in cm^2 . According to published data [186,187], $\epsilon = 6 \cdot 10^{-19}\text{ cm}^2/\text{molecule}$ for carboxylate and is $2 \cdot 10^{-18}\text{ cm}^2/\text{molecule}$ for carbonyl. The value of k found by linearization of curve 2 (Fig.

Table 5
Intermediates in CO–NO reaction on oxide catalysts

Catalyst	Intermediates	Degree of reliability	References
Fe ₂ O ₃	NO _{ads}	L	[170]
CuO/Al ₂ O ₃ , CuO/SiO ₂	Cu ⁺ NO	L	[171,172]
Cr ₂ O ₃ , Cr ₂ O ₃ /SiO ₂	NCO	L	[173,174]
Cu–Cr–O/Al ₂ O ₃	Cu ²⁺ NCO, Cu ⁺ NCO, Cu ⁺ NO, Cu ²⁺ CO, Cu ²⁺ NO, Cu ⁺ CO	L	[176]
LaMO ₃ (M = Cr, Mn, Fe, Co, Ni)	NCO	L	[177]
MgO(N ₂ O + CO)	HCOO [–]	M	[178]
SnO ₂ –CuO	NCO	M	[179]
CuO/SiO ₂	NCO	M	[180]
Cr ₂ O ₃ /SiO ₂	Cr(NO) ₂	M	[181]
Cr ₂ O ₃ /SiO ₂	CO*NO	M	[182]
Cu–Co–O/Al ₂ O ₃	CO _{ads} , CO*NO	H	[183]
CuO/Al ₂ O ₃	Cu ⁺ –CO, Cu–NCO	H	[184,185]

34) in coordinates of a first-order equation is 0.13 min^{-1} . Simple calculation shows that the rate of carboxylate decomposition is about three orders of magnitude less than the rate of CO₂ formation: at 340°C $W_{\text{CO}_2} = 2.6 \cdot 10^{19}$ molecules/min, as well as $W_{\text{COO}^-} = kDS/\epsilon = 2 \cdot 10^{16}$ molecules/min. For carbonyl complex, however, the agreement of the rates is rather good: at 100°C $W_{\text{CO}_2} = 5 \cdot 10^{17}$ molecules/min, and the CO₂ formation rate via carbonyl complex is $2.3 \cdot 10^{17}$ molecules/min ($D_{\text{CO}} = 0.1$ and the conversion constant of the carbonyl is 1 min^{-1} at this temperature).

These calculations also confirm that the CO + NO reaction proceeds via the carbonyl as an intermediate over Cu-containing systems.

The bulk of data on intermediates in the CO + NO reaction over oxide catalysts is presented in Table 5.

5.4. Some regularities of the surface steps proceeding in the CO–NO reaction on metals and oxides

On the basis of the data presented we can conclude that the catalytic properties of metals and oxides are different. Metals are more active. N₂, CO₂ and N₂O are the main reaction products. Oxide are less active, but can work at lower temperatures than metals. The main reaction products are N₂O and CO₂. At still higher temperatures, N₂O decomposes to N₂ and O₂.

The systematic spectrokinetic study carried out on various reaction mixture compositions and temperatures reveals that, under reaction conditions CO_{ads}, NO_{ads}, as well as isocyanate (NCO) and carbonate (CO₂[–]) complexes exist on the surface of supported Pt-group metals. NCO complex is an intermediate in the reaction of N₂ formation. It is formed when an adsorbed nitrogen atom reacts with adsorbed CO and then decomposes, reacting with adsorbed NO. Carbonate complex is a precursor of gaseous CO₂ formation. N₂O is formed via the following reaction:



Thus, the sequence of steps leading to the formation of N₂ includes CO and NO adsorption, NO dissociation and NCO formation.

Over oxides in the low temperature region the main product of the NO–CO reaction is N₂O. Adsorbed NO, CO molecules as well as CO*NO complexes are found to exist by spectral measurements at the surface. These complexes have been established as intermediates in the formation of N₂O. In the high temperature region the degree of reduction of the sample surface increases and an additional route for N₂ formation appears. Isocyanate complexes are recorded in the IR spectra of samples. According to spec-

kinetic measurements, NCO complex is an intermediate in this case. Its formation possibly occurs after NO dissociation over reduced surface sites.

To summarize, the reaction mechanism changes with increasing temperature. At low temperature, carbonyl complex is observed on the surface, and N_2O and CO_2 are the main products. At high temperature, NCO is formed on the surface, N_2 and CO_2 being the main reaction products.

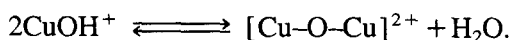
It is possible to construct one reaction scheme for all the catalytic systems studied. CO and NO adsorption results in the formation of a $CO*NO$ complex on the surface, CO_{ads} being an intermediate over supported CuO catalysts, NO_{ads} over simple oxides and $CO*NO$ complex over Cu–Co spinel. The subsequent reaction path depends on the possibility of NO dissociation. Over metals, where it is rather high, atomic nitrogen is formed, reacts with adsorbed CO resulting in NCO, and further formation of N_2 and CO_2 . On oxides, where NO dissociation is not so likely, transformation of the $CO*NO$ complex results in the formation of N_2O .

In other words, the basic difference between metal and oxide catalysts concerning their activity in the CO–NO reaction lies in their different ability to dissociate NO. On metal surfaces this process proceeds rather well, so metal catalysts are more active than oxides and spinels.

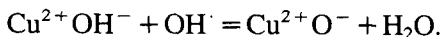
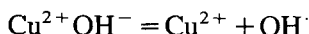
6. NO_x reduction over copper-containing zeolites

6.1. NO reduction by hydrocarbons

The recent discovery of the selective reduction of NO_x to nitrogen by hydrocarbons in lean mixtures (i.e. in mixtures with an excess of oxygen, as in the exhaust gases of Diesel engines) on zeolite catalyst Cu-ZSM5 [188] initiated a series of investigations devoted to this reaction and to the decomposition of NO over zeolites. The state of the copper in the zeolite catalyst was studied by ESR, ESCA, Auger and IR spectroscopy [188–192], and was found to be Cu^{2+} and Cu^+ , the later prevailing under reaction conditions. According to Ref. [188,192], the following reaction occurs:

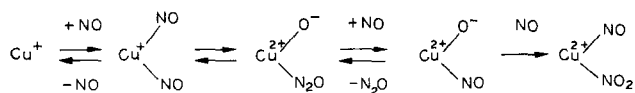


However, the formation of double clusters of copper is doubtful, because of the considerable distance between H^+ ions in H-ZSM5 zeolite. The following mechanism of autoreduction with formation of free radical sites was suggested by Larson et al. [190]:



According to this scheme, water oxidizes Cu^+ sites. It is known that water is a poison in the NO + hydrocarbon reaction in the presence of oxygen. Therefore, Cu^+ sites are active sites under catalytic conditions.

NO decomposition on Cu-ZSM5 proceeds at the same temperature as NO reduction by hydrocarbons. NO decomposition has been studied by spectral methods [188–190,193–195]. In practically all studies dinitrosyl complexes on Cu^+ were observed to form. Their subsequent transformation could be as follows [192]:



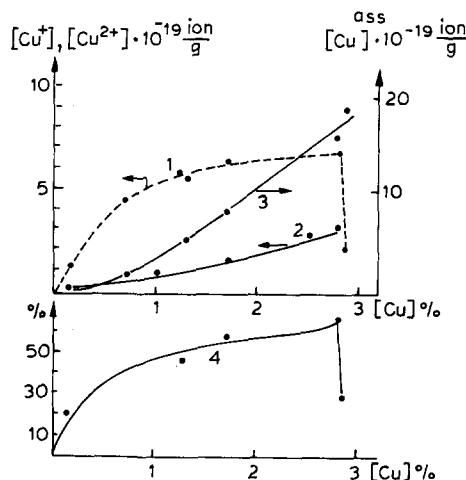
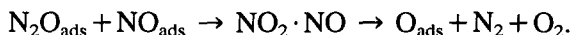


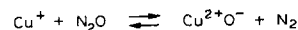
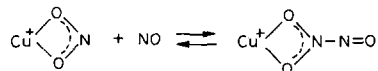
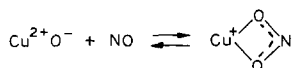
Fig. 38. Quantity of Cu^{2+} ions (1), Cu^+ ions (2) and of Cu associates (3) as well as NO conversion at 600°C (4) versus total quantity of copper in oxidized samples.

Decomposition of the last complex results in the formation of nitrogen and oxygen.

After the NO decomposition, $\text{NO}^{\delta-}$, $(\text{NO})_2^{\delta-}$ complexes on Cu^+ and $\text{NO}^{\delta+}$ on Cu^{2+} were found [194]. During the reaction the intensity of IR bands of $\text{NO}^{\delta-}$, and $(\text{NO})_2^{\delta-}$ decreases, while that of $\text{NO}^{\delta+}$ increases. Also, NO_3^- , NO_2^- and associative $(\text{NO}_2 \cdot \text{NO})$ complexes were found [195]. The last-named complexes are formed by the reaction:

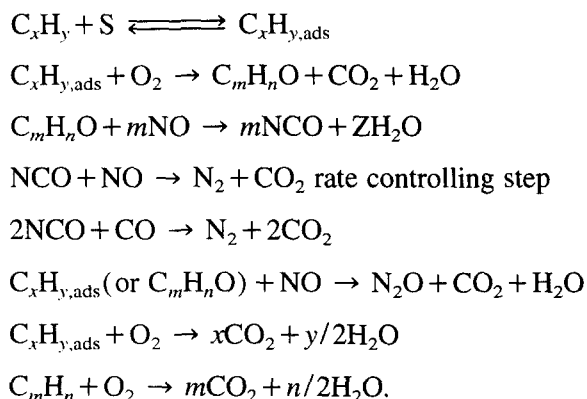


At room temperature, upon NO adsorption on Cu-ZSM5 [190], bands of $\text{Cu}^{2+}-\text{N}^-=\text{N}$ (2156 cm^{-1}), $\text{Cu}^{2+}-\text{NO}$ (1910 cm^{-1}), Cu^+-NO (1811 cm^{-1}), $\text{Cu}^+(\text{NO})_2$ ($1734, 1827 \text{ cm}^{-1}$) and $\text{Cu}^{2+}-\text{O}-\text{N}=\text{O}$ (1631 cm^{-1}) were observed in the IR spectra. At high temperature, as NO decomposition commenced, $\text{Cu}^{2+}-\text{NO}_2$ (2130 cm^{-1}), $\text{Cu}^{2+}-\text{NO}$ (1910 cm^{-1}), $\text{Cu}^{2+}-\langle \text{O} \rangle \text{N}=\text{O}^-$ (1502 cm^{-1}), $\text{Cu}^{2+}-\text{NO}$ (1811 cm^{-1}) and $\text{Cu}^{2+}-\text{O}-\text{N}=\text{O}$ ($1616, 1540, 1574 \text{ cm}^{-1}$) bands were found. The following mechanism of complex transformation and NO decomposition is suggested [190]:

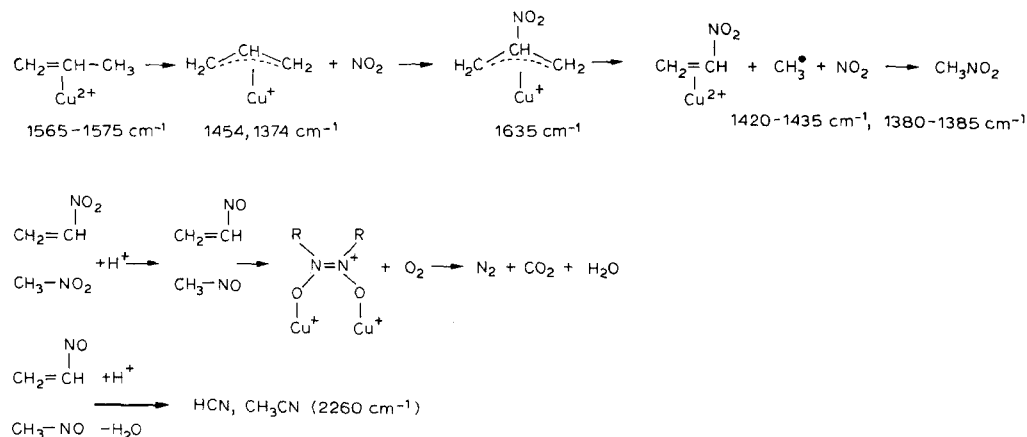


The mechanism of the NO + hydrocarbon reaction in the presence of oxygen was studied by a spectral technique [196–202]. Propene, propane [198] and isobutene [202] were used as reducing agents. Intermediates of hydrocarbons are not so well understood as NO forms. According to TAP reactor experiments (temporal analysis of products) [197], it is possible that coke is formed as an intermediate in this reaction. For example, during the reaction of $C_3H_6 + NO_x$ on Cu-ZSM5 in the presence or absence of oxygen, coke is formed, which then participates in the NO_x reduction, and is more active in the presence of oxygen. Zeolite possibly helps coke to form and maintains copper in the Cu^+ state.

In some cases isocyanate and cyanide complexes were found to be formed under the reaction conditions [199–201]. They can be bound with Cu atoms as well as with Al in zeolite. The reaction proceeds according to the following scheme [200]:

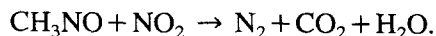


A more detailed scheme, based on IR spectral data in situ is presented in Ref. [201]:



According to this scheme, cyanides are inactive compounds, and isocyanates are not included at all.

The interaction of NO with hydrocarbons in the presence of oxygen has also been studied by spectral techniques on zeolites of ZSM type ion-exchanged with other cations. Over Ce-ZSM5 the $C_3H_6 + NO + O_2$ reaction was studied by IR spectroscopy in situ and by the kinetic response method with gas analysis [203,204]. Bands due to adsorbed NO_2 , NO_3^- , NCO and CH_3NO_2 were observed in the spectra. According to the authors, the following reaction proceeds:



The Ga-ZSM5 catalyst is very selective in the reaction of NO with methane and ethane [205–207]. Such unique properties of the catalyst are explained by dissociative adsorption of methane on Ga-ZSM5, proved by hydrogen exchange between CH_4 and CD_4 . NO reduction by hydrocarbons in the presence of oxygen was also studied on non-zeolite catalysts. Particularly, on $\text{Rh}/\text{Al}_2\text{O}_3$ [208] the $\text{C}_3\text{H}_6 + \text{NO} + \text{O}_2$ reaction proceeds in the following way: NO_2 and NO_3 are formed in an excess of oxygen and interact further with C_3H_6 , resulting in HNO_x and a weakly adsorbed radical, C_3H_5 , which is quickly oxidized by nitrates and nitrites to CO_2 . NO reduction by hydrocarbons on various zeolites modified by ZrO_2 as well as on complex oxides supported over $\gamma\text{-Al}_2\text{O}_3$ has been studied [209,210], R-NO_x , NO_x , nitrates, nitrites and NCO were found in the spectra.

It can be seen from this brief review that the intermediates in the NO reduction on zeolites are not well understood.

We attempted to investigate the main features of the interaction of reagents with atoms and ions of copper, as well as the role of different copper states in the NO reduction on Cu-ZSM5. Copper-containing samples were prepared by the ion-exchange method with of HZSM5 zeolite with 0.15, 0.70, 1.3, 1.7, 2.8% of Cu, and with Na-HZSM5 zeolite with 2.86% of Cu. The Si:Al ratio = 40, the degree of crystallinity = 95%. Fe contamination was not detected by ESR. The amount and coordination of isolated copper ions Cu^{2+} were determined by the ESR technique, and the amount of Cu^+ from TPD spectra after CO adsorption. IR spectroscopy in situ, TPD under flow conditions (N_2 as carrier gas, heating rate $20^\circ\text{C}/\text{min}$) and the ESR technique were used to study processes on the zeolite. The data obtained for NO reduction by propane on samples with various Cu contents show that NO reduction is rather effective at temperatures higher than 400°C (no zeolite activity in the absence of Cu was observed). However, further increasing the temperature (higher than 500°C) does not cause any increase of NO conversion; it even begins to fall with some samples. Nitrogen is the main reaction product, but at low temperatures a small amount of N_2O was recorded.

ESR data show Cu^{2+} ions to be localized in the square pyramidal and square planar coordinations. Fig. 38 shows different amounts of copper ions versus copper concentration, according to data obtained by ESR and TPD techniques. It can be seen that in oxidized samples (curve 2) Cu^+ ions are always present, and their amount continuously increases with Cu concentration. The amount of Cu^{2+} increases in the Cu-ZSM5 catalyst and drops in 2.86% Cu-Na-HZSM5 (curve 1). If the Cu concentration in samples is low practically all ions are isolated; but if it is high, most of them are involved in association (curve 3). In this figure, too (curve 4), the conversion of NO at 600°C is plotted against the Cu content of the sample. An obvious correlation between NO conversion and Cu^{2+} ion concentration in the sample exists, pointing to the possible participation of Cu^{2+} ions in the rate-limiting reaction step (activation of reagent molecules, for example).

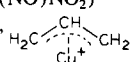
To clarify this problem we carried out a systematic study of samples containing copper ions of different valence and coordination. Our data, based on IR spectroscopy in situ and TPD, show that NO is activated by interaction with either zeolite or Cu^+ ions. When NO interacts with diamagnetic Cu^+ ion it is possible to form a species with an unpaired electron, which is observable by ESR. We failed to record such a complex in our ESR study of the interaction of NO with catalysts. It seems likely that the NO molecule with Cu^+ ions forms not a nitrosyl, but a nitrite complex. Moreover, the 1610 cm^{-1} band usually assigned to vibrations in a nitrite complex of copper ions [190] was recorded in the IR spectra of the samples after NO adsorption.

Oxygen is activated by interaction with reduced states of copper. Oxygen molecules rather effectively transform reduced copper ions to the Cu^{2+} state which is an active one for the catalysts studied. That is why, for example, NO cannot be reduced by propane in the absence of oxygen in gas the phase.

Propane is activated by interaction with acid sites of the zeolite.

Table 6

Intermediates in NO decomposition and reduction by hydrocarbons

Reaction catalyst	Intermediates	Degree of reliability	References
Decomposition of NO on Cu-ZSM5	O _{ads}	M	[188]
	Cu ⁺ NO, Cu(NO) ₂ , Cu(NO ₂) ⁻	M	[189]
	(Cu–O–Cu) ²⁺ , CuOH ⁺	L	[191,192]
	CuNO, Cu(NO) ₂	M	[193]
	Cu ⁺ NO ^{δ-} , Cu ⁺ (NO) ₂ ^{δ-} , Cu ²⁺ NO ^{δ+}	M	[194]
	Cu ⁺ (NO) ₂ , Cu ²⁺ (O)(N ₂ O), Cu ²⁺ (O ⁻)(NO), Cu ²⁺ (NO)(NO ₂)	M	[197]
	Cu ²⁺ –N=N, Cu ²⁺ NO, Cu ⁺ NO, Cu ⁺ (NO) ₂ , Cu ²⁺ –O–N=O, H		[190]
	Cu ²⁺ NO ₂ , Cu ²⁺ ⟨O⟩N=O ⁻		
	Cu ⁺ NO, Cu ²⁺ (NO)NO ₂	M	[197]
	CH ₂ =CH–CH ₃ , 	M	[201]
C ₃ H ₆ + NO + O ₂ on Cu-ZSM5	Cu ²⁺ , NO _{2,ads} , CH ₂ =CH–NO ₂ , CH ₃ NO ₂ , HCN, CH ₃ CN		
	CN, NCO	M	[199]
	Cu ⁺ (NO) ₂ , Cu ⁺ O _{ads}	L	[196]
	NCO, C _m H _m , C _x H _y O, NO _{ads}	M	[200]
	NO _{2,ads} , C _x H _y O	L	[198]
C ₈ H ₈ + NO + O ₂ on Cu-ZSM5	C _x , NO _{ads}	L	[202]
i-C ₄ H ₃ + NO + O ₂ on Cu-ZSM5	NO ₂ ⁻ , NO ₃ ⁻ , CH ₃ NO ₂ , NCO	H	[203,204]
C ₃ H ₆ + NO + O ₂ on Ce-ZSM5	CH _{3,ads}	L	[205–207]
CH ₄ + NO + O ₂ on Ga-ZSM5	C ₃ H _{5,ads} , HNO _x	L	[208]
C ₃ H ₆ + NO + O ₂ on Rh/Al ₂ O ₃	R–NO _x , NO _x , NCO, NO ₂ , NO ₃ ⁻	M	[209]

The bulk of the data obtained shows, not an original activation of reacting molecules (as was assumed above) but rather that some other, stepwise transformation of adsorbed forms on isolated Cu²⁺ ions is a rate-limiting stage of the reduction of NO by propane. We cannot, however deny the role of possible synergetic effects during interaction of the real mixture with the catalyst. But our TPD spectra, recorded after separate adsorption of NO and C₃H₈ and after adsorption of a mixture of the two, do not differ in essence.

Note, too, that in our ESR study of working catalysts we failed to record species containing active carbon, which were supposed to be active sites in Ref. [197].

It should be noted that NO reduction by hydrocarbons has been intensively studied only during the last 2–3 years. But despite this short time, a number of spectral investigations devoted to surface compounds have appeared. Unfortunately, not many of them are reliable enough; they do not satisfy spectrokinetic requirements. The most reliable is the observation of such intermediates as NO adsorption; less reliable observations concern complexes with both NO and hydrocarbons. The bulk of the data on intermediates in NO decomposition and reduction by hydrocarbons are presented in Table 6.

6.2. NO reduction by CO

A TPD study of CO adsorption on oxidized and reduced copper-containing zeolites shows that desorption of CO proceeds at 260–280°C. The quantity of desorbed molecules depends on the redox pretreatment of the sample. Under experimental conditions CO is adsorbed mainly on Cu⁺ ions. So we can consider the quantity of desorbed CO molecules to be a measure of the Cu ion content. The IR spectra after CO adsorption show a band at 2160 cm⁻¹ assigned to vibration in a linear carbonyl CO–Cu⁺. The optical density of this band depends on the pretreatment of the sample and the quantity of embedded copper ions. The position of the band (2160 cm⁻¹) does not change with copper concentration in the

catalyst, but its optical density (D_{2160}) and the intensity of the TPD peak of CO increases with increasing copper concentration.

Kinetic parameters of CO desorption were determined by IR spectroscopy in situ at 170–330°C in following manner: after adsorption of CO on 1.3% Cu-ZSM5 catalyst the flow containing 1% CO was switched to He and the optical density, D_{2160} , was followed. Kinetic curves were treated according to a first-order equation. The temperature dependence of the rate constants gives an activation energy for CO desorption of 12 kcal/mol.

D_{2160} decreases if the flow of nitrogen containing 1.8% of NO at temperatures below 100°C is introduced to a sample with preadsorbed CO, which points to a high reactivity of surface carbonyl. Further investigations of carbonyl reactivity were carried out in the temperature range 80–170°C. Similar experiments were carried out with addition of oxygen. The intensity of the absorption band of the carbonyl complex practically does not change in the presence of oxygen in this temperature region.

This observation is rather interesting: the point is that in all oxide systems the rate of interaction of oxygen with CO is essentially higher than that of NO (see, for example Ref. [149]). We decided to study the nature of this phenomenon.

The change of optical density of the 2160 cm^{-1} band with time after the addition of a flow containing NO is described in first-order equation coordinates. The activation energy of surface carbonyl consumption calculated from the temperature dependence of the rate constant is close to zero. It is known (see, for example, Ref. [211]), that NO molecules adsorbed on platinum-group metals can be substituted by CO molecules from the gas phase. This can possibly occur in our experiments (decrease of optical density D_{2160} , closed to zero activation energy of carbonyl consumption).

To check this assumption we conducted the a following experiment. The sample (2.8% Cu-ZSM5), placed in a cell for recording of diffuse-reflectance IR spectra, was treated with a gas flow containing 1% CO at 50°C and then with nitrogen. After that, the 2160 cm^{-1} band was recorded. Then a flow containing 1.8% of NO was fed to the cell and recordings were made of D_{2160} , concentration of CO at the reactor outlet, and CO_2 and N_2O concentration in the reaction products. Typical results of such experiments are presented in Fig. 39. Calculations based on transmission spectroscopy ($P = 18 \text{ mg}$, $D = 0.42$, $S = 2 \text{ cm}^2$, $\epsilon = 2.10^{-18} \text{ cm}^2/\text{molec}$) show that the number of carbonyl complexes at the surface of the 420 mg sample (such samples are usually used when studied by diffuse-reflectance spectroscopy) is 10^{19} . When NO is fed to the sample, CO, CO_2 and N_2O are found in the gas phase, pointing to the

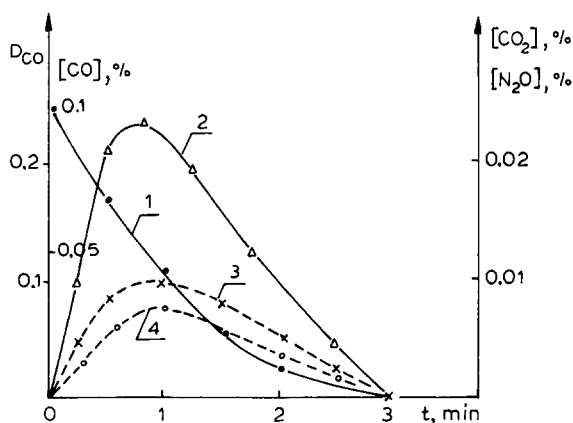


Fig. 39. Time dependencies of CO (2), CO_2 (3) and N_2O (4) concentrations, as well as of optical density of absorption band of Cu^+-CO (1) over 2.8% Cu/ZSM-5 at 1% NO in the reaction mixture. The sample was pretreated at 50°C in CO.

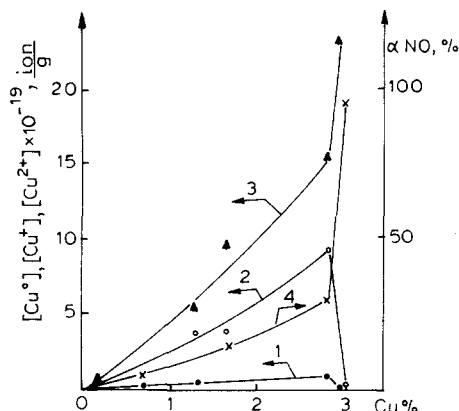


Fig. 40. Quantity of Cu^{2+} (1) ions, Cu^+ (2) ions and of metal Cu (3) as well as NO conversion at 500°C (4) versus total quantity of copper in the sample.

simultaneous occurrence of two processes: substitution and reaction. Quantitative comparison reveals that about 90% of CO is substituted on the surface by NO molecules and only 10% reacts with NO giving N_2O as a main reaction product. Measurements of surface complexes and reaction product concentration show that the Cu^+-CO complex is an intermediate in the reaction.

It seems likely that the reaction products CO_2 and N_2O are formed during the interaction of NO molecules (substituted surface CO species) with CO molecules still remaining on the surface. Such an assumption is also supported by an observed correlation between the concentration of Cu^+ ions in the sample and that of reaction products. This correlation proves once again that at low temperature (50°C in our case) CO and NO react to form N_2O on Cu^+ ions.

We also studied the $\text{CO} + \text{NO}$ reaction in a model mixture, containing 0.18% NO and 0.9% CO in nitrogen. Under the reaction conditions ESR study showed Cu to be reduced: the intensity of the ESR signal of Cu^{2+} is almost the same as the intensity for samples reduced in H_2 at 600°C . N_2 and CO_2 are the main reaction products at temperatures above 300°C . The temperature dependence of the catalyst's activity passes through a maximum. The decrease of activity at high temperatures is likely to be due to a change of catalyst itself (even its color changes). Fig. 40 shows the activity of samples at 500°C (curve 4), the quantity of Cu^{2+} (curve 1), of Cu^+ ions (curve 2), and of Cu^0 (curve 3) versus copper concentration in reduced samples. Curves 3 and 4 reveal a correlation between NO conversion and copper concentration in the sample.

According to current conceptions [149], NO dissociation is one of the most important stage in the $\text{CO} + \text{NO}$ reaction over platinum-group metals. Nitrogen atoms can either recombine, giving nitrogen in the gas phase, or react with adsorbed CO, forming isocyanate complex which in turn can either be an intermediate in NO reduction or can migrate to the support and take no part in the reaction.

Isocyanate complex was also observed under reaction conditions on copper-containing systems [184]. It is formed from the dissociation of NO on copper atoms appearing at the surface of the reduced catalyst at high temperature.

In our case, too, NO dissociation is possibly a rate-determining step. Its occurrence on metal atoms makes the observed correlation between NO conversion and metal atoms concentration in the sample quite understandable.

We attempted to record diffuse-reflectance IR spectra of surface complexes simultaneously with reaction rate. Under reaction conditions at $300\text{--}500^\circ\text{C}$ only a carbonyl complex band was recorded in the

spectra. An increase of the reaction rate is accompanied by a decrease of its band intensity. It is possible that carbonyl is also an intermediate in the high-temperature reduction of NO by CO. This conclusion can be supported by the following estimates. Simple calculations based on transmission spectroscopy ($P=20$ mg, $D=0.2$, $S=2$ cm², $\epsilon=2\cdot 10^{-18}$ cm²/molec) show that there are about $4\cdot 10^{18}$ carbonyl complexes on the surface of the sample used (2.8% Cu-ZSM5, 400 mg). An effective constant of the consumption of these complexes determined from the time dependence of D_{2160} at changing the flow from CO + N₂ to NO + N₂ is 0.9 min⁻¹. On the basis of the proposition that carbonyl is an intermediate, the reaction rate will be $W=kN=3.6\cdot 10^{18}$ molecules/min. The measured rate of NO consumption is $3\cdot 10^{18}$ molecules/min. The good agreement of these values points to the validity of our assumption concerning carbonyl complexes as intermediates in the reduction of NO by CO on Cu-ZSM5.

IR bands of adsorbed NO and of isocyanate complex are absent in the spectra probably due to both low surface coverage under reaction conditions (400°C) and low extinction coefficients in comparison with Cu⁺-CO.

Thus two mechanisms for the reduction of NO by CO on Cu-containing zeolites are valid. One, at low reaction temperatures, implies that NO and CO molecules adsorbed on Cu ions interact resulting in the formation of N₂O and CO₂. Another, at high temperatures, implies that CO adsorbed on Cu⁺ ions interacts with NO dissociatively adsorbed on Cu⁰, giving N₂ and CO₂. The Cu⁺-CO carbonyl was shown to be very reactive. Quantitative measurements show that Cu⁺-CO is an intermediate for both high-temperature and low-temperature reactions.

In a low temperature region, adsorbed CO molecules are substituted by NO molecules, which points to an effective interaction of NO with surface Cu⁺ ions. As has been shown above, the reverse effect was observed on platinum-group metals: the substitution of adsorbed NO molecules by CO from the gas phase. It seems likely that the strong bond of NO with surface of Cu-containing zeolites is the main reason for principal possibility of NO reduction in excess of oxygen.

7. Ammonia oxidation

7.1. Ammonia oxidation over metals

Interest in the reaction of ammonia oxidation is essentially related to the problem of synthesizing nitric acid. Furthermore, NH oxidation under conditions of olefin ammoxidation is an undesirable side reaction, which leads to considerable losses of ammonia. Under industrial conditions the oxidation of ammonia resulting in nitrogen monoxides and water with further formation of nitric acid proceeds at high temperature (800–1000°C) over platinum–rhodium nets, mainly according to a heterogeneous–homogeneous mechanism. Spectral investigations are usually carried out at lower temperatures, under conditions when both nitrogen and nitrogen oxides (N₂O, NO) are formed.

Dann et al. [212] recorded the 2056, 1914, 1650 and 1377 cm⁻¹ absorption bands in their study of the adsorption of ammonia on the surface of polycrystalline platinum. These bands were assigned to C⁻≡N, N=N and N–H vibrations, respectively (on the basis of a comparison of these spectra with spectra of adsorbed N¹⁵H₃ and N¹⁴D₃). According to the authors, carbon exists as an impurity on platinum. It was shown [213–215] that ammonia is adsorbed on metals in a molecular form at low temperatures, and dissociatively at high temperatures, forming NH₂ [216] and/or NH [217], which may possibly be more stable than NH₂. Gorodetski et al. [218] used EELS and TPD techniques to reveal HNO particles on the Pt(111) surface which are likely to decompose further to OH and N_{ads}. Gland and Korchak [220] studied the mechanism of ammonia oxidation under high-vacuum conditions and showed that, in excess

of ammonia, the platinum surface is covered mainly by nitrogen-containing complexes, while in excess of oxygen it is covered by oxygen-containing complexes. After the combined adsorption of ammonia and oxygen an interesting phenomenon was found by Thornburg and Madix [219]: the stabilization of adsorbed oxygen.

This brief review shows that the information currently available on the mechanism of ammonia oxidation is rather contradictory. This is because of the absence of data on intermediate complexes in the reaction. We have tried to obtain such data.

Fourier emission spectroscopy (Section 2) was used to study the reaction on the surface of massive metals. The emission spectra were recorded in the range from 2500 to 400 cm^{-1} . The scan number was 600–6000, normal resolution 8 cm^{-1} . The construction of the cell reactor used is described in Section 2. Metal disks (Cu, Fe, Au, Ag, Pt) of 40 mm diameter and 1 mm thickness were used as samples. Before measurement they were heated in a nitrogen flow up to the required temperature. The spectrum recorded was taken as the black body spectrum. Then nitrogen was replaced by the reaction mixture and after 20 min (for establishment of the reaction equilibrium) the spectrum was recorded once again. Dividing this spectrum by the spectrum of the black body we obtained the spectrum under reaction conditions. The intensity of absorption bands of N_2O (2225 cm^{-1}) and of NH_3 (1630 cm^{-1}) in the gas phase after reaction gives information on the rate of N_2O formation and NH_3 conversion.

Under reaction conditions copper becomes covered by a black film, a very intense and broad band with a maximum at about 1100 cm^{-1} appears in the spectra. Since copper oxides do not have an absorption band above 1000 cm^{-1} , and copper itself has a tendency to form ammines, the spectral pattern described above was assigned to ammines on the copper surface. Its rate of formation is rather large and it is almost impossible to measure the spectra of surface compounds at the surface of copper.

Ammines also can be formed under reaction conditions on gold and silver surface. However, their concentration and the rate of formation is not so high as on the copper surface. On a silver surface at 260–320°C, in addition to the broad band at 1150 cm^{-1} (similar to that on copper), a series of low intensity emission bands (at 2180, 2050, 1970, 1750, 1500–1400 cm^{-1}) is observed. This region of the spectrum (1300–2500 cm^{-1}) is shown in Fig. 41. It can be seen that the intensity of the 2180 cm^{-1} absorption band decreases gradually with increasing temperature. The intensity of other bands passes

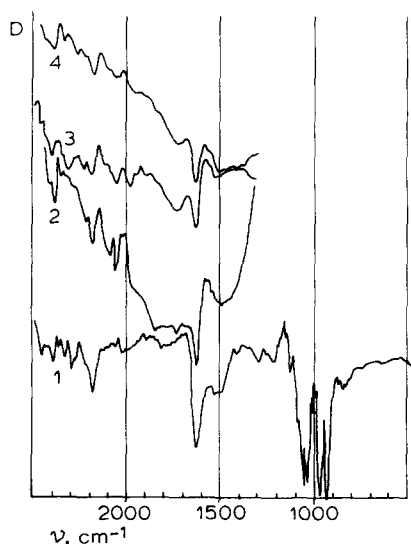


Fig. 41. Emission spectra under ammonia oxidation over Ar at various temperatures: 1, 200°C; 2, 260°C; 3, 320°C; 4, 340°C.

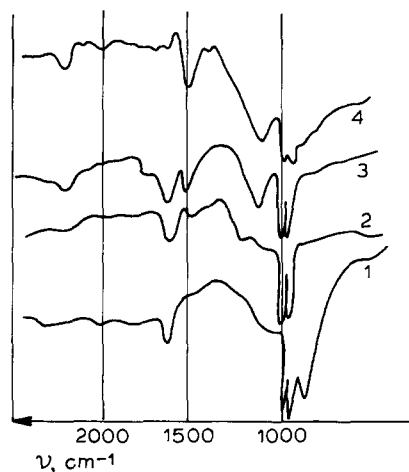


Fig. 42. Emission spectra under ammonia oxidation over Pt at various temperatures: 1, 200°C; 2, 230°C; 3, 260°C; 4, 320°C.

through a maximum at 260°C. Therefore, there are two groups of emission bands which differ in terms of the temperature dependence of their intensity. It should be noted that the band at 2180 cm^{-1} is also observed under reaction conditions on other metals. The bands in the $1900\text{--}2200\text{ cm}^{-1}$ region should be assigned to $\text{C}\equiv\text{N}$ (2180 cm^{-1}) and $\text{N}=\text{N}$ (2050 cm^{-1}) vibrations. The presence of bands in this spectral region is evidence for the dissociative adsorption of ammonia. Other emission bands are possibly due to vibrations of a complex of the type $\text{Me}(\text{NH}_3)_x(\text{NO})_y$ ($1970, 1750\text{ cm}^{-1}$: vibrations of NO, $1400\text{--}1500\text{ cm}^{-1}$ of NH).

An emission band at 1630 cm^{-1} due to ammonia vibration is also recorded in the spectra. Its decreasing intensity with temperature, given a constant feed rate of the reaction mixture, can be used to determine catalyst activity in the reaction. Simultaneously measured temperature dependencies of the catalyst activity and of the intensity of emission bands, when compared, show that the rate of ammonia oxidation becomes noticeable when the intensity of the emission bands in the region $1700\text{--}1800\text{ cm}^{-1}$ and $1400\text{--}1500\text{ cm}^{-1}$ starts to decrease. So it is possible that the complex $\text{Me}(\text{NH}_3)_x(\text{NO})_y$ is an intermediate in the formation of N_2 and N_2O . Complexes of similar type were detected by Naito and Tamaru [222] in their study of NO reduction by ammonia.

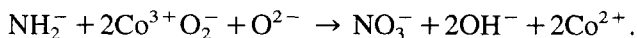
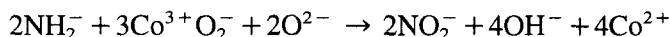
During the oxidation of ammonia on iron, bands at $2180, 2070$, and $1970\text{--}1800\text{ cm}^{-1}$ were recorded in the IR spectra under reaction conditions. The intensity of all bands decreases with increasing temperature. As above, the 2180 and 2070 cm^{-1} bands can be assigned to $\text{C}\equiv\text{N}$ and $\text{N}=\text{N}$ vibrations, respectively [212]. Other bands lie in the region where the vibrations of adsorbed NO molecules are usually recorded. Thus we can assume that adsorbed forms of NO are intermediates in the oxidation of ammonia on iron. Simultaneous measurements of spectral and catalytic properties proved this assumption.

Fig. 42 shows the emission spectra recorded under conditions of ammonia oxidation on platinum. They reveal bands at $2225, 2000$ and 1520 cm^{-1} . The intensities of the 2225 cm^{-1} band (vibrations of gaseous N_2O) and of the 1520 cm^{-1} band (vibrations of the N–H bond in the NH_2 complex) increase with increasing temperature. Comparison of spectral and catalytic data shows that the catalytic activity decreases when the intensity of the 1520 cm^{-1} emission band increases. It seems likely, that at low temperature, the surface of platinum is covered mainly by NH_2 complexes which, in the presence of oxygen, transform slowly to the reaction products. We failed to detect any oxygen-containing complexes on the Pt catalyst, possibly because of their rapid formation and decomposition.

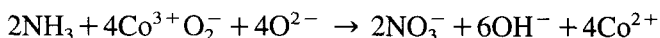
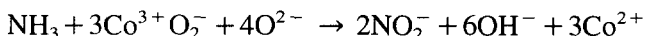
Thus, compounds found on the surface of iron, silver and platinum, are, respectively, adsorbed NO molecules, intricate oxygen-containing complexes and NH_2 complexes. On the basis of measurements of the reaction rate it is possible to place all metals studied in a sequence according to their activity in the ammonia oxidation: $\text{Pt} > \text{Ag} > \text{Au} > \text{Fe}$. This sequence agrees well with that presented in Ref. [223], where it is also noted that N_2 and N_2O are formed in parallel routes, and values of activation energy of NH_3 oxidation are presented (120 kJ/mol for Pt, 64 kJ/mol for Ag and 36 kJ/mol for Fe). Therefore, on the surface of catalysts with high activation energy complexes are observed which take part in the initial steps of the reaction, while on metals with low activation energy, complexes are found which take part in the steps close to the end stage (NO_{ads} on Fe). The general sequence of steps is evidently the same for all catalysts.

7.2. Ammonia oxidation over oxides: introduction

The spectral technique was also used to study the mechanism of ammonia oxidation over oxides. Several schemes have been proposed. In the oxidation of ammonia N_2O , NO and NO_2 complexes on the surface of metal oxides [224], and NO_2^- and NO_3^- complexes on the surface of CoO–MgO catalyst [225] were supposed to be intermediates. The following reaction mechanism was proposed by Zecchina et al. [225] (on the basis of IR and ESR data):

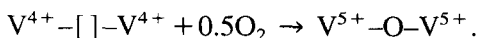
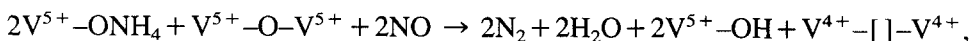
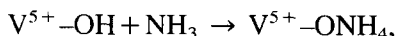


Also it is possible that the reactions

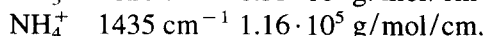
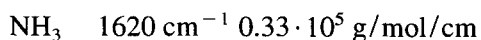


proceed. NO^- complex formation is also possible, but its band in the spectra is masked by bands due to NO_2^- and NO_3^- .

Various surface NH_3 complexes were recorded and identified during NH_3 adsorption over oxides [226–229]. On the surface of MgO an NH_2^- complex was observed under conditions of $\text{NH}_3 + \text{O}_2$ reaction [230]. During the oxidation of ammonia by nitric oxide on a NaY zeolite, an intricate surface complex was found: $(\text{NO})(\text{NH}_3)$. This subsequently decomposes, giving nitrogen and water [222]. Two NH_2^- complexes were found on the surface of Fe/SiO₂: Si– NH_2 (1550 cm^{-1}) and Fe– NH_2 (1610 cm^{-1}). On a vanadium catalyst [232,233] the NH_4^+ complex is supposed to be an intermediate in the oxidation of ammonia by NO. The following scheme is proposed for the reaction:



Alsdorf et al. [234] estimated the extinction coefficients of NH_3 and NH_4^+ complexes on $\text{MoO}_2\text{–SiO}_2$:



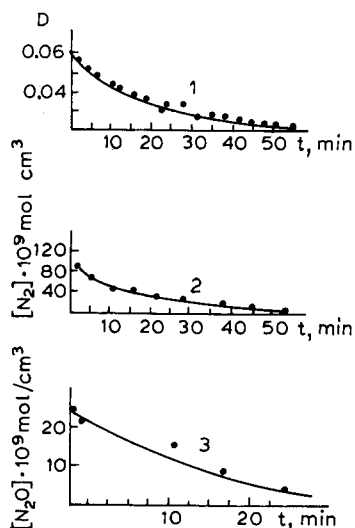


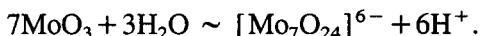
Fig. 43. Ammonia oxidation on MoO_3 . Time dependencies of NH_4^+ optical density (1), as well as of N_2 (2) and N_2O (3) concentration at 360°C after ammonia switching off from the reaction mixture.

We can compare these values and the values presented by Davydov et al. [38]: $\epsilon_{1430} = 2.15 \cdot 10^5 \text{ cm}^2/\text{mol}$ and $\epsilon_{1610} = 5.9 \cdot 10^5 \text{ cm}^2/\text{mol}$. We carried out a transmission and diffuse-reflectance IR spectrokinetic study of the oxidation of ammonia on the surface of MoO_3 [235], ZnO [236], Fe_2O_3 [237] and Cr_2O_3 [238,239].

7.3. Ammonia oxidation on MoO_3

Measurements were carried out in a catalytic microreactor, which served simultaneously as an IR cell. The catalyst was pressed into 60–70 mg pellets with an area of 2 cm^2 . The total weight of the catalyst in the experiment was about 1 g.

Treatment of MoO_3 with a mixture of ammonia and oxygen at $25\text{--}400^\circ\text{C}$ gives rise to a single band at 1430 cm^{-1} . In agreement with Tsyganenko et al. [226], this band is assigned to the bending vibrations of the NH_4^+ complex. The formation of NH_4^+ complex at the surface of an oxide catalyst is usually related to the catalyst's acidity. However, there is still no generally accepted opinion concerning the nature of the acid sites of the MoO_3 surface. We assume that there are several sources of protons for the formation of NH_4^+ . One can be associated with stabilization of Mo^{5+} ions, and another with the formation of polymolybdate species, for example, according to the equation:



In order to determine whether NH_4^+ complexes participate in the formation of N_2 and N_2O , we used the response method. Ammonia was excluded from the reagent mixture and the concentrations of NH_3 , N_2 and N_2O at the reactor outlet were followed. The change in the optical density of the 1430 cm^{-1} band ($D_{\text{NH}_4^+}$) over time was measured simultaneously. Typical results of such experiments are given in Fig. 43, which shows that the reaction products (N_2 and N_2O) are formed over a long period after ammonia had disappeared from the reactor zone. A drop in $D_{\text{NH}_4^+}$ over time was noted. It is natural to assume that the formation of N_2 and N_2O may proceed as a result of the reaction of the NH_4^+ surface complex with oxygen. In this case, the rate of nitrogen formation should be a function of the rate of decomposition of

the NH_4^+ surface complex. Information on this rate may be obtained by following $D_{\text{NH}_4^+}$ over time. If the formation of N_2 and N_2O occurs by parallel routes, the change in the NH_4^+ concentration at the surface will be described by the following equation:

$$-d\theta_{\text{NH}_4^+}/dt = k_1\theta_{\text{NH}_4^+} + k_2\theta_{\text{NH}_4^+} \quad (7.1)$$

Here, k_1 and k_2 are the effective constants for the consumption of the NH_4^+ complex to give N_2 and N_2O . Using the well known equation (Eq. (2.2)), we obtain

$$-dD_{\text{NH}_4^+}/dt = k_1D_{\text{NH}_4^+} + k_2D_{\text{NH}_4^+} \quad (7.2)$$

This equation quite satisfactorily describes the observed change in $D_{\text{NH}_4^+}$ over time and thus permits us to determine the sum $(k_1 + k_2)$.

The change of the nitrogen concentration in the reaction space in the case of nitrogen formation from NH_4^+ complexes adsorbed on the surface is described by the following equation:

$$V_r d[\text{N}_2]/dt = 0.5k_1\theta_{\text{NH}_4^+} - F[\text{N}_2], \quad (7.3)$$

where $[\text{N}_2]$ is the nitrogen concentration in the reaction space (mol/cm^3); V_r is the volume of the reaction space (cm^3); F is the flow rate (cm^3/min); and $\theta_{\text{NH}_4^+}$ is the amount of NH_4^+ complexes in the sample (mol).

A similar equation may be written for the change in the N_2O concentration in the reaction space

$$V_r d[\text{N}_2\text{O}]/dt = 0.5k_2\theta_{\text{NH}_4^+} - F[\text{N}_2\text{O}]. \quad (7.4)$$

We find $d[\text{N}_2]/dt$ and $d[\text{N}_2\text{O}]/dt$ by graphical differentiation of the time dependencies of $[\text{N}_2]$ and $[\text{N}_2\text{O}]$. Thus, the sum $(k_1 + k_2)$ may be determined from the spectral data using Eq. (7.2) and from the kinetic data using Eqs. (7.3) and (7.4).

$$V_r (d[\text{N}_2\text{O}]/dt + d[\text{N}_2]/dt) = 0.5(k_1 + k_2)\theta_{\text{NH}_4^+} - F([\text{N}_2\text{O}] + [\text{N}_2]). \quad (7.5)$$

Substituting the sum $(k_1 + k_2)$ found from Eq. (7.2) into Eq. (7.5), we may calculate $\theta_{\text{NH}_4^+}$ at different moments in time. The ratio of $(\theta_{\text{NH}_4^+})_1$ and $(\theta_{\text{NH}_4^+})_2$ calculated at times t_1 and t_2 is the same as the ratio of the optical densities $(D_{\text{NH}_4^+})_1$ and $(D_{\text{NH}_4^+})_2$ measured at the same moments of time. This finding justifies the hypothesis of parallel formation of N_2 and N_2O from the NH_4^+ complex. In addition, the possibility of calculating $\theta_{\text{NH}_4^+}$ at a moment of time t and knowledge of the optical density $D_{\text{NH}_4^+}$ at the same moment of time allows us to determine the extinction coefficient at the maximum of the 1430 cm^{-1} band, which is difficult to find experimentally.

The extinction coefficient estimated for 310°C agrees quite well with the value obtained experimentally using SiO_2 probes with different amounts of $(\text{NH}_4)_6\text{Mo}_7\text{O}_{24}$ [234].

Similar calculations carried out using the experimental data at $300\text{--}400^\circ\text{C}$ indicate a systematic decrease of ϵ with increasing temperature (to $0.68 \cdot 10^4\text{ cm}^2/\text{mol}$ at 380°C). Knowledge of the value of ϵ , in turn, permits the determination of k_1 and k_2 . These are only slightly temperature dependent. This finding indicates that the surface coverage by oxygen (θ_0), which may decrease with increasing temperature, is included within the experimentally determined values of k_1 and k_2 .

A study of the dependence of the reaction rate on the ammonia concentration showed that the rate of N_2O formation increases with increasing optical density of the 1430 cm^{-1} band. The rate of nitrogen formation increases with increasing ammonia concentration until NH_3 is present in the gas phase (Fig. 44).

The values for $k_1'\theta_0$ and $k_2'\theta_0$ determined from the segments of the curves for $[\text{N}_2] = f(t)$ and $[\text{N}_2\text{O}] = f(t)$ when NH_3 is absent from the gas phase were found to be equal to those obtained by spectral

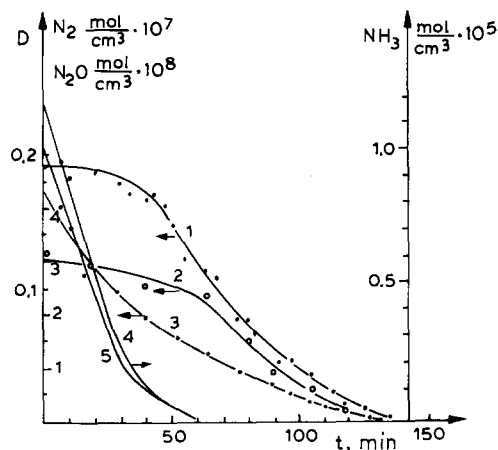
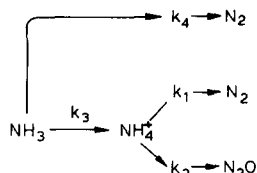


Fig. 44. Ammonia oxidation on MoO_3 . NH_4^+ optical density (1), as well as N_2 (2), N_2O (3) and ammonia (4 — inlet and 5 — outlet) concentrations versus time at 360°C .

measurements (Fig. 43). Knowing $k_1'\theta_0$ and $k_2'\theta_0$, we may calculate the steady-state rates of formation of N_2 and N_2O , assuming that, even in the presence of ammonia, N_2 and N_2O are obtained upon decomposition of the NH_4^+ surface complex.

In accordance with Eqs. (7.3) and (7.4), the steady-state rate of nitrogen formation (W_{N_2}) is equal to $1/2k_1\theta_0\theta_{\text{NH}_4^+}$ and that of N_2O formation ($W_{\text{N}_2\text{O}}$) is equal to $W_{\text{N}_2\text{O}} = 1/2k_2\theta_0\theta_{\text{NH}_4^+}$. Simple calculations show that the calculated value of $W_{\text{N}_2\text{O}}$ is equal to the experimental value. The calculated W_{N_2} is about one-half of the experimental value. The following experimental scheme may be proposed on the basis of the available data:



(7.6)

N_2O is formed only through the surface NH_4^+ complex. The formation of nitrogen proceeds via two routes: (1) through NH_4^+ ; and (2) through a mechanism which is not detailed in the present work. Knowing $k_1\theta_0$ and $k_2\theta_0$, we may easily separate the routes of nitrogen formation. The reaction rate through the route 1 is $W_1 = 1/2k_1'\theta_0\theta_{\text{NH}_4^+}$, while the rate through the pathway 2 is $W_2 = k_4[\text{NH}_3]$. Studying the dependence of W_2 on the NH_3 concentration at different temperatures we may evaluate the activation energy of nitrogen formation through the pathway 2. This activation energy was found to be 50 kJ/mol.

The dependence of the reaction rate on the oxygen concentration was studied under steady-state conditions. A typical result of these experiments is shown in Fig. 45. The rates of formation of N_2 , N_2O and $D_{\text{NH}_4^+}$ do not change when the oxygen content decreases from 90 to 75%. The independence of the reaction rate on the oxygen pressure at high oxygen concentrations indicates that adsorbed oxygen participates in the reaction.

Upon decreasing the oxygen content yet further, the rate of N_2O formation decreases linearly, while $D_{\text{NH}_4^+}$ increases linearly. The curve for W_{N_2} has two linear segments, reflecting the two reaction pathways.

Kinetic analysis of data presented in Figs. 43, 44, 45 on the basis of Eq. (7.6) shows that the value of θ_0 is maintained constant with decreasing ammonia concentration in the gas phase, i.e., with increasing oxygen concentration. Steady-state values of θ_0 decrease with increasing temperature. Knowing the value

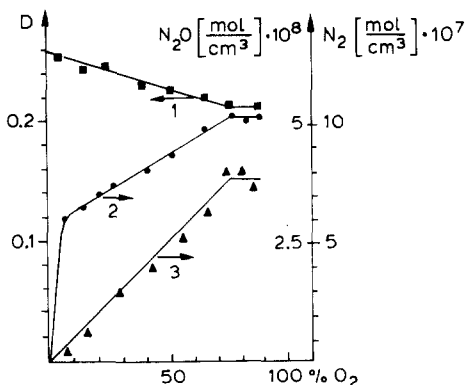


Fig. 45. NH_4^+ optical density (1), N_2 (2) and N_2O (3) concentrations versus oxygen content in the reaction mixture at 380°C .

of θ_0 we can calculate true values of the rate constants ($k' = k/\theta_0$) of the formation of N_2O and N_2 (through the route 1) and the corresponding values of the activation energies: $E_{\text{N}_2\text{O}} = 126 \text{ kJ/mol}$ and $E_{\text{N}_2} = 118 \text{ kJ/mol}$.

It should be noted that there are no literature data concerning the NH_4^+ surface complex as an intermediate in the reaction. This fact can be attributed to the lack of spectral studies on the transformation of surface complexes under ammonia oxidation conditions. It is also possible that only the first reaction step, related to the formation and oxidation of the NH_4^+ complex, may be observed spectrokinetically on such low activity catalysts as molybdenum oxide.

7.4. Ammonia oxidation on ZnO and Fe_2O_3

Treatment of a ZnO catalyst with a mixture of $\text{NH}_3 + \text{O}_2$ at $325\text{--}365^\circ\text{C}$ causes the appearance of two adsorbed bands: a weak one at 1625 cm^{-1} (due to vibrations of gaseous ammonia), and an intense one at 2200 cm^{-1} , assigned on the basis of spectral and chromatographic data to vibrations of the surface N_2O complex. The 2200 cm^{-1} absorption band appears in the spectra only after heating the sample in the reaction mixture to a temperature $T > 325^\circ\text{C}$, and disappears subsequent cooling. Treatment of the catalyst in oxygen as well as in the presence of the reaction products (N_2 and N_2O) causes no absorption in this spectral region. Admission of ammonia to the catalyst which has been treated in oxygen causes the appearance of the absorption band at 2200 cm^{-1} . Perhaps surface oxygen takes part in the formation of a surface complex: $\text{N}_2\text{O}_{\text{ads}}$.

Replacing the reaction mixture by oxygen leads to a rapid decrease in the intensity of the 2200 cm^{-1} absorption band. These data indicate that NH_3 and O_2 take part in the formation of the complex, whereas only oxygen is involved in its consumption stage.

To determine the role of the surface compound absorbing at 2200 cm^{-1} ($\text{N}_2\text{O}_{\text{ads}}$) in the reaction of ammonia oxidation we performed stationary spectrokinetic experiments with measurements of the transmission spectra. We simultaneously measured the rate of formation of the products (N_2 and N_2O) and the optical density of the absorption band at 2200 cm^{-1} (D_{2200}), which is proportional to the concentration of surface complexes. Typical experimental results are shown in Figs. 46 and 47. At constant oxygen content (40 vol.-%), both the reaction rate and the surface compound concentration increase with increasing ammonia concentration and ceases to change when the ammonia content in the reaction mixture exceeds 20%.

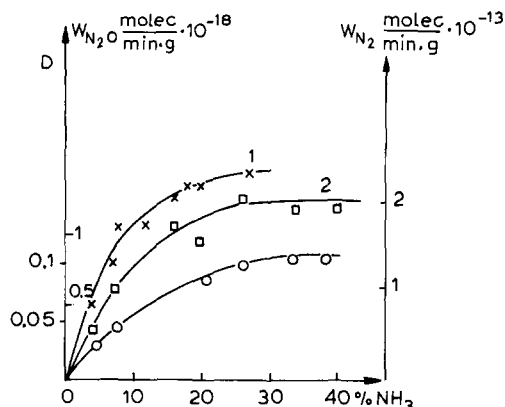


Fig. 46. N_2O (1) and N_2 (2) formation rates, as well as optical density of surface compound (D_{2200}) (3) versus ammonia content in the reaction mixture at 360°C . $[\text{O}_2] = 40\%$.

At a constant ammonia concentration, the reaction rate increases but the concentration of $\text{N}_2\text{O}_{\text{ads}}$ decreases with increasing oxygen concentration. This behavior of the parameters means that oxygen may be presumed to be involved in the consumption of the $\text{N}_2\text{O}_{\text{ads}}$ complex. It also follows from Fig. 46 that the rate of N_2O formation is proportional to the optical density of the absorption band of $\text{N}_2\text{O}_{\text{ads}}$:

$$W_{\text{N}_2\text{O}} = kD_{2200}. \quad (7.7)$$

Values of k calculated at various temperatures:

T (K)	615	633	648
k	7.5	9.1	12.5

were used to estimate the activation energy of the reaction. The value obtained (57 kJ/mol) agrees rather well with the available estimates [223], pointing to the possibility of $\text{N}_2\text{O}_{\text{ads}}$ being an intermediate in the reaction.

To compare quantitatively the rates of $\text{N}_2\text{O}_{\text{ads}}$ consumption and of $\text{N}_2\text{O}_{\text{gas}}$ formation we carried out nonsteady-state spectrokinetic measurements using diffuse reflectance spectroscopy. We simultaneously measured the reaction rate ($W_{\text{N}_2\text{O}}$) and the intensity of the 2200 cm^{-1} absorption band after a rapid change of the reaction mixture composition. A typical kinetic curve, obtained at 340°C after the reaction

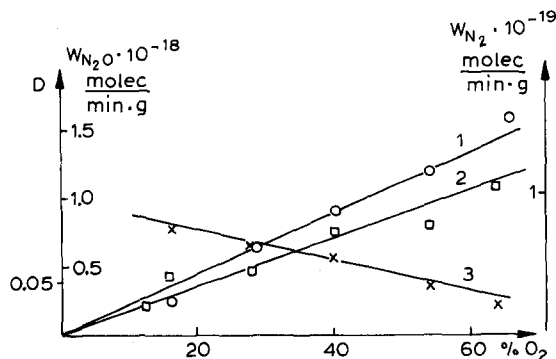


Fig. 47. N_2O (1) and N_2 (2) formation rates, as well as optical density of surface compound (D_{2200}) (3) versus oxygen content in the reaction mixture at 360°C . $[\text{NH}_3] = 20\%$.

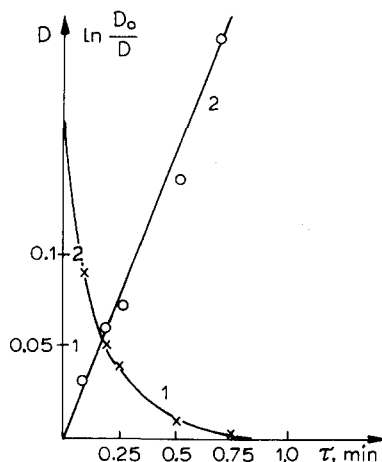


Fig. 48. Time dependence of optical density of surface compound (D_{2200}) after turning off ammonia flow from the reaction mixture (1) and its treatment according to the first-order Eq. (2). $T = 340^\circ\text{C}$.

mixture was replaced by oxygen (curve 1), as well as the results (curve 2) of its treatment according to the first-order equation are shown in Fig. 48. The corresponding rate constant for the consumption of the surface N_2O complex is 0.12 s^{-1} . The steady-state rate of N_2O formation in the gas phase at 613 K is $1.08 \cdot 10^{11}$ molecules/s/cm² ($0.58 \cdot 10^{18}$ molecules/min/g). If N_2O appears in the gas phase as a result of desorption of the surface N_2O complex, then the reaction rate can be expressed as

$$W_{\text{N}_2\text{O}} = k\theta_{\text{N}_2\text{O}}. \quad (7.8)$$

In order to evaluate $\theta_{\text{N}_2\text{O}}$, a coefficient that relates the band intensity and the surface coverage should be determined experimentally from the spectroscopic data. The experiments were performed in the following way. The products of desorption of the surface complex, which were formed upon replacing the reaction mixture by oxygen, were frozen out at 200 K in a trap filled with silica gel. The N_2O content in the gas which evolved after heating the trap was determined by chromatography. At 613 K, the intensity of the band, which is equal to 0.17, turns out to correspond to a surface concentration of the complexes of $7.1 \cdot 10^{11}\text{ cm}^{-2}$. The rate of N_2O evolution into the gas phase, calculated using Eq. (7.8), will thus reach $0.85 \cdot 10^{11}$ molecules/s/cm². This value is in agreement with the experimentally obtained rate of N_2O formation ($1.08 \cdot 10^{11}$ molecules/s/cm²). Such an agreement seems to be a sound argument in favor of the hypothesis that the observed surface complex $\text{N}_2\text{O}_{\text{ads}}$ is an intermediate in the oxidation of ammonia on ZnO.

It is known [223] that the formation of N_2 and N_2O occurs simultaneously during the low-temperature oxidation of NH_3 , i.e., the main regularities in the formation of these products are very much the same. Therefore, a formal relationship between W_{N_2} and $[\text{N}_2\text{O}_{\text{ads}}]$ is revealed. However, the value of the rate of $\text{N}_2\text{O}_{\text{ads}}$ conversion does not coincide with the rate of N_2 formation. This means that a common complex, a precursor of both N_2 and N_2O , is formed and decomposed in the stages preceding the desorption of the $\text{N}_2\text{O}_{\text{ads}}$ complex.

The results of the diffuse-reflectance IR investigation of the oxidation of ammonia on the surface of $\alpha\text{-Fe}_2\text{O}_3$ are shown in Fig. 49. Two absorption bands of hydroxyl groups (at 3650 and 3750 cm^{-1}) are recorded after treatment of the catalyst in flowing of oxygen (400°C , 1 h) with subsequent cooling to 220°C (spectrum 1). In the presence of ammonia the 3650 cm^{-1} absorption band splits into two bands at 3650 and 3620 cm^{-1} , pointing to the interaction of OH groups with ammonia molecules. An NH_4^+ complex is formed as a result of this interaction and we can see its absorption band at 1420 cm^{-1}

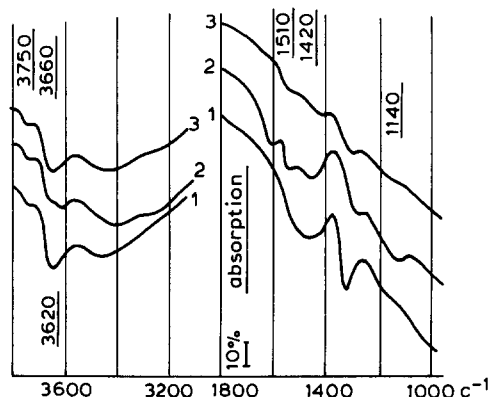


Fig. 49. Diffuse reflectance spectra during ammonia oxidation over Fe_2O_3 : 1, initial spectrum, $T=220^\circ\text{C}$, oxygen; 2, $\text{NH}_3 + \text{O}_2$, $T=220^\circ\text{C}$; 3, $\text{NH}_3 + \text{O}_2$, $T=320^\circ\text{C}$.

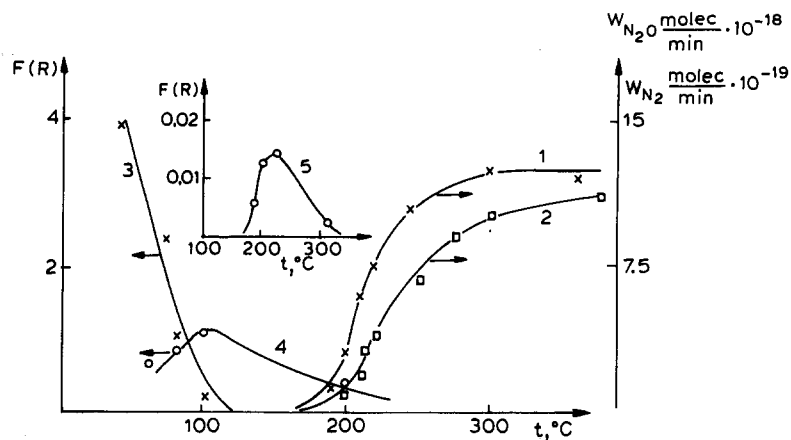


Fig. 50. Intensity of 1440 cm^{-1} (3), 1620 cm^{-1} (4) and 2080 cm^{-1} (5) absorption bands in units of Kubelka Munk function $F(R)$, as well as $W_{\text{N}_2\text{O}}$ (2) and W_{N_2} (1) versus temperature over Cr_2O_3 .

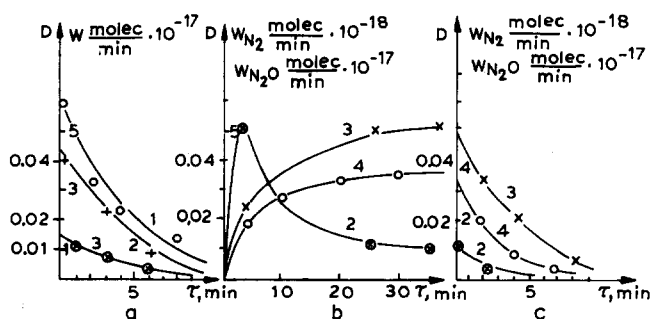


Fig. 51. Time dependencies of optical densities of 1620 cm^{-1} (1) and of 2080 cm^{-1} (4), as well as of W_{N_2} (2) and $W_{\text{N}_2\text{O}}$ (3), (a) after ammonia is turned off from the flow; (b) during transition to steady state; (c) after ammonia is turned off from the reaction mixture (D_{2080} was followed). Cr_2O_3 at 240°C .

(spectrum 2). Also the bands of coordinatively bound ammonia (at 1140 and 1620 cm^{-1}) and of the surface NH_2 complex (at 1520 cm^{-1} , low intense) are recorded.

Thus, under reaction conditions there are OH-groups, coordinatively bound ammonia, NH_4^+ and NH_2

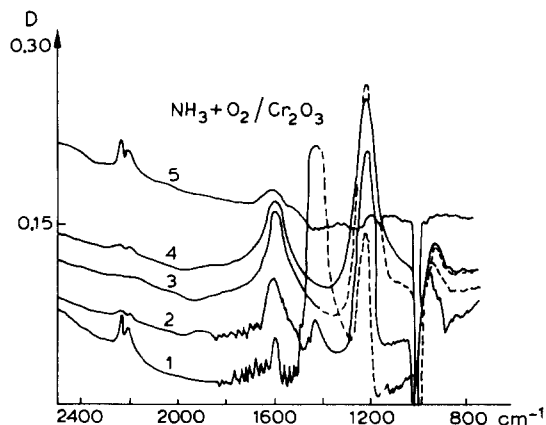


Fig. 52. FTIR spectra during ammonia oxidation over Cr_2O_3 at: 1, 150°C; 2, 220°C; 3, 230°C; 4, 250°C; 5, 320°C.

complexes on the surface of the catalyst. We performed a spectrokinetic study of their role in the reaction and have found that:

- NH_2 complex is an intermediate;
- N_2 and N_2O are formed in parallels; and
- the activation energy of the reaction is 95 kJ/mol, which is quite close to the value determined by Golodets [223].

7.5. Ammonia oxidation on Cr_2O_3

Under steady-state reaction conditions absorption bands at 1150, 1220, 1440, 1620 and 2080 cm^{-1} were recorded on the surface of Cr_2O_3 . Depending on the pretreatment of the sample (reduction or oxidation), one observes adsorption bands at 1150 cm^{-1} (for reduction) or 1220 cm^{-1} (for oxidation). They were assigned to the vibrations of ammonia, coordinatively bound with Cr^{2+} , or Cr^{3+} , respectively [38]. The absorption band at 1620 cm^{-1} is also assigned to these vibrations. The 1440 cm^{-1} absorption band is due to vibrations of NH_4^+ complex, which is likely to be formed from water present in the reaction

Table 7
Intermediates in NH oxidation

Catalyst	Intermediates	The degree of reliability	References
Pt(111)	HNO	L	[218]
Pt	NH_2	M	[221]
Ag	$(\text{NH}_3)_x(\text{NO})_y$	M	[221]
Fe	NO_{ads}	M	[221]
Metal oxides	$\text{N}_2\text{O}_{\text{ads}}$, NO_{ads} , NO_2	L	[224]
CoO–MgO	NO_2^- , NO_3^-	L	[225]
Transition metal oxides	$\text{NH}_{3,\text{ads}}$	L	[226–229]
MgO ($\text{NH}_3 + \text{NO}_2$)	$\text{NH}_{3,\text{ads}}$	M	[230]
$\text{Fe}_2\text{O}_3/\text{SiO}_2$	Fe-NH_2 , Si-NH_2	L	[231]
V_2O_5	NH_4^+	L	[232,233]
MoO_3	NH_4^+	H	[235]
ZnO	$\text{N}_2\text{O}_{\text{ads}}$	H	[236]
Fe_2O_3	OH , $\text{NH}_{3,\text{ads}}$, $\text{N}_2\text{O}_{\text{ads}}$, NH_4^+ , NH_2	M	[237]
Cr_2O_3	$\text{NH}_{3,\text{ads}}$, NO_{ads}	H	[238]

mixture. The 2080 cm^{-1} absorption band appears in the spectra only after treatment of the sample in the reaction mixture at $200\text{--}220^\circ\text{C}$, and disappears when the flow of ammonia is turned off. Typical temperature dependencies of the optical densities (D) and of the reaction rate are shown in Fig. 50. D_{1440} decreases (curve 3) and D_{1620} passes through a maximum (curve 4) with increasing temperature. At about 200°C the reaction products N_2 (curve 1) and N_2O (curve 2) start to be released and the absorption band at 2080 cm^{-1} appears (curve 5).

The reaction rate and D_{2080} increase linearly with increasing concentration of NH_3 up to 8% and then stop changing. These values depend in the same way on the concentration of oxygen. The reaction rate is proportional to the concentration of surface complex absorbing at 2080 cm^{-1} , so we believe this complex to be an intermediate in the reaction. It can be observed only under reaction conditions and contains both nitrogen and oxygen atoms (because the only vibrations which can absorb in this spectral region in the $\text{NH}_3 + \text{O}_2/\text{Cr}_2\text{O}_3$ system are the vibrations of the N–O bond). We assigned this absorption band to the vibrations of the adsorbed molecule $\text{NO}^{\delta+}$, ruling out other possible surface compounds:

— nitrites, nitrates and N–H, because their absorption bands are recorded in another spectral region; and

— HNO_{ads} , because its vibration frequencies are $\nu_{\text{NH}} = 3280\text{ cm}^{-1}$, $\nu_{\text{NO}} = 800\text{ cm}^{-1}$ and $\delta_{\text{NH}} = 1540\text{ cm}^{-1}$ [218].

The surface compound absorbing at 1620 cm^{-1} is thought to be an intermediate in the reaction. To check these assumptions we carried out nonsteady-state spectrokinetic measurements. The typical experimental results obtained after turning off the ammonia flow (curves a and c) as well as during the process of establishing stationary reaction conditions (curve b) are shown in Fig. 51. The characteristic reaction time is close to the time of conversion of surface complexes absorbing at 1620 cm^{-1} (a) and 2080 cm^{-1} (b,c), pointing to their involvement as intermediates in the reaction. Moreover, using the value of the extinction coefficient for the coordinatively bound ammonia [38], $\epsilon_{1620} = 0.9 \cdot 10^{-18}\text{ cm}^2/\text{molecule}$ and the transmission spectral data ($5.04 \cdot 10^{18}$ complexes on the surface of the 180 mg sample at $D_{1620} = 0.38$, $S = 2\text{ cm}^2$, $p = 30\text{ mg}$), as well as the consumption rate constant of 0.22 min^{-1} (determined from curve 1 of Fig. 51), we can calculate the consumption rate of the coordinatively bound ammonia. If it is a precursor of the reaction products (N_2 and N_2O) then, taking into account the reaction stoichiometry, $2 \cdot (W_{\text{N}_2} + W_{\text{N}_2\text{O}}) = k \cdot N_{\text{NH}_3} = 1.1 \cdot 10^{18}\text{ molecules/min}$.

The reaction rate determined from the experimental data (Fig. 51) equals $1.2 \cdot 10^{18}\text{ molecules/min}$. The very close coincidence of these two values furnishes definite proof that the coordinatively bound ammonia is an intermediate in the reaction under study.

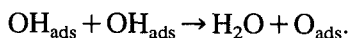
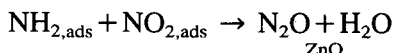
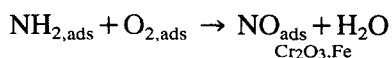
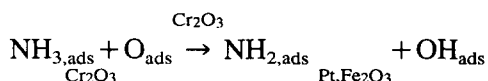
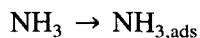
This system was also studied by the FTIR absorption spectroscopy and the following facts were discovered. Under reaction conditions at low temperature (ca. 150°C) an intense 1420 cm^{-1} band appears in the spectra of the sample pretreated in wet air. This is due to NH_4^+ (Fig. 52, spectrum 1). The 2220 cm^{-1} band assigned to the reaction product $\text{N}_2\text{O}_{\text{gas}}$ is also present in the spectra. The intensity of these two bands decreases sharply with increasing temperature up to $220\text{--}230^\circ\text{C}$ (spectra 2 and 3). At the same time the intensity of the 1220 cm^{-1} absorption band (due to the vibrations of coordinatively bound ammonia) increases and passes through a maximum at 250°C . At this temperature the absorption band of $\text{N}_2\text{O}_{\text{ads}}$ (spectra 4 and 5) appears again and becomes more intense. Thus we see that there are at least two routes for ammonia oxidation. One (low-temperature) proceeds through the formation and further conversion of the ammonia ion (the coordinatively bound ammonia is absent on the surface at this temperature); the other proceeds through the coordinatively bound ammonia. It is natural to assume that the sequence of steps of these two reactions are different, resulting in the formation of the same products.

7.6. Ammonia oxidation over oxides: conclusion

The results of the spectrokinetic study of the low temperature oxidation of ammonia on the surface of both metals and oxides reveal the following regularity: the lower the activation energy for the catalyst studied, the closer is the structure of the intermediate complex to the structure of the final product, and vice versa.

Data obtained for the Cr_2O_3 catalyst show that there are at least two directions by which the ammonia oxidation proceeds. One starts with the formation of the ammonia ion, and the other with the formation of coordinatively bound ammonia.

It was noted [240] that complexes which take part in the slowest steps of the reaction have the highest probability of being detected spectrally. When the reaction conditions change or the catalyst itself changes another reaction step possibly becomes the slowest in the process. The spectra recorded may also change. However, the total sequence of the reaction steps from reagents to products will possibly not change. On the basis of this point of view we have constructed the following sequence for the transformation of surface complexes (the catalysts are also indicated, where the relevant intermediates were observed spectrally):



We know, too, that there is another sequence which starts with NH_4^+ formation. Unfortunately, no reliable data on further conversion of the ammonia ion are available at present.

The validity of the scheme presented above could be proved directly if it were possible to simultaneously observe all the complexes listed, and to measure the rates of their subsequent conversion up to the reaction products. At present, this is evidently not possible because of the insufficient sensitivity of the available spectrometric equipment. The only method we currently have is to study this sequence by parts. Table 7 presents the bulk of the data on the intermediates in the oxidation of ammonia.

8. General conclusions

In Sections 2–7 we have presented the basic regularities of the surface steps of the following reactions: propene oxidation to acrolein, $\text{CO} + \text{NO}$ interaction and ammonia oxidation. They were obtained on the basis of the spectrokinetic studies.

As a rule, a variety of intermediates are observed at the surface of different catalysts under the same reaction conditions. Their existence is usually explained by the assumption of a great variety of reaction

mechanisms. It is possible, however, to select catalysts on the surface of which several intermediate compounds may be observed at the same time and their consecutive conversion to the reaction products may be followed. This permits us to hope that we shall be able to construct a chemically noncontroversial reaction scheme, which will be true for all catalysts of a given kind. Note that this is possible only on the basis of the investigation of a single reaction on a variety of catalysts.

The study of the nature of the reaction intermediates over various catalysts is not a simple task. The fact is that different catalysts have inherently different optical properties. We managed to overcome this problem by using a great variety of spectral techniques. Thus, emission spectroscopy was used to obtain information on the intermediates of ammonia oxidation over bulk metals. Diffuse-reflectance spectroscopy was used to study processes at the surface of catalysts which are not very active. The results of these experiments permit us to determine the role of surface compounds in the reaction.

Quantitative analysis of spectral data is based on the values of the extinction coefficients. There are two possible ways to determine them: on the basis of independent measurements of the absorbing substance concentration and on the basis of spectrokinetic measurements.

Note that, in general, almost all previous investigations of surface intermediates were not sufficiently reliable. Only the coincidence of the reaction rate with the rate of conversion of the surface compound evidences that this compound is a intermediate in the reaction. These two rates can be measured and thus compared during the nonsteady-state study of the reaction process. Such nonsteady-state investigations of C_3H_3 oxidation, $NO + CO$ reaction, $NO +$ hydrocarbons reaction and ammonia oxidation were performed by the present authors at the Institute of Chemical Physics in Moscow.

Note, too, that spectral as well as kinetic measurements of the surface processes have, as a rule, a rather low time resolution. This problem can be solved only by construction of new surface methods which would allow us to study rapid processes (at least in the millisecond range). At present the best prospect in this regard, is, the so-called TAP reactor (temporal analysis of products) [41].

Our results allow the derivation of some rules of the Polyanyi type (the correlation between the activation energy of the reaction and that of the conversion of surface compounds). In some cases the activation energy of the reaction decreases if the intermediates observed become structurally more close to the reaction products. But insufficient data are available to draw definite conclusions.

We often obtained a spectral recording of the surface compounds which have been formed on the active part of the catalyst and then diffused to the support. Their characteristic feature is the very weak (if at all noticeable) response to the reaction conditions (pressure, temperature, reagent mixture composition). One of the basic mechanisms of such diffusion and the further accumulation of the surface compounds on the support (or on a phase of a complex catalyst or on a plane of a simple one) is spillover. The surface compound accumulated in this way may serve as a reservoir for the feed of the main reaction path if the reaction conditions are changed. In complex reactions these accumulated compounds may serve as bridges between different active sites.

Our reaction mechanisms, although quite reasonable, are still to a great extent hypothetical. But we are sure that further investigations of surface intermediates will help us to make more progress towards the establishment of the mechanisms of the catalytic reactions.

References

- [1] S.L. Kiperman, *Osnovy khimicheskoi kinetiki v geterogennom katalise* (Chemical kinetics in heterogenous catalysis, Russian), Moscow, Khimiya, 1979.
- [2] O.V. Krylov and L.Ya. Margolis, *The problems of kinetic and catalysis* (Russian) Moscow, Nauka, 19 (1985) 5.
- [3] K. Tamaru, *Dynamic Heterogenous Catalysis*, Academic Press, New York, San Francisco, 1978.

- [4] V.A. Matyshak, A.A. Ukharskii and A.A. Kadushin, *Zhurnal Prikl. Spektroskopii* (Russian), 24 (1971) 179.
- [5] P.V. Kurman, V.A. Matyshak, A.A. Kadushin and G.P. Korneichuk, *Ibid.*, 36 (1982) 685.
- [6] A. Bell, *Springer Ser. Chem. Phys.*, 34 (1984) 23.
- [7] S.M. Govern, B.S.H. Royce and J. Benziger, *Appl. Opt.*, 24 (1985) 1512.
- [8] St. Pons, *J. Electron. Spectr. Rel. Phenom.*, 45 (1987) 303.
- [9] H.G. Karge, W. Abke, E.P. Boldingth and H. Laniecki, *Proc. 6th Iberoamer. Symp. Catal.*, Lisboa, 1 (1984) 582.
- [10] A.M. Bradshaw, *Surf. Sci.*, 158 (1985) 624.
- [11] L. Little, *Infrared Spectra of Adsorbed Species*, Academic Press, London, 1966.
- [12] K. Nakamoto, *Infrared Spectra of Inorganic and Coordination Compounds*, Wiley and Sons, New York, 1964.
- [13] A. Smith, *Applied Infrared Spectroscopy*, Wiley and Sons, New York, 1979.
- [14] A. Zecchina, G. Spoto and S. Bordiga, *EuropaCat-1, Book of Abstracts, Montpellier*, Vol. 1, 1993, p. 71.
- [15] W. Wendlandt and H.G. Hecht, *Reflectance Spectroscopy*, Interscience Publishers, New York, 1966.
- [16] V.B. Kazansky, V.Yu. Borovkov and L.M. Kustov, *Proc. 8th Congr. on Catalysis, Weinheim*, Vol. 3, 1984, p. 3.
- [17] P.R. Griffiths, *Chemical Infrared Fourier Transform Spectroscopy*, Wiley and Sons, London, 1975.
- [18] J.B. Bates, *Fourier Transform Infrared Emission Spectroscopy*, Academic Press, Vol.1, 1978.
- [19] P. Baraldi and G. Fabbri, *Appl. Spectrosc.*, 38 (1984) 668.
- [20] A.W. Mantz, S.A. Shafer and K.H. Rao, *Appl. Optics*, 15 (1967) 589.
- [21] P. Baraldi and G. Fabbri, *Appl. Spectrosc.*, 26 (1972) 593.
- [22] P. Baraldi and G. Fabbri, *Spectrochim. Acta*, 39A (1983) 669.
- [23] N. Sheppard, in J.P. Durig (Editor), *Analytical Application of FT-IR to Molecular and Biological Systems*, NATO Advanced Study Institutes Series, Dordrecht, Holland, 1980, p. 125.
- [24] J.R. Aronson, A.G. Emslie, F.E. Ruecia, C.R. Smallman, E.M. Smith and P.F. Strong, *Appl. Optics*, 18 (1979) 2622.
- [25] A.B. Pluchino, *Ibid.*, 20 (1981) 531.
- [26] J. Hvistendaehe, E. Pytter and H.A. Oye, *Appl. Spectrosc.*, 37 (1983) 182.
- [27] P.H.G. Van Kasteran and L.H. Smeets, *Reprint from SPIE, V.29-Fourier Transform Spectroscopy*, Society of Photo-Optical Instrumentation Engineers, 1981.
- [28] T. Wadayama, Y. Hanata and W. Suetaka, *Surf. Sci.*, 158 (1985) 579.
- [29] J. Mink, T. Srilagyi, S. Wachholz and D. Kunat, *J. Mol. Struct.*, 141 (1986) 389.
- [30] R.G. Tobin, R.B. Phelps and P.L. Richards, *Surf. Sci.*, 183 (1987) 427.
- [31] P.L. Richards and R.G. Tobin, in J.T. Yates and T.E. Madey (Editors), *Methods Surf. Caract. (Vibr. Spectr. Mol. Surf.)*, 1 (1987) 417.
- [32] P.C.M. Van Woerkom and R.L. de Groot, *Appl. Optics*, 21 (1982) 3114.
- [33] P.C.M. Van Woerkom, P. Blok and H.J. Van Veenendaal, *Appl. Optics*, 19 (1980) 2546.
- [34] P.C.M. Van Woerkom, *J. Mol. Struct.*, 79 (1982) 31.
- [35] V.A. Matyshak, E. Lofler and K.-H. Schnabel, *Kinetika i Kataliz*, 28 (1987) 1389.
- [36] M. Boudart, *Uspekhi Khimii*, 43 (1974) 317.
- [37] O.V. Krylov, *Kinetika i Kataliz*, 21 (1980) 79.
- [38] A.A. Davydov, *IR Spectroscopy in the Surface Chemistry of Oxides* (in Russian), Nauka, Novosibirsk, 1984.
- [39] T. Konno and M. Kobayashi, *Proc. 8th Int. Congr. on Catalysis, Basel, Weinheim*, Vol. 3, 1984, p. 217.
- [40] P.T. Connor, S. Kovenkloglu and D.C. Shelly, *Appl. Catal.*, 71 (1991) 247.
- [41] J.T. Gleaves, J.R. Ebner and T.C. Kuechler, *Catal. Rev.*, 30 (1989) 43.
- [42] G.D. Svoboda, J.T. Gleaves and P.L. Mills, *Proc. 2nd Int. Congr. New Developments in Selective Oxidation*, Amsterdam, Elsevier, 1994, p. 481.
- [43] R.A. Van Santen and H.P.C.E. Kuipers, *Adv. Catal.*, 35 (1987) 265.
- [44] X. Bao, B. Pettinger, G. Ertl and R. Schlögl, *Ber. Bunsenges. Phys. Chem.*, 97 (1993) 322.
- [45] C. Martin, I. Martin and V. Rives, *J. Chem. Soc. Faraday Trans.*, 89 (1993) 4131.
- [46] L.Ya. Margolis, *Hydrocarbons Oxidation on Heterogeneous Catalysts* (Russian) Moscow, Khimiya, 1977.
- [47] C.R. Adams and T.J. Jennings, *J. Catal.*, 2 (1963) 63.
- [48] C.R. Adams and T.J. Jennings, *J. Catal.*, 3 (1964) 549.
- [49] M. Imachi, R.L. Kuczkowski, J.T. Groves and N.W. Cant, *J. Catal.*, 82 (1983) 355.
- [50] G. Busca, G. Ramis, V. Lorenzelli, A. Jamin and J.C. Lavalley, *Spectrochim. Acta A*, 43 (1987) 489.
- [51] D.R. Conlson, P.L. Mills and K. Kourtakis, in P. Ruiz and B. Delmon (Editors), *New Developments in Selective Oxidation by Heterogeneous Catalysis*, Vol. 72, 1992, p. 305.
- [52] C. Martin, I. Martin, C. Mendizabal and V. Rives, *Proc. 10th Int. Congr. on Catal.*, Akademiai Kiado, Budapest, C., 1993, p. 1987.
- [53] F. Trifiro, L. Kubelkova and I. Pasguon, *J. Catal.*, 19 (1970) 121.
- [54] K.P. Zhdanova and N.I. Popova, *Kinetika i Kataliz*, 9 (1968) 1301.
- [55] Ya.B. Gorokhovatskii and S.V. Gerey, *Proc. 1st Japan-Soviet Catalysis Seminar*, Tokyo, 1971.
- [56] A.A. Davydov, V.G. Mikhachenko, V.D. Sokolovskij and G.K. Boreskov, *J. Catal.*, 55 (1978) 299.
- [57] A.A. Efremov, J. Tikhy and A.A. Davydov, *Kinetika i Kataliz*, 21 (1978) 154.
- [58] A.A. Davydov, A.A. Efremov, V.G. Mikhachenko and V.D. Sokolovskij, *J. Catal.*, 58 (1979) 1.

- [59] M. Carbuceschio, C. Centi, P. Forzatti, F. Trifiro and P.L. Villa, *J. Catal.*, 10 (1987) 307.
- [60] G.W. Keulks and Z. Yu, *Proc. 8th Congr. on Catalysis, Basel, Weinheim*, Vol. 3, 1984, p. 289.
- [61] T. Ono, K.W. Hulleg and R.L. Kuczkowski, *J. Catal.*, 123 (1990) 236.
- [62] A.A. Davydov, *Kinetika i Kataliz*, 34 (1993) 699.
- [63] A.A. Davydov and T.A. Gordymova, *Zhurnal Fizicheskoi Khimii*, 93 (1993) 2025.
- [64] E. Garrone, A. Zecchina and F.S. Stone, *J. Catal.*, 62 (1980) 396.
- [65] I.L.C. Frerics, R. Bowman and P.V. Geenan, *J. Catal.*, 65 (1980) 315.
- [66] A.A. Davydov and A.A. Efremov, *Kinetika i Kataliz*, 24 (1983) 1434.
- [67] K. Dyrek and M. Labanovska, *Appl. Catal.*, 23 (1986) 63.
- [68] A.A. Davydov, *Proc. 7th Soviet–Japan Seminar on Catalysis, Irkutsk*, 1983, p. 178.
- [69] E.A. Aliev, K.Yu. Adzhamov and T.G. Alhasov, *Proc. 4th All-Union Conference on Catalysis, Moscow*, Vol. 2, 1986, p. 12.
- [70] A.A. Kadushin, N.A. Koutyreva, V.A. Matyshak and O.S. Morozova, *Kinetika i Kataliz*, 22 (1981) 233.
- [71] A.A. Kadushin, P.V. Kurman, N.A. Koutyreva and V.A. Matyshak, *Kinetika i Kataliz*, 24 (1983) 1258.
- [72] O.S. Morozova, A.A. Ukharskii and A.A. Kadushin, *Proc. 3rd Int. Symp. Heterogeneous Catalysis, Varna*, 1975, p. 379.
- [73] K. Nakanishi, *Infrared Spectra and Structure of Organic Compounds* Nankodo Company Limited, Tokyo, 1962.
- [74] S.Z. Roginskii, *Adsorption and Catalysis on Heterogeneous Surface (in Russian)*, Moscow, AN SSSR, 1948.
- [75] A.A. Davydov, Yu.M. Shchekochihin and N.P. Keier, *Kinetika i kataliz*, 10 (1969) 1341.
- [76] C.K. Adams, H.H. Voge, C.Z. Morgan and W.E. Armstrong, *J. Catal.*, 3 (1964) 379.
- [77] O.V. Isaev, *Thesis*, Moscow, 1968.
- [78] A. Ramstetter and M. Baerns, *J. Catal.*, 109 (1993) 303.
- [79] H.H. Kung and M.C. Kung, *Adv. Catal.*, 33 (1985) 159.
- [80] S. De Rossi, M. Lo Jacono, M. Gardini and P. Portu, *J. Catal.*, 146 (1994) 126.
- [81] O.V. Krylov, *Vestnik AN SSSR*, 1 (1983) 26.
- [82] V.A. Matyshak, P.V. Kurman and M.Yu. Koutyrev, *Khim. Fizika (Russian)* 3 (1984) 1138.
- [83] Ref. 73, p. 51.
- [84] A.A. Firsova, M.Yu. Koutyrev and L.Ya. Margolis, *Dokl. AN SSSR*, 263 (1982) 147.
- [85] M.Yu. Koutyrev and K.N. Spiridonov, *Proc. 4th Conference on Oxidative Catalysis, Baku*, Vol. 1, 1978, p. 14.
- [86] H. Shinjoh, H. Muraki and Y. Fujitani, *Proc. 1st Int. Symp. Catal. Autom. Pollution Control Processes*, 1986, p. 187.
- [87] V.I. Panchishnyi, *The Problems of Kinetics and Catalysis (Russian)* Moscow, Nauka, Vol. 18, 1981, p. 145.
- [88] K.C. Taylor, in R.L. Klimisch (Editor), *The Catalytic Chemistry of Nitrogen Oxides*, Plenum Press, New York, 1975, p. 173.
- [89] J.C. Schlatter and K.C. Taylor, *J. Catal.*, 49 (1977) 42.
- [90] W. Adlhoeh and H.G. Lintz, *Surf. Sci.*, 78 (1978) 58.
- [91] W.C. Hecker and A.T. Bell, *J. Catal.*, 84 (1983) 200.
- [92] R.E. Hendershot and R.S. Hansen, *J. Catal.*, 98 (1986) 150.
- [93] L.H. Dubois, P.K. Nahsma and G.A. Somorjai, *J. Catal.*, 65 (1980) 318.
- [94] R.J. Gorte and L.D. Schmidt, *Surf. Sci.*, 111 (1981) 266.
- [95] M.W. Lesley and L.D. Schmidt, *Surf. Sci.*, 155 (1985) 215.
- [96] W.F. Banholzer, R.E. Parise and R.I. Masel, *Ibid.*, 155 (1985) 653.
- [97] E.W. Scharf and J.B. Benziger, *J. Catal.*, 136 (1992) 346.
- [98] H. Conrad, G. Ertl, J. Kuppers and E.E. Satta, *Faraday Discuss.*, 58 (1974) 116.
- [99] P.A. Thiel, W.H. Weinberg and J.T. Yates, *J. Chem. Soc.*, 71 (1979) 1643.
- [100] L.H. Dubois, P.K. Hansma and G.A. Somorjai, *J. Catal.*, 65 (1980) 318.
- [101] M.L. Unland, *J. Phys. Chem.*, 77 (1973) 1952.
- [102] T.W. Root, L.D. Schmidt and B. Fisher, *Surf. Sci.*, 150 (1985) 173.
- [103] M.L. Unland, *J. Catal.*, 31 (1973) 459.
- [104] J.W. London and A.T. Bell, *J. Catal.*, 31 (1973) 96.
- [105] F. Solymosi, J. Sarkany and A. Schauer, *J. Catal.*, 46 (1977) 297.
- [106] F. Solymosi and J. Rasko, *J. Catal.*, 63 (1980) 217.
- [107] D.D. Eley, G.H. Kiwanuka and C.H. Rochester, *J. Chem. Soc. Faraday Trans. 1*, 69 (1973) 2062.
- [108] B.A. Morrow and I.A. Cody, *Ibid.*, 71 (1975) 1021.
- [109] A. Guillet, H. Coudurier and J.B. Donnet, *Bull. Soc. Chim. Fr.*, N 7–8 (1975) 1563.
- [110] R.A. Dalla Betta and M. Shelef, *J. Mol. Catal.*, 1 (1976) 431.
- [111] F. Solymosi and T. Bansagi, *J. Phys. Chem.*, 83 (1979) 552.
- [112] M.F. Brown and R.D. Gonzalez, *J. Catal.*, 44 (1976) 477.
- [113] A.A. Davydov and A.T. Bell, *J. Catal.*, 49 (1977) 345.
- [114] F. Solymosi and J. Sarkany, *Appl. Surf. Sci.*, 3 (1979) 68.
- [115] J. Rasko and F. Solymosi, *J. Catal.*, 71 (1981) 219.
- [116] R.G. Gorte, L.D. Schmidt and B.A. Sexton, *J. Catal.*, 67 (1981) 387.
- [117] W.C. Hecker and A.T. Bell, *J. Catal.*, 85 (1984) 389.

- [118] W.C. Hecker and A.T. Bell, *J. Catal.*, 88 (1984) 288.
- [119] F. Solymosi, L. Volgyesi and J. Sarkany, *J. Catal.*, 54 (1978) 336.
- [120] R. Dictor, *J. Catal.*, 109 (1988) 89.
- [121] K. Ashley, M. Lazaga, M.G. Samant, H. Seki and M.P. Philpott, *Surf. Sci.*, 219 (1989) L519.
- [122] D.K. Paul, M.L. McKee, S.D. Worley, N.W. Hoffman, D.H. Ash and J. Gatney, *J. Phys. Chem.*, 93 (1989) 4598.
- [123] T. Bansagi, J. Rasko and F. Solymosi, *Mag. Kem. Folyoirat*, 90 (1984) 345.
- [124] E.A. Hyde and R. Rudman, *J. Chem. Soc. Faraday Trans. 1*, 80 (1984) 531.
- [125] A. Arai and H. Tominaga, *J. Catal.*, 43 (1976) 131.
- [126] J. Kiss and F. Solymosi, *Surf. Sci.*, 135 (1983) 243.
- [127] J. Rasko, L. Volgyesi, M. Lanes and F. Solymosi, *Proc. 8th Int. Congr. Catalysis, Basel, Weinheim, Vol. 3, 1984*, p. 671.
- [128] R.J.H. Voorhoeve, C.K.N. Patel, L.E. Trimble, R.J. Kerl and R.K. Gallander, *J. Catal.*, 45 (1976) 279.
- [129] R.J.H. Voorhoeve, C.K.N. Patel, L.E. Trimble and R.J. Kerl, *J. Catal.*, 54 (1978) 102.
- [130] R.J.H. Voorhoeve and L.E. Trimble, *J. Catal.*, 54 (1978) 269.
- [131] C.C. Chang and L.L. Hegedus, *J. Catal.*, 57 (1979) 361.
- [132] H. Niiyama, M. Tanaka, H. Iida and E. Echigoya, *Bull. Chem. Soc. Japan*, 49 (1976) 2047.
- [133] R. Nakamura, R. Nakai, K. Sugiyama and E. Echigoya, *Bull. Chem. Soc. Japan*, 54 (1981) 1950.
- [134] V. Rives-Armai and B. Munuera, *Appl. Surf. Sci.*, 6 (1980) 122.
- [135] D. Lorimer and A.T. Bell, *J. Catal.*, 59 (1979) 223.
- [136] R.F. Van Slooten and S. Niewenhuys, *J. Catal.*, 122 (1990) 429.
- [137] J. Regalbuto and E.E. Wolf, *J. Catal.*, 95 (1985) 558.
- [138] G.M. Alikina, A.A. Davydov, I.S. Sazonova and V.V. Popovskii, *React. Kinet. Catal. Lett.*, 27 (1985) 279.
- [139] J. Regalbuto, P.J. Kaul and E.E. Wolf, *Proc. 8th Int. Congr. Catalysis, Basel, Weinheim, Vol. 3, 1984*, p. 353.
- [140] E. Guglielminotti and F. Boccuzzi, *J. Catal.*, 141 (1993) 486.
- [141] T. Yamada, I. Matsuo, J. Nakamura and K.I. Tanaka, *Surf. Sci.*, 231 (1990) 304.
- [142] D. Forster and D.H.L. Goodgame, *J. Chem. Soc. A*, (1965) 1286.
- [143] A.H. Norlury and A.C.P. Sinha, *J. Chem. Soc. A*, (1968) 1598.
- [144] B.A. Morrow, W.N. Sont and A. St. Onge, *J. Catal.*, 62 (1980) 304.
- [145] R. Hierl, H.P. Urbach and H. Knozinger, *Proc. 10th Int. Congr. Catal., Akademiai Kiado, Budapest, C., 1993*, p. 2697.
- [146] V.A. Shvets, M.O. Osmanov, A.A. Tarasov and V.B. Kazanskii, *Kinetika i Kataliz*, 31 (1990) 645.
- [147] V.A. Matyshak, M.M. Slinko, A.A. Kadushin and O.V. Krylov, *Proc. 7th French-Soviet Seminar on Catalysis, Strasbourg, 1986*, p. 1.
- [148] V.A. Matyshak, M.M. Slinko, R.A. Gazarov, V.I. Panchishnyi, A.A. Kadushin and O.V. Krylov, *Proc. 4th All-Union Conference on Catalysis, Moscow, Vol. 2, 1986*, p. 312.
- [149] R.A. Gazarov, V.A. Matyshak and M.M. Slinko, *Itogi Nauki i Tehniki, Moscow, VINITI, 1986*, pp. 3–100.
- [150] V.A. Matyshak, M.M. Slinko, R.A. Gazarov, V.I. Panchishnyi, A.A. Kadushin and O.V. Krylov, *Kinetika i Kataliz*, 27 (1986) 167.
- [151] V.A. Matyshak, R.A. Gazarov, V.I. Panchishnyi and A.A. Kadushin, *Kinetika i Kataliz*, 29 (1988) 1123.
- [152] V.A. Matyshak, R.A. Gazarov, V.I. Panchishnyi and A.A. Kadushin, *Kinetika i Kataliz*, 29 (1988) 1130.
- [153] V.A. Matyshak, R.A. Gazarov, V.I. Panchishnyi and A.A. Kadushin, *Kinetika i Kataliz*, 29 (1988) 1389.
- [154] V.A. Matyshak, *Kinetika i Kataliz*, 33 (1992) 1168.
- [155] V.A. Matyshak, R.A. Gazarov, V.I. Panchishnyi and A.A. Kadushin, *Kinetika i Kataliz*, 29 (1988) 1381.
- [156] V.A. Matyshak, M.M. Slinko, R.A. Gazarov, O.V. Krylov, S. Dzvigai and E. Haber, *Kinetika i Kataliz*, 30 (1989) 155.
- [157] A.C. Yang and C.W. Garland, *J. Phys. Chem.*, 61 (1957) 504.
- [158] M.A. Babaeva, Thesis, Leningrad, LGU, 1984.
- [159] S.D. Worley, C.A. Rice, G.A. Mattson, C.W. Curtis, J.A. Guin and A.R. Tarrer, *J. Chem. Phys.*, 76 (1982) 20.
- [160] S.H. Oh and J.E. Carpenter, *J. Catal.*, 101 (1986) 104.
- [161] H.G. Lintz, *Surf. Sci.*, 108 (1981) 426.
- [162] K.C. Taylor and J.C. Schlatter, *J. Catal.*, 63 (1980) 53.
- [163] B.G. Baker and R.F. Peterson, *Proc. 6th. Int. Congr. Catalysis, London, 1976*, Preprint B-37.
- [164] M. Shelef, K. Otto and J. Gandi, *J. Catal.*, 12 (1968) 361.
- [165] E.R.S. Winter, *J. Catal.*, 34 (1974) 440.
- [166] M. Shelef and K. Otto, *J. Catal.*, 10 (1968) 408.
- [167] T.G. Alkhazov, G.Z. Gasan-Zade, M.O. Ocmanov and M.Yu. Sultanov, *Kinetika i Kataliz*, 16 (1975) 1230.
- [168] G.V. Glasneva, I.S. Sazonova and N.P. Keier, *Dokl. AN SSSR*, 213 (1973) 364.
- [169] I.S. Sazonova, G.M. Alikina, G.V. Glasneva, N.P. Keier, N.E. Bogdanchikova and V.G. Devyatov, *Kinetika i Kataliz*, 18 (1977) 441.
- [170] G.V. Glazneva, A.A. Davydov, I.C. Sazonova, Yu.M. Shchekochichin and N.P. Keier, *Kinetika i Kataliz*, 19 (1978) 997.
- [171] Yu.A. Lochoy, Z. Musil and A.A. Davydov, *Ibid.*, 20 (1979) 256.
- [172] Yu.A. Lochoy, Z. Musil and A.A. Davydov, *Proc. 2nd All-Union Conference on Catalysis, Moscow, Vol. 1, 1978*, p. 305.
- [173] J. Rasko and F. Solymosi, *J. Mol. Catal.*, 3 (1977) 305.
- [174] F. Solymosi and J. Rasko, *J. Catal.*, 65 (1980) 235.
- [175] J.W. London and A.T. Bell, *J. Catal.*, 31 (1973) 32.

- [176] M.O. Osmanov, A.A. Tarasov, V.A. Shvets and V.B. Kazanskii, *Dokl. AN SSSR*, 304 (1989) 1395.
- [177] J.M.D. Tascon, L. Gonzalez Tejuca and C.H. Rochester, *J. Catal.*, 95 (1989) 558.
- [178] B. Hori and N. Takezawa, *Catal. Lett.*, 12 (1992) 283.
- [179] P.G. Harrison and E.W. Thornton, *J. Chem. Soc. Farad. Trans. 1*, 74 (1978) 2604.
- [180] J.W. London and A.T. Bell, *J. Catal.*, 31 (1973) 96.
- [181] S.S. Shin, D.S. Shihabi and R.G. Sgueries, *Proc. 6th Int. Congr. Catalysis*, London, 1976, Preprint B-36.
- [182] E. Garrone, E. Guglielminotti and A. Zecchina, *J. Chem. Soc. Farad. Trans. 1*, 20 (1984) 2723.
- [183] D. Panayotov, V. Matyshak, A. Sklyarov, A. Vlasenko and D. Mechandjiev, *Appl. Catal.*, 24 (1986) 37.
- [184] M.A. Ismailov, R.B. Akhverdiev, V.S. Gadji-Kasumov, R.G. Sarmurzina, V.I. Panchishnyi and V.A. Matyshak, *Kinetika i Kataliz*, 34 (1993) 117.
- [185] M.A. Ismailov, R.B. Akhverdiev, V.S. Gadji-Kasumov and V.A. Matyshak, *Kinetika i Kataliz*, 33 (1992) 611.
- [186] Y. Amenomiya, *Appl. Spectrosc.*, 38 (1978) 484.
- [187] B.E. Nieuwenhuys, *Surf. Sci.*, 126, (1983) 307.
- [188] M. Iwamoto, *Proc. Meeting of Catalytic Technology for Removal of NO*, Tokyo, 1990, p. 17.
- [189] J. Valon and W.K. Hall, *J. Phys. Chem.*, 97 (1993) 5211.
- [190] S. Larsen, A.W. Aylor, A.T. Bell and J.A. Reimer, *Proc. US-Russia Workshop on Environmental Catalysis*, Wilmington, Delaware, 1994, p. 21.
- [191] E.S. Shpiro, W. Grunert, R.W. Joyner and G.N. Baeva, *Catal. Lett.*, 24 (1994) 159.
- [192] J. Sarkani, J.L. d'Itri and W.M.H. Sachtler, *Catal. Lett.*, 16 (1992) 242.
- [193] M. Shelef, *Catal. Lett.*, 15 (1992) 305.
- [194] M. Iwamoto, H. Yahiro, K. Mizuno, W.X. Zhang, Y. Miye and H. Furukawa, *J. Phys. Chem.*, 96 (1992) 9360.
- [195] J. Vallyon and W.K. Hall, *J. Phys. Chem.*, 97 (1993) 1204.
- [196] R. Burch and P.J. Millingham, *Appl. Catal.*, B2 (1993) 71.
- [197] G.P. Ansell, A.F. Diwail and S.E. Golunski, *Appl. Catal.*, B2 (1993) 81.
- [198] M. Sasaki, H. Hamada, V. Kintaichi and T. Ito, *Catal. Lett.*, 15 (1992) 297.
- [199] N.W. Hayes, W. Grunert, G.J. Hutchings, R.W. Joyner and E.S. Shpiro, *J. Chem. Soc., Chem. Commun.*, (1994) 531.
- [200] H. Yahiro, Y. Yu-u, H. Takeda, N. Mizuno, M. Iwamoto and Shokubai, 35 (1993) 130.
- [201] N. Hayes, R.W. Joyner and E.S. Shpiro, *Appl. Catal.*, to be published.
- [202] J.O. Petunchi, G. Sill and W.K. Hall, *Appl. Catal.*, B2 (1993) 303.
- [203] H. Yasuda, T. Miyamoto, C. Yokoyama and M. Misono, *Shokubai*, 35 (1993) 386.
- [204] C. Yokoyama, H. Yasuda and M. Misono, *Shokubai*, 35 (1993) 122.
- [205] T. Tabata and M. Kokitsu, *Catal. Lett.*, 25 (1994) 393.
- [206] K. Yogo, M. Ihara, I. Terasaki and E. Kikuchi, *Chem. Lett.*, 2 (1993) 229.
- [207] K. Yogo, M. Ihara, I. Terasaki, H. Watanabe and E. Kikuchi, *Shokubai*, 35 (1993) 126.
- [208] S. Naito and M. Tanimoto, *Chem. Lett.*, 11 (1993) 1935.
- [209] V.A. Sadykov, A.Ya. Rozovskii, V.V. Lunin and V.A. Matyshak, *Proc. US–Russia Workshop on Environmental Catalysis*, Wilmington, Delaware, 1994, p. 20.
- [210] A.N. Ilichev, A.A. Ukharskii and V.A. Matyshak, *Kinetika i Kataliz*, (1994) to be published.
- [211] R.M. Lambert and G.M. Comri, *Surf. Sci.*, 46 (1974) 61.
- [212] D.S. Dann, M.W. Severson, W.G. Golden and J. Overend, *Spectrochim. Acta*, 37A (1981) 815.
- [213] W. Erleg and H. Ibach, *Surf. Sci.*, 119 (1982) L357.
- [214] J.E. Parmenter, Y. Wang, C.B. Mulling and W.H. Weinberg, *J. Chem. Phys.*, 88 (1988) 5225.
- [215] Y. Zhou, S. Akhter and J.M. White, *Surf. Sci.*, 202 (1988) 357.
- [216] I.C. Bassignana, K. Wagemann, J. Kuppers and G. Ertl, *Surf. Sci.*, 175 (1986) 22.
- [217] G.S. Selwyu and M.C. Lin, *Stud. Laser Proc.*, 1983, p. 115.
- [218] V.V. Gorodetskii, M.Y. Smirnov and A.R. Cholech, *Proc. 10th Intern. Congr. on Catal.*, Akademiai Kiado, Budapest, B., 1993, p. 1587.
- [219] D.M. Thornburg and R.J. Madix, *Surf. Sci.*, 220 (1989) 268.
- [220] J.L. Gland and V.N. Korchak, *J. Catal.*, 53 (1978) 9.
- [221] V.A. Matyshak, E. Lofler and K.H. Schnabel, *Kinetika i Kataliz*, 28 (1987) 1389.
- [222] S. Naito and K. Tamaru, *J. Phys. Chem.*, 87 (1983) 315.
- [223] G.I. Golodets, *Geterogennye Kataliticheskie Reakzii s Uchastiem Molekulyarnogo Kisloroda*, Kiev, Naukova Dumka, 1977.
- [224] Y. Murakami, Y. Kosaki and U. Matokoura, *Nipp. Kagaki Kaishi*, 5 (1977) 612.
- [225] E.E. Platero, S. Coluccia and A. Zecchina, *J. Catal.*, 103 (1987) 270.
- [226] A.A. Tsyganenko, D.V. Posdnyakov and V.N. Filimonov, *J. Mol. Struct.*, 29 (1979) 299.
- [227] F.B. Kasumov, A.A. Efremov, A.A. Davydov, K.Yu. Adzhamov and T.G. Alkhazov, *Kinetika i Kataliz*, 23 (1982) 700.
- [228] Yu.V. Belokopytov, K.M. Kholiyavenko and S.V. Gerej, *J. Catal.*, 60 (1979) 1.
- [229] D. Bianchi, J.L. Bernard, M. Camelot, R. Benall-Chaoui and S.J. Teichner, *Bull. Soc. Chem. France*, (1980) 275.
- [230] E. Borello, S. Coluccia and A. Zecchina, *J. Catal.*, 93 (1985) 331.
- [231] C. Johnston, N. Jorgensen, C.H. Rochester, *J. Chem. Soc., Farad. Trans. 1*, 84 (1988) 2001.

- [232] P.A. Rajadhyaksha and H. Knozinger, *Appl. Catal.*, 51 (1989) 81.
- [233] M. Casior, J. Haber, T. Machey and T. Czeppe, *J. Mol. Catal.*, 43 (1988) 359.
- [234] E. Alsdorf, W. Hanke and K.H. Schnabel, *J. Catal.*, 98 (1986) 82.
- [235] V.A. Matyshak, A.A. Kadushin, I.S. Burkhardt and K.H. Schnabel, *Kinetika i Kataliz*, 26 (1985) 334.
- [236] V.A. Matyshak, A.A. Ukharskii and O.N. Silchenkova, *Kinetika i Kataliz*, 35 (1994).
- [237] E.N. Amirbekov, V.A. Matyshak, *Primenenie Opticheskoi Spektroskopii v Adsorbzii i Katalise*, Leningrad, LGU, 1988, p. 123.
- [238] V.A. Matyshak, O.N. Silchenkova, I.N. Staroverova and V.N. Korchak, *Kinetika i Kataliz*, 1995, to be published.
- [239] L.M. Røev and A.V. Alekseev, *Elementarnye Fotoprozessy v Molekylakh*, Moscow–Leningrad, Nauka, 1966, p. 346.
- [240] V.A. Matyshak, *Kinetika i Kataliz*, 30 (1989) 160.